

**Network Centric Systems  
Raytheon Company  
McKinney, TX 75071**

---

**EER-2006-34171-002  
Engineering Evaluation Report**

**January 31, 2006**

# **JCAA/JG-PP LEAD-FREE SOLDER PROJECT: FAILURE ANALYSIS OF TEST VEHICLES SUBJECTED TO COMBINED ENVIRONMENTS TEST**

by  
Jeff Bradford  
Robert Champaign  
Marlin Downey  
Theresa Hendricks  
Jodi Roepsch

---

Approved for public release; distribution is unlimited.

---



**Abstract**

Raytheon conducted the combined environments test (CET) for the Joint Council on Aging Aircraft/Joint Group on Pollution Prevention Lead-Free Solder project. Using performance requirements of the aerospace and military electronics community, this project validated lead-free solders as potential replacements for conventional tin-lead solders used in circuit card assemblies.

The solder alloys tested include: Sn3.9Ag0.6Cu, Sn3.4Ag1.0Cu3.3Bi, Sn0.7Cu0.05Ni and Sn37Pb. These solder alloys were used to assemble various components on three different printed wiring board test vehicles: manufacture, rework and hybrid. The test vehicles were subjected to a CET consisting of thermal cycling from -55 to +125 degrees Celsius at a ramp rate of 20 degrees Celsius per minute, dwell at the temperature extremes for 15 minutes and pseudorandom vibration of 10 g<sub>rms</sub> for the last 10 minutes of the dwell periods. After every 50 cycles, the vibration level was increased by 5 g<sub>rms</sub> until a maximum of 55 g<sub>rms</sub> was reached.

The Raytheon Failure Analysis Laboratory located in McKinney, Texas performed failure analysis on the test vehicles including destructive physical analysis, scanning electron microscopy and energy dispersive spectroscopy.



**Contents**

Abstract .....	i
Contents.....	iii
List of Figures .....	iii
List of Tables.....	ix
Foreword.....	1
Summary.....	2
Introduction.....	3
Methods, Assumptions and Procedures.....	3
Combined Environments Test .....	3
HALT Chamber.....	4
Test Profile.....	4
Test Execution .....	5
Microsection.....	5
Scanning Electron Microscopy (SEM) / Energy Dispersive Spectroscopy (EDS) .....	6
Results and Discussion.....	7
Manufactured Test Vehicles Results and Discussion.....	7
Tin-Lead Solder .....	8
Tin-Silver-Copper Solder.....	26
Tin-Silver-Copper-Bismuth Solder .....	43
Tin-Copper Solder .....	58
Rework Test Vehicle Results and Discussion.....	61
Tin-Silver-Copper-Bismuth Solder .....	62
Hybrid Test Vehicle Results and Discussion.....	74
Tin-Lead Solder .....	75
Tin-Silver-Copper Solder.....	82
Tin-Silver-Copper-Bismuth Solder .....	87
Conclusions.....	93
Manufactured Test Vehicles .....	93
BGA-225.....	93
CLCC-20.....	93
PDIP-20 .....	94
PLCC-20.....	94
TQFP-144 .....	94
TQFP-208 .....	95
TSOP-50.....	95
Reworked Tin-Silver-Copper-Bismuth Soldered TQFP-208 Components on Rework Test Vehicles .....	95
Hybrid Test Vehicles.....	95
CSP-100 .....	95
Hybrid-30 .....	96
References.....	97
Appendixes.....	98
Appendix A: List of Microsectioned Components on Manufactured Test Vehicles .....	99
Appendix B: List of Microsectioned Components From Rework Test Vehicles .....	101
Appendix C: List of Microsectioned Components From Hybrid Test Vehicles .....	102
List of Symbols, Abbreviations and Acronyms .....	103

**List of Figures**

Figure 1	QualMark Model OVS-4 HALT/HASS Chamber.....	4
Figure 2	Initial Combined Environments Test Profile .....	5
Figure 3	Test Vehicle Layout in Test Chamber .....	5
Figure 4	Microsection Laboratory.....	6

**JCAA/JG-PP Lead-Free Solder Project: Failure Analysis of Test Vehicles Subjected to Combined Environments Test**

**List of Figures**

Figure 5 Carl Zeiss SMT 1550 VP-SEM..... 6

Figure 6 SEM Micrograph of SnPb Soldered SnPb BGA-225 on Manufactured Test Vehicle (SN 30, U55, Bump 14) ..... 8

Figure 7 SEM Micrograph of SnPb Soldered SnPb BGA-225 on Manufactured Test Vehicle (SN 32 U43, Bump 1) ..... 9

Figure 8 SEM Micrograph of SnPb Soldered SnPb CLCC-20 on Manufactured Test Vehicle (SN 31, U22, Lead 16) ..... 10

Figure 9 SEM Micrograph of SnPb Soldered SnPb CLCC-20 on Manufactured Test Vehicle (SN 31, U22, Lead 16) ..... 10

Figure 10 SEM Micrograph of SnPb Soldered SnPb CLCC-20 on Manufactured Test Vehicle (SN 31, U22, Lead 1) ..... 10

Figure 11 SEM Micrograph of SnPb Soldered SnPb CLCC-20 on Manufactured Test Vehicle (SN 31, U22, Lead 1) ..... 11

Figure 12 EDS Spectra of SnPb Soldered SnPb CLCC-20 on Manufactured Test Vehicle (SN 31, U22, Lead 1) ..... 11

Figure 13 SEM Micrograph of SnPb Soldered SnPb CLCC-20 on Manufactured Test Vehicle (SN 31, U22, Lead 1) ..... 12

Figure 14 EDS Spectra of SnPb Soldered SnPb CLCC-20 on Manufactured Test Vehicle (SN 31, U22, Lead 1) ..... 12

Figure 15 SEM Micrograph of SnPb Soldered SnPb CLCC-20 on Manufactured Test Vehicle (SN 31, U46, Lead 11) ..... 13

Figure 16 SEM Micrograph of SnPb Soldered SnPb CLCC-20 on Manufactured Test Vehicle (SN 31, U46, Lead 5) ..... 13

Figure 17 SEM Micrograph of SnPb Soldered Sn PDIP-20 on Manufactured Test Vehicle (SN 31, U30, Lead 10) ..... 15

Figure 18 SEM Micrograph of SnPb Soldered Sn PDIP-20 on Manufactured Test Vehicle (SN 31, U30, Lead 10) ..... 15

Figure 19 SEM Micrograph of SnPb Soldered Sn PDIP-20 on Manufactured Test Vehicle (SN 31, U30, Lead 10) ..... 15

Figure 20 SEM Micrograph of SnPb Soldered Sn PDIP-20 on Manufactured Test Vehicle (SN 34, U49, Lead 10) ..... 16

Figure 21 SEM Micrograph of SnPb Soldered AuPdNi PDIP-20 on Manufactured Test Vehicle (SN 34, U49, Lead 10) ..... 16

Figure 22 SEM Micrograph of SnPb Soldered Sn PLCC-20 on Manufactured Test Vehicle (SN 32, U28, Lead 16) ..... 17

Figure 23 SEM Micrograph of SnPb Soldered Sn PLCC-20 on Manufactured Test Vehicle (SN 32, U28, Lead 16) ..... 18

Figure 24 SEM Micrograph of SnPb Soldered Sn TQFP-144 on Manufactured Test Vehicle (SN 30, U1, Lead 144) ..... 19

Figure 25 SEM Micrograph of SnPb Soldered Sn TQFP-144 on Manufactured Test Vehicle (SN 30, U1, Lead 144) ..... 19

Figure 26 SEM Micrograph of SnPb Soldered Sn TQFP-144 on Manufactured Test Vehicle (SN 34, U1, Lead 144) ..... 20

Figure 27 SEM Micrograph of SnPb Soldered Sn TQFP-144 on Manufactured Test Vehicle (SN 34, U1, Lead 144) ..... 20

Figure 28 SEM Micrograph of SnPb Soldered Sn TQFP-144 on Manufactured Test Vehicle (SN 30, U1, Lead 144) ..... 21

Figure 29 EDS Spectra of SnPb Soldered Sn TQFP-144 on Manufactured Test Vehicle (SN 30, U1, Lead 144) ..... 21

Figure 30 SEM Micrograph of SnPb Soldered AuPdNi TQFP-208 on Manufactured Test Vehicle (SN 30, U57, Lead 104) ..... 22

Figure 31 SEM Micrograph of SnPb Soldered SnPb TSOP-50 on Manufactured Test Vehicle (SN 31, U24, Lead 1) ..... 23

Figure 32 SEM Micrograph of SnPb Soldered SnPb TSOP-50 on Manufactured Test Vehicle (SN 32 U26, left side) ..... 24

**JCAA/JG-PP Lead-Free Solder Project: Failure Analysis of Test Vehicles Subjected to Combined Environments Test**

**List of Figures**

Figure 33 SEM Micrograph of SnPb Soldered SnPb TSOP-50 on Manufactured Test Vehicle (SN 32 U26, left side) ..... 24

Figure 34 SEM Micrograph of SnPb Soldered SnPb TSOP-50 on Manufactured Test Vehicle (SN 32 U26, left side) ..... 25

Figure 35 SEM Micrograph of SnPb Soldered SnPb TSOP-50 on Manufactured Test Vehicle (SN 32 U26, left side) ..... 25

Figure 36 SEM Micrograph of SnAgCu Soldered SnPb BGA-225 on Manufactured Test Vehicle (SN 100, U5, Bump 15R) ..... 27

Figure 37 SEM Micrograph of SnAgCu Soldered SnPb BGA-225 on Manufactured Test Vehicle (SN 100, U5, Bump 15R) ..... 27

Figure 38 SEM Micrograph of SnAgCu Soldered SnAgCu BGA-225 on Manufactured Test Vehicle (SN 101, U55, Bump 1A) ..... 28

Figure 39 SEM Micrograph of SnAgCu Soldered SnAgCu BGA-225 on Manufactured Test Vehicle (SN Board 102, U6, Bump 14R) ..... 28

Figure 40 SEM Micrograph of SnAgCu Soldered SnPb CLCC-20 on Manufactured Test Vehicle (SN 99, U46, Lead 25) ..... 29

Figure 41 SEM Micrograph of SnAgCu Soldered SnPb CLCC-20 on Manufactured Test Vehicle (SN 99, U46, Lead 1) ..... 30

Figure 42 SEM Micrograph of SnAgCu Soldered SnPb CLCC-20 on Manufactured Test Vehicle (SN 99, U46, Lead 1) ..... 30

Figure 43 SEM Micrograph of SnAgCu Soldered SnAgCu CLCC-20 on Manufactured Test Vehicle (SN 101, U17, Lead 15) ..... 31

Figure 44 SEM Micrograph of SnAgCu Soldered Sn PDIP-20 on Manufactured Test Vehicle (SN 99, U11, Lead 1) ..... 32

Figure 45 SEM Micrograph of SnAgCu Soldered Sn PDIP-20 on Manufactured Test Vehicle (SN 99, U11, Lead 1) ..... 32

Figure 46 SEM Micrograph of SnAgCu Soldered Sn PDIP-20 on Manufactured Test Vehicle (SN 99, U11, Lead 1) ..... 33

Figure 47 EDS Spectra of SnAgCu Soldered Sn PDIP-20 on Manufactured Test Vehicle (SN 99, U11, Lead 1) ..... 33

Figure 48 SEM Micrograph of SnAgCu Soldered AuPdNi PDIP-20 on Manufactured Test Vehicle (SN 99, U23, Lead 1) ..... 34

Figure 49 EDS Spectra of SnAgCu Soldered AuPdNi PDIP-20 on Manufactured Test Vehicle (SN 99, U23, Lead 1) ..... 34

Figure 50 SEM Micrograph of SnAgCu Soldered AuPdNi PDIP-20 on Manufactured Test Vehicle (SN 99, U23, Lead 1) ..... 35

Figure 51 EDS Spectra of SnAgCu Soldered AuPdNi PDIP-20 on Manufactured Test Vehicle (SN 99, U23, Lead 1) ..... 35

Figure 52 SEM Micrograph of SnAgCu Soldered Sn PLCC-20 on Manufactured Test Vehicle (SN 102, U47, Lead 15) ..... 36

Figure 53 SEM Micrograph of SnAgCu Soldered Sn PLCC-20 on Manufactured Test Vehicle (SN 102, U47, Lead 15) ..... 36

Figure 54 SEM Micrograph of SnAgCu Soldered Sn TQFP-144 on Manufactured Test Vehicle (SN 101, U58, Lead 144) ..... 37

Figure 55 SEM Micrograph of SnAgCu Soldered AuPdNi TQFP-208 on Manufactured Test Vehicle (SN 101, U3, Lead 105) ..... 38

Figure 56 SEM Micrograph of SnAgCu Soldered AuPdNi TQFP-208 on Manufactured Test Vehicle (SN 103, U31, Lead 208) ..... 39

Figure 57 SEM Micrograph of SnAgCu Soldered AuPdNi TQFP-208 on Manufactured Test Vehicle (SN 101, U3, Lead 105) ..... 39

Figure 58 EDS Spectra of SnAgCu Soldered AuPdNi TQFP-208 on Manufactured Test Vehicle (SN 101, U3, Lead 105) ..... 39

Figure 59 SEM Micrograph of SnAgCu Soldered AuPdNi TQFP-208 on Manufactured Test Vehicle (SN 101, U3, Lead 105) ..... 40

**JCAA/JG-PP Lead-Free Solder Project: Failure Analysis of Test Vehicles Subjected to Combined Environments Test**

**List of Figures**

Figure 60 SEM Micrograph of SnAgCu Soldered AuPdNi TQFP-208 on Manufactured Test Vehicle (SN 101, U3, Lead 105) ..... 40

Figure 61 SEM Micrograph of SnAgCu Soldered SnPb TSOP-50 on Manufactured Test Vehicle (SN 99, U16, Lead 25) ..... 42

Figure 62 SEM Micrograph of SnAgCu Soldered SnCu TSOP-50 on Manufactured Test Vehicle (SN 100, U39, Lead 1) ..... 42

Figure 63 SEM Micrograph of SnAgCu Soldered SnPb TSOP-50 on Manufactured Test Vehicle (SN 101, U62, Lead 15) ..... 42

Figure 64 SEM Micrograph of SnAgCuBi Soldered SnAgCu BGA-225 on Manufactured Test Vehicle (SN 113, U4, Bump 1R) ..... 44

Figure 65 SEM Micrograph of SnAgCuBi Soldered SnAgCu BGA-225 on Manufactured Test Vehicle (SN 113, U4, Bump 1R) ..... 44

Figure 66 SEM Micrograph of SnAgCuBi Soldered SnAgCu BGA-225 on Manufactured Test Vehicle (SN 142, U55, Bump 15A) ..... 45

Figure 67 SEM Micrograph of SnAgCuBi Soldered SnAgCu BGA-225 on Manufactured Test Vehicle (SN 142, U55, Bump 15A) ..... 45

Figure 68 SEM Micrograph of SnAgCuBi Soldered SnAgCu BGA-225 on Manufactured Test Vehicle (SN 142, U55, Bump 15A) ..... 45

Figure 69 SEM Micrograph of SnAgCuBi Soldered SnPb BGA-225 on Manufactured Test Vehicle (SN 142, U56, Bump 1R) ..... 46

Figure 70 SEM Micrograph of SnAgCuBi Soldered SnPb BGA-225 on Manufactured Test Vehicle (SN 142, U2, Bump 1R) ..... 46

Figure 71 SEM Micrograph of SnAgCuBi Soldered SnPb CLCC-20 on Manufactured Test Vehicle (SN 113, U9, Lead 5) ..... 48

Figure 72 SEM Micrograph of SnAgCuBi Soldered SnPb CLCC-20 on Manufactured Test Vehicle (SN 113, U9, Lead 5) ..... 48

Figure 73 SEM Micrograph of SnAgCuBi Soldered SnPb CLCC-20 on Manufactured Test Vehicle (SN 141, U46, Lead 11) ..... 49

Figure 74 SEM Micrograph of SnAgCuBi Soldered SnAgCuBi CLCC-20 on Manufactured Test Vehicle (SN 141, U45, Lead 1) ..... 49

Figure 75 SEM Micrograph of SnAgCuBi Soldered Sn PLCC-20 on Manufactured Test Vehicle (SN 140, U54, Lead 10) ..... 50

Figure 76 SEM Micrograph of SnAgCuBi Soldered Sn PLCC-20 on Manufactured Test Vehicle (SN 140, U54, Lead 10) ..... 50

Figure 77 SEM Micrograph of SnAgCuBi Soldered Sn PLCC-20 on Manufactured Test Vehicle (SN 140, U54, Lead 10) ..... 51

Figure 78 EDS Spectra of SnAgCuBi Soldered Sn PLCC-20 on Manufactured Test Vehicle (SN 140, U54, Lead 10) ..... 51

Figure 79 SEM Micrograph of SnAgCuBi Soldered Sn TQFP-144 on Manufactured Test Vehicle (SN 139, U1, Lead 109) ..... 52

Figure 80 SEM Micrograph of SnAgCuBi Soldered AuPdNi TQFP-208 on Manufactured Test Vehicle (SN 139, U57, Lead 104) ..... 53

Figure 81 SEM Micrograph of SnAgCuBi Soldered AuPdNi TQFP-208 on Manufactured Test Vehicle (SN 142, U31, Lead 125) ..... 54

Figure 82 SEM Micrograph of SnAgCuBi Soldered AuPdNi TQFP-208 on Manufactured Test Vehicle (SN 142, U31, Lead 125) ..... 54

Figure 83 SEM Micrograph of SnAgCuBi Soldered AuPdNi TQFP-208 on Manufactured Test Vehicle (SN 142, U31, Lead 52) ..... 55

Figure 84 SEM Micrograph of SnAgCuBi Soldered SnPb TSOP-50 on Manufactured Test Vehicle (SN 141, U24, Lead 1) ..... 56

Figure 85 SEM Micrograph of SnAgCuBi Soldered SnCu TSOP-50 on Manufactured Test Vehicle (SN 142, U25, Lead 25) ..... 56

Figure 86 SEM Micrograph of SnAgCuBi Soldered SnCu TSOP-50 on Manufactured Test Vehicle (SN 142, U25, Lead 25) ..... 57

Figure 87	EDS Spectra of SnAgCuBi Soldered SnCu TSOP-50 on Manufactured Test Vehicle (SN 142, U25, Lead 25) .....	57
Figure 88	SEM Micrograph of SnCu Soldered Sn PDIP-20 on Manufactured Test Vehicle (SN 140, U51, Lead 10) .....	58
Figure 89	SEM Micrograph of SnCu Soldered AuPdNi PDIP-20 on Manufactured Test Vehicle (SN 142, U35, Lead 10) .....	59
Figure 90	SEM Micrograph of SnCu Soldered AuPdNi PDIP-20 on Manufactured Test Vehicle (SN 142, U35, Lead 10) .....	59
Figure 91	SEM Micrograph of SnCu Soldered Sn PDIP-20 on Manufactured Test Vehicle (SN 140, U51) .....	60
Figure 92	EDS Spectra of SnCu Soldered Sn PDIP-20 on Manufactured Test Vehicle (SN 140, U51) .....	60
Figure 93	SEM Micrograph of SnCu Soldered Sn PDIP-20 on Manufactured Test Vehicle (SN 140, U51) .....	61
Figure 94	EDS Spectra of SnCu Soldered Sn PDIP-20 on Manufactured Test Vehicle (SN 140, U51) .....	61
Figure 95	SEM Micrograph of Reworked AuPdNi TQFP-208 Soldered with Tin-Silver-Copper-Bismuth Solder Alloy on Rework Test Vehicles (SN 200, U57, Lead Left) .....	63
Figure 96	SEM Micrograph of Reworked AuPdNi TQFP-208 Soldered with Tin-Silver-Copper-Bismuth Solder Alloy on Rework Test Vehicles (SN 200, U57, Lead Left) .....	64
Figure 97	SEM Micrograph of Reworked AuPdNi TQFP-208 Soldered with Tin-Silver-Copper-Bismuth Solder Alloy on Rework Test Vehicles (SN 200, U57, Lead Left) .....	64
Figure 98	SEM Micrograph of Reworked AuPdNi TQFP-208 Soldered with Tin-Silver-Copper-Bismuth Solder Alloy on Rework Test Vehicles (SN 200, U57, Lead Left) .....	65
Figure 99	SEM Micrograph of Reworked AuPdNi TQFP-208 Soldered with Tin-Silver-Copper-Bismuth Solder Alloy on Rework Test Vehicles (SN 200, U57, Lead Right) .....	65
Figure 100	SEM Micrograph of Reworked AuPdNi TQFP-208 Soldered with Tin-Silver-Copper-Bismuth Solder Alloy on Rework Test Vehicles (SN 200, U57, Lead Right) .....	66
Figure 101	SEM Micrograph of Reworked AuPdNi TQFP-208 Soldered with Tin-Silver-Copper-Bismuth Solder Alloy on Rework Test Vehicles (SN 200, U57, left side lead, board interface).....	66
Figure 102	EDS Spectra of Reworked AuPdNi TQFP-208 Soldered with Tin-Silver-Copper-Bismuth Solder Alloy on Rework Test Vehicles (SN 200, U57, left side lead, board interface).....	66
Figure 103	SEM Micrograph of Reworked AuPdNi TQFP-208 Soldered with Tin-Silver-Copper-Bismuth Solder Alloy on Rework Test Vehicles (SN 200, U57, left side lead, component interface).....	67
Figure 104	EDS Spectra of Reworked AuPdNi TQFP-208 Soldered with Tin-Silver-Copper-Bismuth Solder Alloy on Rework Test Vehicles (SN 200, U57, left side lead, component interface).....	67
Figure 105	SEM Micrograph of Reworked AuPdNi TQFP-208 Soldered with Tin-Silver-Copper-Bismuth Solder Alloy on Rework Test Vehicles (SN 201, U57, Lead 20) .....	67
Figure 106	SEM Micrograph of Reworked AuPdNi TQFP-208 Soldered with Tin-Silver-Copper-Bismuth Solder Alloy on Rework Test Vehicles (SN 201, U57, Lead 20) .....	68
Figure 107	SEM Micrograph of Reworked AuPdNi TQFP-208 Soldered with Tin-Silver-Copper-Bismuth Solder Alloy on Rework Test Vehicles (SN 203, U3, Lead Left) .....	68
Figure 108	SEM Micrograph of Reworked AuPdNi TQFP-208 Soldered with Tin-Silver-Copper-Bismuth Solder Alloy on Rework Test Vehicles (SN 203, U3, board interface) .....	69
Figure 109	EDS Spectra of Reworked AuPdNi TQFP-208 Soldered with Tin-Silver-Copper-Bismuth Solder Alloy on Rework Test Vehicles (SN 203, U3, board interface) .....	69
Figure 110	SEM Micrograph of Reworked AuPdNi TQFP-208 Soldered with Tin-Silver-Copper-Bismuth Solder Alloy on Rework Test Vehicles (SN 203, U3, Lead Left) .....	69
Figure 111	SEM Micrograph of Reworked AuPdNi TQFP-208 Soldered with Tin-Silver-Copper-Bismuth Solder Alloy on Rework Test Vehicles (SN 203, U3, Lead Left) .....	70
Figure 112	SEM Micrograph of Reworked AuPdNi TQFP-208 Soldered with Tin-Silver-Copper-Bismuth Solder Alloy on Rework Test Vehicles (SN 203, U3, Lead Right) .....	70
Figure 113	SEM Micrograph of Reworked AuPdNi TQFP-208 Soldered with Tin-Silver-Copper-Bismuth Solder Alloy on Rework Test Vehicles (SN 204, U57, Lead 105) .....	71
Figure 114	SEM Micrograph of Reworked AuPdNi TQFP-208 Soldered with Tin-Silver-Copper-Bismuth Solder Alloy on Rework Test Vehicles (SN 204, U57, Lead 105) .....	71
Figure 115	SEM Micrograph of Reworked AuPdNi TQFP-208 Soldered with Tin-Silver-Copper-Bismuth Solder Alloy on Rework Test Vehicles (SN 204, U57, Lead 105) .....	72

Figure 116	EDS Spectra of Reworked AuPdNi TQFP-208 Soldered with Tin-Silver-Copper-Bismuth Solder Alloy on Rework Test Vehicles (SN 204, U57, Lead 105) .....	72
Figure 117	SEM Micrograph of Reworked AuPdNi TQFP-208 Soldered with Tin-Silver-Copper-Bismuth Solder Alloy on Rework Test Vehicles (SN 204, U57, Lead 105) .....	73
Figure 118	SEM Micrograph of Reworked AuPdNi TQFP-208 Soldered with Tin-Silver-Copper-Bismuth Solder Alloy on Rework Test Vehicles (SN 204, U57, Lead 105) .....	73
Figure 119	SEM Micrograph of Reworked AuPdNi TQFP-208 Soldered with Tin-Silver-Copper-Bismuth Solder Alloy on Rework Test Vehicles (SN 204, U57, Lead 105) .....	74
Figure 120	SEM Micrograph of SnPb Soldered SnPb CSP-100 Components on Hybrid Test Vehicles (SN 301, U36, Bump A) .....	76
Figure 121	SEM Micrograph of SnPb Soldered SnPb CSP-100 Components on Hybrid Test Vehicles (SN 301, U36, Bump A) .....	76
Figure 122	SEM Micrograph of SnPb Soldered SnPb CSP-100 Components on Hybrid Test Vehicles (SN 301, U36, Bump J) .....	76
Figure 123	SEM Micrograph of SnPb Soldered SnPb CSP-100 Components on Hybrid Test Vehicles (SN 301, U37, Bump D) .....	77
Figure 124	SEM Micrograph of SnPb Soldered SnPb CSP-100 Components on Hybrid Test Vehicles (SN 302, U60, Bump J) .....	77
Figure 125	SEM Micrograph of SnPb Soldered SnPb CSP-100 Components on Hybrid Test Vehicles (SN 302, U60, Bump J) .....	77
Figure 126	SEM Micrograph of SnPb Soldered SnPb CSP-100 Components on Hybrid Test Vehicles (SN 301, U36, Bump A) .....	78
Figure 127	SEM Micrograph of SnPb Soldered SnPb CSP-100 Components on Hybrid Test Vehicles (SN 301, U37, BUMP E) .....	78
Figure 128	EDS Spectra of SnPb Soldered SnPb CSP-100 Components on Hybrid Test Vehicles (SN 301, U37, BUMP E) .....	78
Figure 129	SEM Micrograph of SnPb Soldered SnPb CSP-100 Components on Hybrid Test Vehicles (SN 301, U36, BUMP A) .....	79
Figure 130	SEM Micrograph of SnPb Soldered SnPb Hybrid-30 Components on Hybrid Test Vehicles (SN 301, U50, Lead A) .....	80
Figure 131	SEM Micrograph of SnPb Soldered SnPb Hybrid-30 Components on Hybrid Test Vehicles (SN 301, U50, Lead A) .....	80
Figure 132	SEM Micrograph of SnPb Soldered SnPb Hybrid-30 Components on Hybrid Test Vehicles (SN 306, U50, Lead E) .....	80
Figure 133	SEM Micrograph of SnPb Soldered SnPb Hybrid-30 Components on Hybrid Test Vehicles (SN 305, U33, Lead C) .....	81
Figure 134	SEM Micrograph of SnPb Soldered SnPb Hybrid-30 Components on Hybrid Test Vehicles (SN 305, U33, Lead D) .....	81
Figure 135	SEM Micrograph of SnAgCu Soldered SnAgCu CSP-100 Components on Hybrid Test Vehicles (SN 325, U19, Bump A) .....	83
Figure 136	SEM Micrograph of SnAgCu Soldered SnAgCu CSP-100 Components on Hybrid Test Vehicles (SN 325, U19, Bump C) .....	83
Figure 137	SEM Micrograph of SnAgCu Soldered SnAgCu CSP-100 Components on Hybrid Test Vehicles (SN 325, U19, Bump G) .....	83
Figure 138	SEM Micrograph of SnAgCu Soldered SnAgCu Hybrid-30 Components on Hybrid Test Vehicles (SN 326, U32, Lead F) .....	84
Figure 139	SEM Micrograph of SnAgCu Soldered SnAgCu Hybrid-30 Components on Hybrid Test Vehicles (SN 326, U33, LEAD A) .....	85
Figure 140	EDS Spectra of SnAgCu Soldered SnAgCu Hybrid-30 Components on Hybrid Test Vehicles (SN 326, U33, LEAD A) .....	85
Figure 141	SEM Micrograph of SnAgCu Soldered SnAgCu Hybrid-30 Components on Hybrid Test Vehicles (SN 326, U32, LEAD A) .....	86
Figure 142	EDS Spectra of SnAgCu Soldered SnAgCu Hybrid-30 Components on Hybrid Test Vehicles (SN 326, U32, LEAD A) .....	86

Figure 143 SEM Micrograph of SnAgCuBi Soldered SnAgCu CSP-100 Components on Hybrid Test Vehicles (SN 333, U37, Bump A) ..... 88

Figure 144 SEM Micrograph of SnAgCuBi Soldered SnAgCu CSP-100 Components on Hybrid Test Vehicles (SN 333, U37, BUMP A) ..... 88

Figure 145 EDS Spectra of SnAgCuBi Soldered SnAgCu CSP-100 Components on Hybrid Test Vehicles (SN 333, U37, BUMP A)..... 88

Figure 146 SEM Micrograph of SnAgCuBi Soldered SnAgCuBi Hybrid-30 Components on Hybrid Test Vehicles (SN 332, U33, Lead A) ..... 90

Figure 147 SEM Micrograph of SnAgCuBi Soldered SnAgCuBi Hybrid-30 Components on Hybrid Test Vehicles (SN 332, U33, Lead B) ..... 90

Figure 148 SEM Micrograph of SnAgCuBi Soldered SnAgCuBi Hybrid-30 Components on Hybrid Test Vehicles (SN 336, U50, Lead A) ..... 91

Figure 149 SEM Micrograph of SnAgCuBi Soldered SnAgCuBi Hybrid-30 Components on Hybrid Test Vehicles (SN 336, U50, Lead B) ..... 91

Figure 150 SEM Micrograph of SnAgCuBi Soldered SnAgCuBi Hybrid-30 Components on Hybrid Test Vehicles (SN 336, U50, Lead E) ..... 91

Figure 151 SEM Micrograph of SnAgCuBi Soldered SnAgCuBi Hybrid-30 Components on Hybrid Test Vehicles (SN 337, U33, Lead A) ..... 92

Figure 152 SEM Micrograph of SnAgCuBi Soldered SnAgCuBi Hybrid-30 Components on Hybrid Test Vehicles (SN 337, U 33, Lead A) ..... 92

Figure 153 SEM Micrograph of SnAgCuBi Soldered SnAgCuBi Hybrid-30 Components on Hybrid Test Vehicles (SN 337, U50, Lead A) ..... 92

**List of Tables**

Table 1 Summary of Intermetallic Compound Thickness on Tin-Lead Solder Joints of BGA-225 Components on Manufactured Test Vehicles ..... 8

Table 2 Summary of Intermetallic Compound Thickness on Tin-Lead Solder Joints of CLCC-20 Components on Manufactured Test Vehicles ..... 9

Table 3 Summary of Intermetallic Compound Thickness on Tin-Lead Solder Joints of PDIP-20 Components on Manufactured Test Vehicles ..... 14

Table 4 Summary of Intermetallic Compound Thickness on Tin-Lead Solder Joints of PLCC-20 Components on Manufactured Test Vehicles ..... 17

Table 5 Summary of Intermetallic Compound Thickness on Tin-Lead Solder Joints of TQFP-144 Components on Manufactured Test Vehicles ..... 18

Table 6 Summary of Intermetallic Compound Thickness on Tin-Lead Solder Joints of TQFP-208 Components on Manufactured Test Vehicles ..... 22

Table 7 Summary of Intermetallic Compound Thickness on Tin-Lead Solder Joints of TSOP-50 Components on Manufactured Test Vehicles ..... 23

Table 8 Summary of Intermetallic Compound Thickness on Tin-Silver-Copper Solder Joints of BGA-225 Components on Manufactured Test Vehicles ..... 26

Table 9 Summary of Intermetallic Compound Thickness on Tin-Silver-Copper Solder Joints of CLCC-20 Components on Manufactured Test Vehicles ..... 29

Table 10 Summary of Intermetallic Compound Thickness on Tin-Silver-Copper Solder Joints of PDIP-20 Components on Manufactured Test Vehicles ..... 31

Table 11 Summary of Intermetallic Compound Thickness on Tin-Silver-Copper Solder Joints of PLCC-20 Components on Manufactured Test Vehicles ..... 35

Table 12 Summary of Intermetallic Compound Thickness on Tin-Silver-Copper Solder Joints of TQFP-144 Components on Manufactured Test Vehicles ..... 37

Table 13 Summary of Intermetallic Compound Thickness on Tin-Silver-Copper Solder Joints of TQFP-208 Components on Manufactured Test Vehicles ..... 38

Table 14 Summary of Intermetallic Compound Thickness on Tin-Silver-Copper Solder Joints of TSOP-50 Components on Manufactured Test Vehicles ..... 41

Table 15 Summary of Intermetallic Compound Thickness on Tin-Silver-Copper-Bismuth Solder Joints of BGA-225 Components on Manufactured Test Vehicles ..... 43

**JCAA/JG-PP Lead-Free Solder Project: Failure Analysis of Test Vehicles Subjected to Combined Environments Test**

**List of Tables**

Table 16	Summary of Intermetallic Compound Thickness on Tin-Silver-Copper-Bismuth Solder Joints of CLCC-20 Components on Manufactured Test Vehicles.....	47
Table 17	Summary of Intermetallic Compound Thickness on Tin-Silver-Copper-Bismuth Solder Joints of PLCC-20 Components on Manufactured Test Vehicles.....	49
Table 18	Summary of Intermetallic Compound Thickness on Tin-Silver-Copper-Bismuth Solder Joints of TQFP-144 Components on Manufactured Test Vehicles.....	52
Table 19	Summary of Intermetallic Compound Thickness on Tin-Silver-Copper-Bismuth Solder Joints of TQFP-208 Components on Manufactured Test Vehicles.....	53
Table 20	Summary of Intermetallic Compound Thickness on Tin-Silver-Copper-Bismuth Solder Joints of TSOP-50 Components on Manufactured Test Vehicles.....	55
Table 21	Summary of Intermetallic Compound Thickness on Tin-Copper Solder Joints of PDIP-20 Components on Manufactured Test Vehicles.....	58
Table 22	Summary of Intermetallic Compound Thickness on Reworked TQFP-208 Soldered with Tin-Silver-Copper-Bismuth Solder Alloy on Rework Test Vehicles.....	62
Table 23	Summary of Intermetallic Compound Thickness on Tin-Lead Solder Joints of CSP-100 Components on Hybrid Test Vehicles.....	75
Table 24	Summary of Intermetallic Compound Thickness on Tin-Lead Solder Joints of Hybrid-30 Components on Hybrid Test Vehicles.....	79
Table 25	Summary of Intermetallic Compound Thickness on Tin-Silver-Copper Solder Joints of CSP-100 Components on Hybrid Test Vehicles.....	82
Table 26	Summary of Intermetallic Compound Thickness on Tin-Silver-Copper Solder Joints of Hybrid-30 Components on Hybrid Test Vehicles.....	84
Table 27	Summary of Intermetallic Compound Thickness on Tin-Silver-Copper-Bismuth Solder Joints of CSP-100 Components on Hybrid Test Vehicles.....	87
Table 28	Summary of Intermetallic Compound Thickness on Tin-Silver-Copper-Bismuth Solder Joints of Hybrid-30 Components on Hybrid Test Vehicles.....	89
Table 29	List of Microsectioned Components on Manufactured Test Vehicles.....	99
Table 30	List of Microsectioned Components From Rework Test Vehicles.....	101
Table 31	List of Microsectioned Components From Hybrid Test Vehicles.....	102

## **Foreword**

The use of tin-lead solders in defense electronics manufacturing is threatened by environmental regulatory actions and free market forces. Although currently exempt from legislation, there is a concern that the use of lead in aerospace and military electronics may be banned in the future. Even with an exemption, aerospace and military electronics may still be impacted by the consumer electronics manufacturers' move to lead-free products. As more commercial electronics manufacturers move to lead-free technology to comply with the environmental regulation, aerospace and military programs will find it more difficult to procure electronic components fabricated with tin-lead solder. While work has been done to determine lead-free reliability for commercial electronic products, there has been little data published on the reliability of lead-free solders on high reliability, high performance military electronic products. In November 2000, a project was initiated by the Department of Defense (DoD) and a consortium of the DoD, National Aeronautics and Space Administration (NASA), and several defense electronics contractors was formed to evaluate lead-free solders to conduct solder joint reliability testing of lead-free solder alloys.

The combined environments test was one of several tests selected by the consortium to determine the reliability of lead-free solders under combined thermal cycle and vibration environmental exposures. The test was conducted from October 7, 2004 through June 3, 2005 using a QualMark Model OVS-4 HALT/HASS chamber located in the Raytheon Environmental Test Laboratory (ETL) in McKinney, Texas. The combined environments test was performed utilizing a temperature range of -55 to 125 degrees Celsius with 20 degree Celsius per minute temperature ramp. The dwell time at each temperature extreme was fifteen minutes. A ten  $g_{rms}$  pseudorandom vibration was applied during the last 10 minutes of both the cold and hot soaks. After 50 cycles, the vibration levels were incremented by 5  $g_{rms}$  and cycling was continued for an additional 50 cycles. This process was repeated until a significant number of solder joints failed or 55  $g_{rms}$  was reached. ETL personnel ran 15 test vehicles in the chamber at a time. The 45 test vehicles were tested in three different groups.

The test vehicle was a circuit card assembly designed per IPC-SM-785 and IPC-9701 to evaluate solder joint reliability. The test vehicle printed circuit board was designed with daisy-chained pads that are complementary to the daisy chain in the components. The test vehicles were assembled per ANSI/J-STD-001, Class 3 requirements by BAE Systems. There were three variations of the test vehicle; "manufactured", "rework" and "hybrid". The purpose of the "manufactured" test vehicle was to simulate the construction of current military circuit card assembly technology. The purpose of the "rework" test vehicle was to simulate the construction of older, legacy military circuit card assembly technology for testing the suitability of using lead-free solder in repairing older hardware built with tin-lead solder. The purpose of the "hybrid" test vehicle was to test the hybrid and CSP components.

The lead-free solder alloys tested were tin-silver-copper, tin-silver-copper-bismuth and tin-copper. The baseline solder alloy was eutectic tin-lead. Tin-silver-copper solder alloys are currently the leading choice of the electronics industry for lead-free solder. Tin-silver-copper-bismuth alloy was tested because bismuth has been shown to enhance the long-term thermal cycle reliability of solder joints. Tin-copper solder alloys are commonly used in wave solder applications by consumer electronics manufacturers.

The manufacture test vehicles were tested for 550 cycles. The rework test vehicles were only tested for 536 cycles because the chamber experienced an over temperature condition during cycle 537. The hybrid test vehicles were tested for 500 cycles.

ITB, Inc. contracted with Raytheon to conduct failure analysis of the test vehicles after they had been subjected to the combined environments test. Raytheon's Failure Analysis Laboratory (FAL) in McKinney, Texas conducted the failure analysis. This report summarizes the results of that failure analysis.

## **Summary**

Raytheon Materials and Process Engineering selected the components to be analyzed from each of the manufactured, rework and hybrid test vehicles. FAL microsectioned those components and analyzed the solder joints using a scanning electron microscope (SEM). Backscattered electron micrographs and secondary electron micrographs were taken of the samples. The SEM was used in conjunction with energy dispersive spectroscopy (EDS) for elemental analysis.

In general, solder joint cracks on BGA components were more prevalent near the component side interface, although some joints failed near the board side interface. The difference in cycles to fail relate to the component location on the board since the induced stress a component receives during CET will vary depending on its location on the board.

All the CLCC solder joint failures occurred as the result of cracks propagating through the bulk solder. Two components were missing that had SnAgCu solder and finish. Both parts appeared to have failed due to cracks extending through the bulk solder. Component U17 on board 142 with SnAgCuBi solder and finish failed after one cycle. No explanation of this early failure was found.

The PDIP-20 devices with SnCu solder and AuPdNi finish did not have cracks in the solder joints but had cracks identified in the PWB. The PDIP devices that exhibited early life failure failed through the solder whereas the devices with late failure had cracks through the board material.

Virtually, no cracks were present in the PLCC-20 solder joints. Of the three solder types examined, the SnAgCuBi solder appeared to be in the best condition. The most severe cracking was present in the SnPb solder with Sn finish joints. None of these devices had been identified as electrical failures.

With all types of solder, cracks were present in TQFP-144 solder joints to varying degrees of severity. In each type of metallurgy, at least one joint on a device cracked all the way through the solder.

All of the manufactured TQFP-208 leads evaluated were found to have partial cracks in the solder that extended varying distances into the solder bond. None of the solder bonds examined were found to be fractured completely through. There was a slight difference in the TQFP-208 components that were soldered with SnAgCuBi solder.

The U57 TQFP-208 devices soldered with SnAgCuBi on rework test vehicles had separation between the lead intermetallics and solder. The U3 TQFP-208 devices soldered with SnAgCuBi on rework test vehicles were missing due to the fracture of the joints. Microvoids were identified in the solder at the pad interface. The U3 devices failed very early in comparison to the U57 devices. This was most likely the result of poor wetting of the solder at the time of rework.

The TSOP components all appear to have failed as a result of crack propagation through the solder joint. The only significant difference noted between the different groups of TSOP components was the way the TSOPs utilizing the SnAgCuBi solder alloy and SnPb finish failed. It should be noted that the components were all missing from this particular group after test, therefore these conclusions are based on analysis of the remaining solder at the board pad interface only.

All of the CSP-100 devices examined had minor cracking in the PWB near the edges of the pad. Solder joints made of SnPb solder and SnPb finish had minor cracks in the solder on the PWB side of the joint. The devices with the SnAgCu solder and SnAgCu finish had solder joints with cracks that extended completely through the solder on the PWB side of the joint. Solder joints with the SnAgCuBi solder and SnAgCu finish had cracks that varied in severity, some of which extended completely through the solder on the board side of the joints. No differences were identified that could explain the difference between the early and late failures.

Of the Hybrid devices examined, all but one had cracks in the PWB. These cracks were minor and were located either at the edge of the pad on the PWB or at the edge of the solder mask. There was no trend with solder or finish to determine location of these minor cracks.

## **Introduction**

The use of conventional tin-lead solder in aerospace and military electronics manufacturing is being threatened today by environmental concerns and increasing regulations concerning lead. The regulations began with banning lead additives in gasoline and paint products. This pressure to reduce or remove lead is growing and has lead environmentalists and regulators to focus their attention on eliminating lead from electronics.

The use of tin-lead solders in defense electronics manufacturing is threatened by European, Asian and United States environmental regulatory actions and free market forces. The European Union has adopted legislation that governs the re-use and recycling of electronics waste known as the Waste from Electrical and Electronic Equipment (WEEE) Directive. In addition, Europe has begun implementing the Restriction of Hazardous Substances Directive (RoHS) that bans the use of lead and other substances starting on 1 July 2006. Japan has taken an active role in eliminating lead from consumer electronics with many major Japanese electronics companies announcing the move to lead-free electronics. The U.S. Environmental Protection Agency (EPA) has cited lead and lead compounds as one of the top seventeen chemicals imposing the greatest threat to human health. In implementing Executive Order 12856, the EPA has reduced the reporting threshold for lead and lead compounds to 100 pounds per year thereby increasing reporting by 13% at an estimated average report cost of \$23,700 per using facility. This reporting requirement has imposed an estimated added administrative burden of \$95 million to the electronics industry. Future U.S. regulatory action may ban all solders containing lead.

Although currently exempt from the European legislation, there is a concern that a legislative body may ban the use of lead in aerospace and military electronics. Even with an exemption, aerospace and military electronics will be impacted by the consumer electronics manufacturers' move to lead-free products. As more commercial electronics manufacturers move to lead-free technology to comply with the European legislation, aerospace and military programs will find it more difficult to procure electronic components fabricated with tin-lead solder. The commercial electronics sector is driving component and board suppliers to provide primarily lead-free surface finishes and alloys. Electronic component manufacturers are switching to lead-free lead finishes. Lead-free components are finding their way into aerospace and military electronics under government acquisition reform initiatives. It is possible that parts with lead-containing finishes may become impossible to procure or the acquisition costs for military grade lead-containing components will become prohibitive. The price of tin-lead solder may rise or the supplies of tin-lead solder may dwindle due to the lower market demand. The aerospace and military community may have little leverage once the lead-free movement gains momentum.

While work has been done to determine lead-free reliability for commercial general and dedicated service electronic products, there has been little comprehensive data published on the reliability of lead-free solders on high reliability, high performance electronic products. In November 2000, a project was initiated by the Department of Defense (DoD). A consortium was formed to evaluate lead-free solders and to determine whether they are suitable for use in high reliability electronics. The consortium consisted of a partnership between the DoD, National Aeronautics and Space Administration (NASA), and several defense electronics contractors to conduct solder joint reliability testing of lead-free solder alloys. The Joint Council on Aging Aircraft (JCAA) and the Joint Group on Pollution Prevention (JG-PP) managed the project.

ITB, Inc. contracted with Raytheon to conduct failure analysis of the test vehicles subjected to the combined environments test. Raytheon's Failure Analysis Laboratory (FAL) in McKinney, Texas conducted the failure analysis.

This report summarizes the results of that failure analysis.

## **Methods, Assumptions and Procedures**

### **Combined Environments Test**

The combined environments test (CET) was conducted in accordance with the Joint Test Protocol, "*Joint Test Protocol, J-01-EM-026-P1, for Validation of Alternatives to Eutectic Tin-Lead Solders used in Manufacturing and Rework of Printed Wiring Assemblies*" (Revised April 2004) by Raytheon Materials and Process Engineering.

## JCAA/JG-PP Lead-Free Solder Project: Failure Analysis of Test Vehicles Subjected to Combined Environments Test Methods, Assumptions and Procedures

and Raytheon Environmental Test Laboratory (ETL). The purpose of the CET was to determine the reliability of solders under combined thermal cycle and vibration environmental exposures. The combined environments test was based on MIL-STD-810F, Method 520.2 and a modified Highly Accelerated Life Test (HALT), a process in which products are subjected to accelerated environments to find weak links in the design and manufacturing process. The project stakeholders felt that the combined environments test would provide a quick method to identify comparative reliability differences between the lead-free solder alloys against the eutectic tin-lead solder baseline.

### ***HALT Chamber***

The CET was conducted using a QualMark Model OVS-4 HALT/HASS chamber. The chamber is located in the Raytheon ETL in McKinney, Texas. A photograph of the chamber is provided in Figure 1. The chamber utilizes liquid nitrogen for cooling and nichrome heater elements for heating. The chamber has thermal capability ranges from -100 to 200 degrees Celsius with ramp rates of up to 60 degrees Celsius per minute. The pseudorandom vibration spectra are generated by pneumatically driven vibrators attached to the bottom of the table with maximum levels of 60  $g_{rms}$  and six degrees of freedom (X, Y, & Z axes with rotation in each axis simultaneously). The thermal and vibration environments can be applied separately or combined.



**Figure 1** QualMark Model OVS-4 HALT/HASS Chamber

### ***Test Profile***

The CET was performed utilizing a temperature range of -55 to 125 degrees Celsius with 20 degree Celsius per minute temperature ramp. The dwell times at each temperature extreme consisted of a six-minute temperature stabilization time plus a 15-minute soak. A 10  $g_{rms}$  pseudorandom vibration was applied for the last ten minutes of the cold and hot soaks. The test profile is graphically represented in Figure 2. Testing was continued until sufficient solder joint failure data was generated to obtain statistically significant Weibull plots indicating relative solder joint reliability. If significant failure rates were not evident after 50 cycles, the vibration levels were incremented by 5  $g_{rms}$  and cycling was continued for an additional 50 cycles. This process was repeated until a significant number of solder joints failed or 55  $g_{rms}$  was reached. During cycle 501 through 550, vibration stress was applied continuously at 55  $g_{rms}$  during the thermal cycle. The test was stopped after 550 cycles.

# JCAA/JG-PP Lead-Free Solder Project: Failure Analysis of Test Vehicles Subjected to Combined Environments Test Methods, Assumptions and Procedures

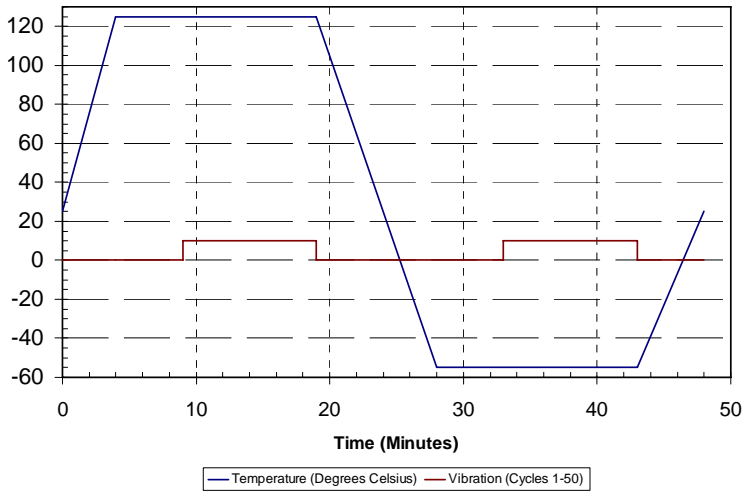


**Figure 2** Initial Combined Environments Test Profile

## Test Execution

A quality control inspector from McKinney Circuit Card Assembly inspected the test vehicles to J-STD-001, Class 3 requirements. Ribbon cables were manually soldered to the test vehicle P1 and P2 plated-through holes using eutectic tin-lead solder. Epoxy adhesive was used to bond the ribbon cables to the test vehicles to provide strain relief to the cables.

ETL personnel ran 15 test vehicles in the chamber at a time. The test vehicles were tested in three different groups. Manufactured test vehicles were tested first, and then the rework test vehicles and the hybrid test vehicles were tested last. ETL fabricated aluminum holding fixtures that held nine test vehicles in the first level and six test vehicles on the second level (see Figure 3). The test vehicles were loaded in the fixture in random documented order.



**Figure 3** Test Vehicle Layout in Test Chamber

## Microsection

Microsectioning is a destructive technique performed to discover and document the materials and processes used to manufacture components, down to sub-micron features. This allows for the discovery of flaws and/or other mechanisms, which cause component failure.

## JCAA/JG-PP Lead-Free Solder Project: Failure Analysis of Test Vehicles Subjected to Combined Environments Test Methods, Assumptions and Procedures

The first step in microsectioning is to select the plane in the sample through which the area of interest may be exposed. A cut is then made in the sample, parallel to this area, and then mounted in an epoxy resin. This captures the sample, helping to ensure planarity and prevent any additional damage from occurring. The potted sample is then ground with ever-finer abrasives until the area to be examined is reached.

Analysis of this microsectioned surface can then be accomplished using various techniques such as optical and electron microscopy and energy dispersive spectroscopy.



**Figure 4** Microsection Laboratory (Part of Raytheon Failure Analysis Laboratory Located in McKinney, Texas)

### Scanning Electron Microscopy (SEM) / Energy Dispersive Spectroscopy (EDS)

A Field Emission Scanning Electron Microscope (FE-SEM) is a tool capable of high resolution imaging on the nanometer scale. Magnifications as high as 500,000x are obtainable. Imaging is a necessary technique in the failure analysis of components and assemblies.

The system used for this analysis is the Carl Zeiss SMT 1550 VP-SEM (see Figure 5). Backscattered electron micrographs and secondary electron micrographs were taken of the samples. The backscattered electron micrographs indicate atomic number information while the secondary electron micrographs give topographical information. The microsections were coated with a conductive coating of either iridium or gold prior to imaging to provide a conductive path to ground. A path to ground is necessary for the best imaging capabilities.



**Figure 5** Carl Zeiss SMT 1550 VP-SEM

The SEM was used in conjunction with energy dispersive spectroscopy (EDS) for elemental analysis. The INCA 300 Si detector EDS was utilized for phase and intermetallic identification for this study.

EDS can qualitatively and quantitatively determine elemental information. A spectrum is acquired in the area of interest. When a beam is focused on the sample, x-rays are generated laterally and vertically in the sample. The region from which the x-rays are detected is referred to as the excitation volume. The excitation volume is directly related to the density of the material present and acceleration voltage.

EDS is limited to detecting elements boron and above in the periodic table. Boron can only be detected if the concentration is high enough. Trace elements cannot be detected by this method. Detection limits are material dependent, but for the most part, a concentration of 0.2-percent by weight and above can be seen. In some instances, there is overlap of elements making detection difficult under certain circumstances. For example, the major peaks of bismuth (Bi) and lead (Pb) overlap. If bismuth concentration is too low in comparison to the lead concentration, the bismuth cannot be identified.

## **Results and Discussion**

### **Manufactured Test Vehicles Results and Discussion**

The manufacture test vehicles were exposed to combined environments testing for 550 cycles. A number of solder joint failures were detected at ten cycles or lower deemed to be outliers and excluded from analysis by team consensus. The team felt these early life failures were due to manufacturing or testing anomalies and the data should be excluded to prevent skewing the test results. The test vehicles were inspected for lead damage. No apparent broken leads were observed during post-test inspection at 30x magnification using a binocular microscope. The solder joint failure data were analyzed and reported in August 2005.<sup>1</sup>

Raytheon Materials & Process Engineering selected the components to be microsectioned and is tabulated in Table 29 on page 99. The components analyzed included the early life failures, good (failure free) components, missing components (fell off during the test), and components with different component finish and solder alloy combinations. The SEM/EDS results are segregated by the solder alloy and component type in the following sections.

---

<sup>1</sup> Jeff Bradford, Joe Felty, and Bill Russell, JCAA/JG-PP Lead-Free Solder Project: Combined Environments Test, 2005.

**Tin-Lead Solder**

*BGA-225*

**Table 1** Summary of Intermetallic Compound Thickness on Tin-Lead Solder Joints of BGA-225 Components on Manufactured Test Vehicles

SN	REFDES	Lead Finish	Lead	IMC Thickness, IC (um)	IMC Thickness, PWB (um)	IMC at IC	IMC at PWB	Observations
30	U55	SnPb	1	1.141 4.688	2.769 3.568	NiSn & *CuSn	CuSn	Minor cracking in solder on component side. Bumps 2 and 3 similar in appearance.
30	U55	SnPb	8	827.2nm 2.390	1.704 3.337	NiSn & *CuSn	CuSn	No cracking in solder joint. Notches occurring in solder bumps, no cracks. Other bumps have a similar appearance.
30	U55	SnPb	16	2.153 2.422	1.747 4.527	NiSn & *CuSn	CuSn	No cracking in solder joint.
32	U43	SnPb	16	701.2nm 1.895	2.128 3.745	NiSn & *CuSn	CuSn	Minor cracking in solder at upper left and right corners and lower left corner.
32	U43	SnPb	1	1.413 2.609	2.340 3.594	NiSn & *CuSn	CuSn	Crack extends all the way through the solder on component side. Some have cracks on PWB side. Most bumps have cracking to some extent.
32	U43	SnPb	8	638.3nm 1.572	1.855 2.922	NiSn & *CuSn	CuSn	Minor cracking at the component side interface.

\* Note the copper (Cu) at the component side interface is the result of Cu migrating from the board side to the component side during reflow.

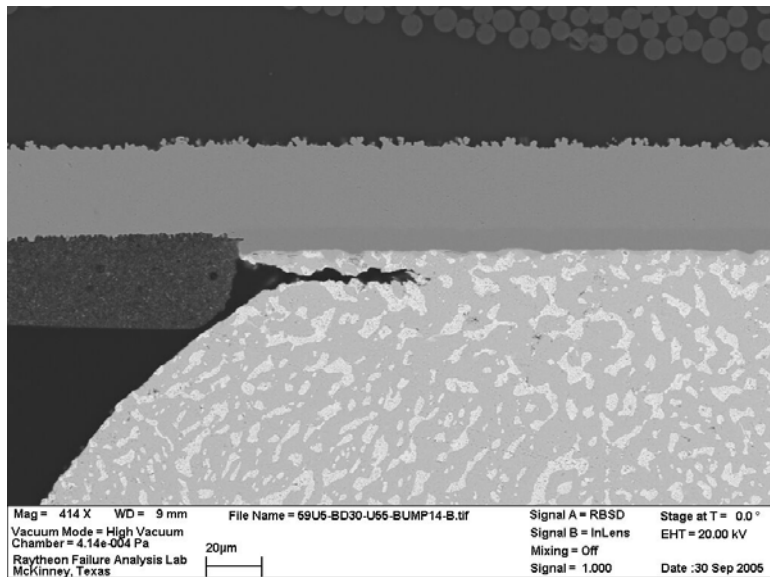


**Figure 6** SEM Micrograph of SnPb Soldered SnPb BGA-225 on Manufactured Test Vehicle (SN 30, U55, Bump 14) Minor cracking is present in the solder. There is again some evidence of work hardening in the solder. The cracks identified in the BGA samples do not extend all the way through the solder.

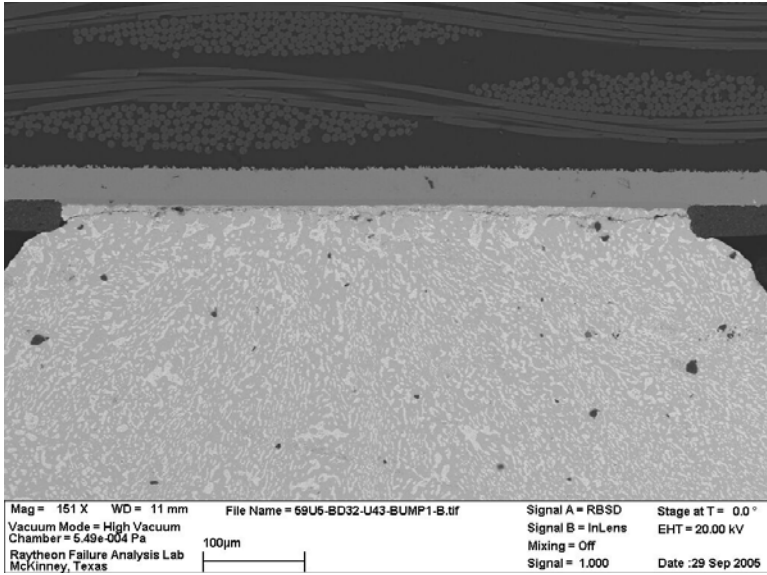


**Figure 7** SEM Micrograph of SnPb Soldered SnPb BGA-225 on Manufactured Test Vehicle (SN 32 U43, Bump 1) Crack through the solder near the component interface.

*CLCC-20*

**Table 2** Summary of Intermetallic Compound Thickness on Tin-Lead Solder Joints of CLCC-20 Components on Manufactured Test Vehicles

SN	REFDES	Lead Finish	Lead	IMC Thickness, IC (um)	IMC Thickness, PWB (um)	IMC at IC	IMC at PWB	Observations
31	U22	SnPb	16	795.7nm 2.577	1.255 3.040	NiSn Some Cu	CuSn	Crack in solder below component. Crack initiates on inside portion of joint below component. Voiding present.
31	U22	SnPb	1	1.358	1.920 3.607	NiSn Some Cu	CuSn	Crack extends all the way through the solder joint.
31	U46	SnPb	11	753.4nm 1.449	1.683 2.996	NiSn Some Cu	CuSn	Crack in solder on underside of component extends into fillet. Large void below in solder below component.
31	U46	SnPb	6	734.8nm 2.067	1.037 2.829	NiSn Some Cu	CuSn	Crack extends all the way through the solder.

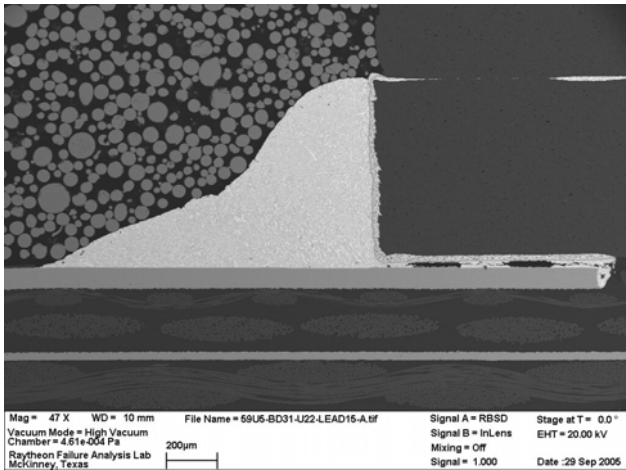


**Figure 8** SEM Micrograph of SnPb Soldered SnPb CLCC-20 on Manufactured Test Vehicle (SN 31, U22, Lead 16) Crack propagating from inside of solder joint below component. Some voiding present in this area as well. The joint is not cracked all the way through the solder.

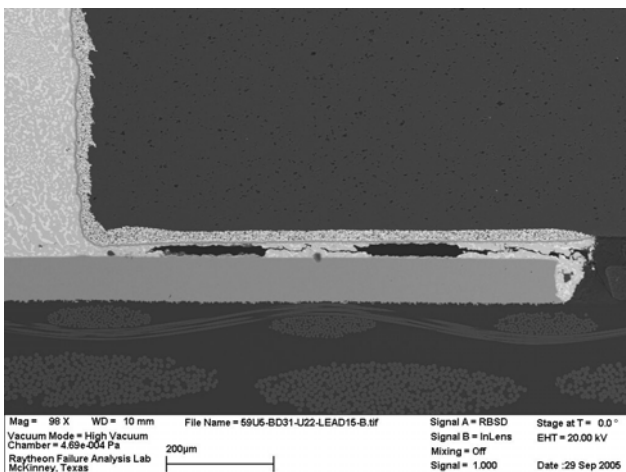


**Figure 9** SEM Micrograph of SnPb Soldered SnPb CLCC-20 on Manufactured Test Vehicle (SN 31, U22, Lead 16) Higher magnification view of solder joint seen in the previous image.

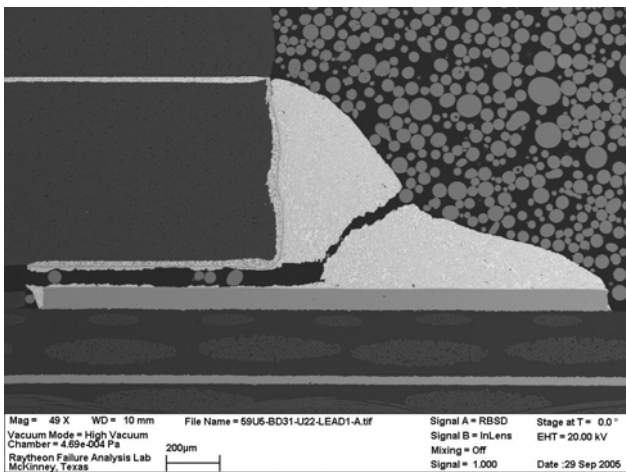


**Figure 10** SEM Micrograph of SnPb Soldered SnPb CLCC-20 on Manufactured Test Vehicle (SN 31, U22, Lead 1) Crack propagates all the way through the joint. See the EDS elemental data of the solder to board and component interfaces in Figure 11, Figure 12, Figure 13, and Figure 14.

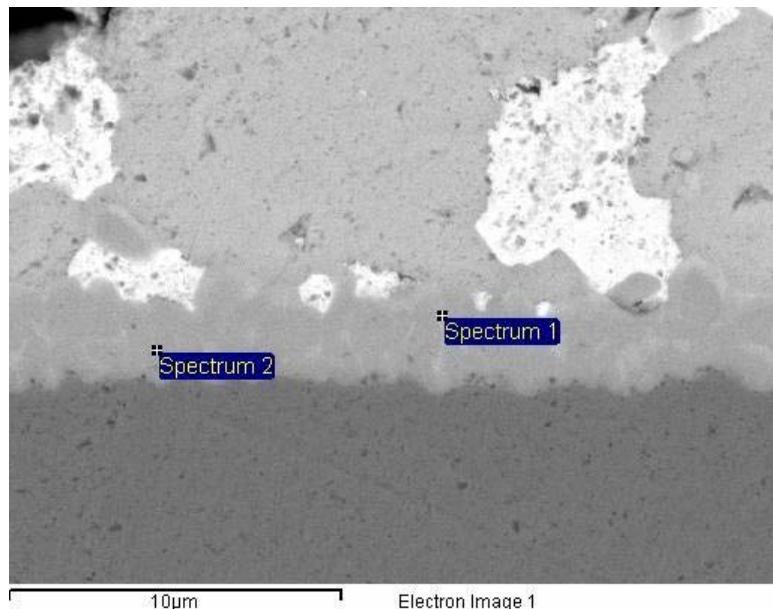


**Figure 11** SEM Micrograph of SnPb Soldered SnPb CLCC-20 on Manufactured Test Vehicle (SN 31, U22, Lead 1) Solder to board interface, the IMC is CuSn, however some phases of AuSn are also present.

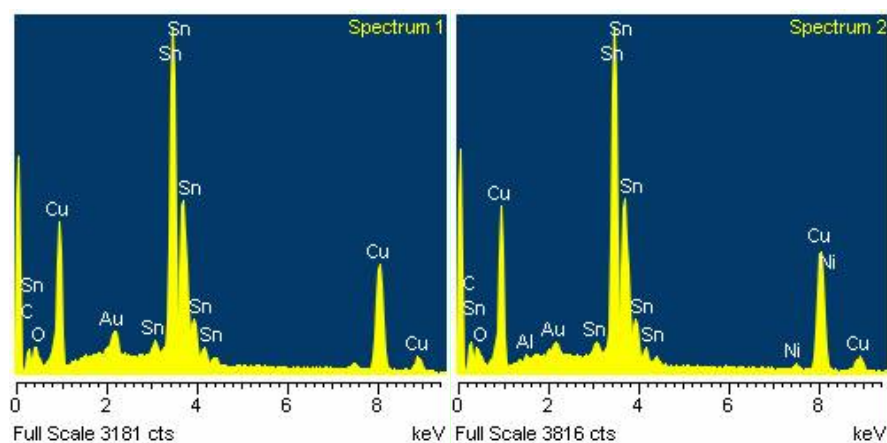


**Figure 12** EDS Spectra of SnPb Soldered SnPb CLCC-20 on Manufactured Test Vehicle (SN 31, U22, Lead 1) CuSn intermetallic zone at the board interface. Some phases of AuSn are also present.

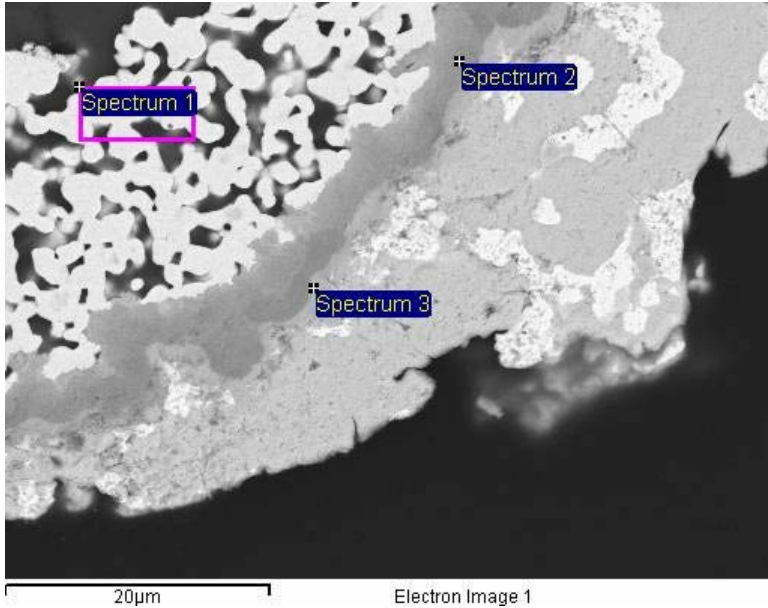


**Figure 13** SEM Micrograph of SnPb Soldered SnPb CLCC-20 on Manufactured Test Vehicle (SN 31, U22, Lead 1) Solder to component interface

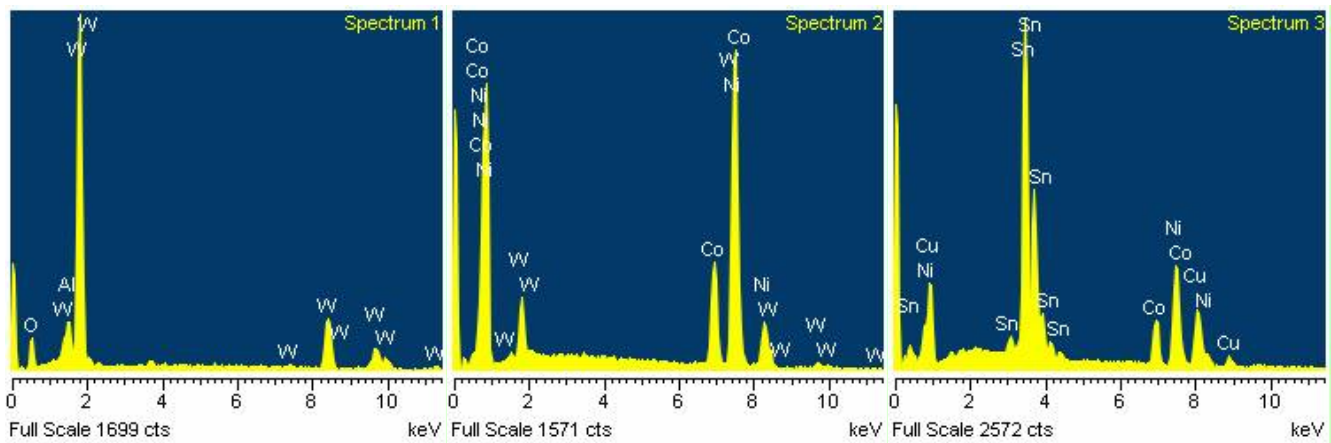


**Figure 14** EDS Spectra of SnPb Soldered SnPb CLCC-20 on Manufactured Test Vehicle (SN 31, U22, Lead 1) Solder to component interface, Spectrum 1 indicates a tungsten (W) thickfilm; Spectrum 2 is a nickel-cobalt (Ni/Co) layer; Spectrum 3 indicates a nickel-tin (Ni/Sn) intermetallic compound zone. The data also suggest some copper (Cu) has migrated from the board to the component interface.

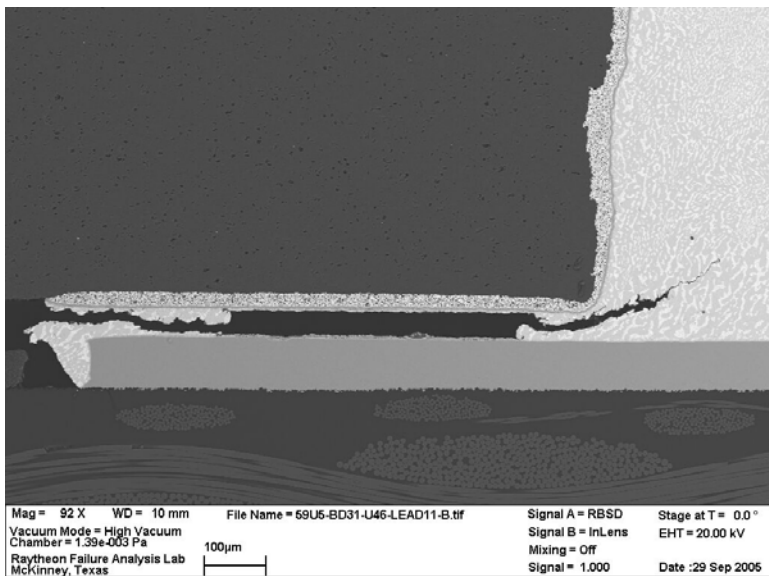


**Figure 15** SEM Micrograph of SnPb Soldered SnPb CLCC-20 on Manufactured Test Vehicle (SN 31, U46, Lead 11) Crack does not extend through the solder joint. There appears to be some voiding in the solder below the component.

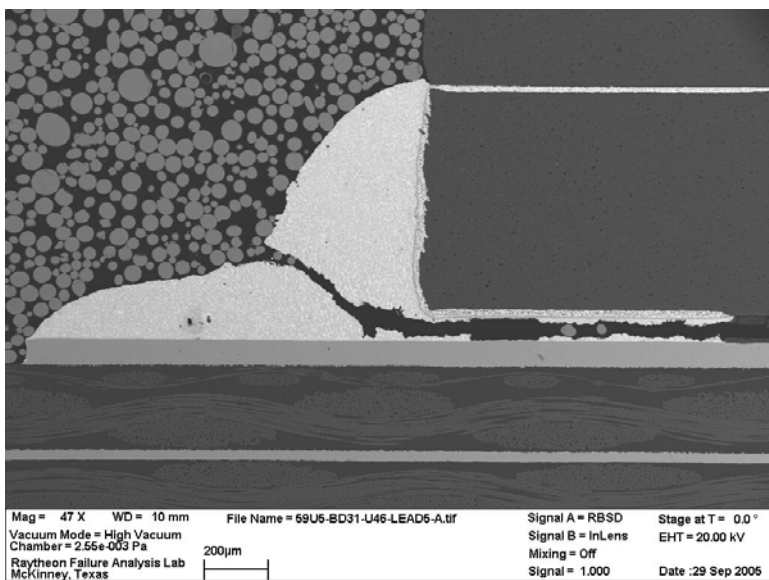


**Figure 16** SEM Micrograph of SnPb Soldered SnPb CLCC-20 on Manufactured Test Vehicle (SN 31, U46, Lead 5) Cracks propagate through entire joint.

PDIP-20

**Table 3** Summary of Intermetallic Compound Thickness on Tin-Lead Solder Joints of PDIP-20 Components on Manufactured Test Vehicles

SN	REFDES	Lead Finish	Lead	IMC Thickness, Lead Side (um)	IMC Thickness, Board Side (um)	IMC at IC	IMC at PWB	Observations
31	U30	Sn	10	1.619 2.916	1.670 1.991	CuSn	NiSn Cu	Crack in solder on both sides of lead and board. Crack extends a significant distance along lead. Voiding present, minor cracks in PWB. Other leads similar in appearance.
31	U30	Sn	1	1.282 2.083	1.219 2.956	CuSn	NiSn Cu	Crack in solder on both sides of lead near PWB to solder interface on both sides of PWB. Voiding present.
31	U30	Sn	5	1.035 3.264	1.582 2.316	CuSn	NiSn Cu	Crack in solder on both sides of lead near PWB to solder interface on both sides of PWB. Voiding present.
34	U49	AuPdNi	10	310.2nm 756.1nm	1.446 3.011	CuSn	NiSn Cu	Crack in solder on both sides of lead near PWB to solder interface, both sides of PWB. Severe in some areas. *
34	U49	AuPdNi	1	434.8nm 1.228	1.217 2.757	CuSn	NiSn Cu	Crack in solder on both sides of lead near PWB to solder interface, both sides of PWB. Voiding present. *
34	U49	AuPdNi	5	531.1nm 1.953	1.030 2.576	CuSn	NiSn Cu	Crack in solder on both sides of lead near PWB to solder interface, both sides of PWB. Voiding present. *
34	U59	AuPdNi	10	480.0nm 663.6nm	1.158 1.999	CuSn	NiSn Cu	Crack in solder on both sides of lead near PWB to solder interface, both sides of PWB. Voiding present. *
34	U59	AuPdNi	1	371.0nm 514.4nm	903.7nm 2.405	CuSn	NiSn Cu	Crack in solder on both sides of lead near PWB to solder interface, both sides of PWB. Voiding present. *
34	U59	AuPdNi	5	409.0nm 690.9nm	1.205 2.347	CuSn	NiSn Cu	Crack in solder on both sides of lead near PWB to solder interface, both sides of PWB. Voiding present. *

\* Cracks did not extend all the way through the hole. Crack does not account for electrical failure. Minor cracking in PWB.

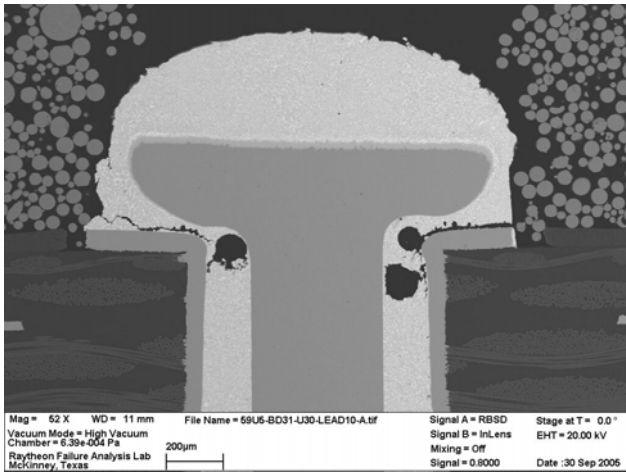


**Figure 17** SEM Micrograph of SnPb Soldered Sn PDIP-20 on Manufactured Test Vehicle (SN 31, U30, Lead 10) Crack in solder on both sides of lead and board. Crack extends a significant distance along lead. Voiding is present in the solder in the area of cracking. Other leads similar in appearance.

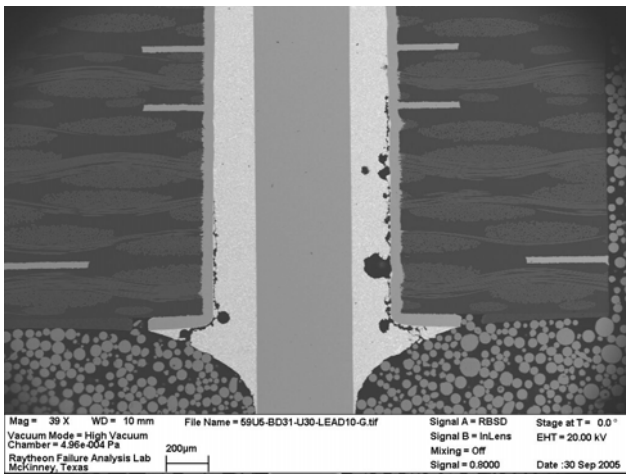


**Figure 18** SEM Micrograph of SnPb Soldered Sn PDIP-20 on Manufactured Test Vehicle (SN 31, U30, Lead 10) Opposite side of board also has cracking nearest the PWB interface. Voiding is also present.

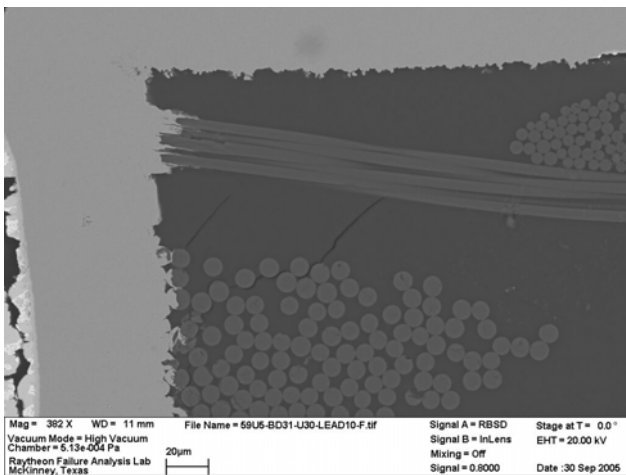


**Figure 19** SEM Micrograph of SnPb Soldered Sn PDIP-20 on Manufactured Test Vehicle (SN 31, U30, Lead 10) Minor cracks in PWB.

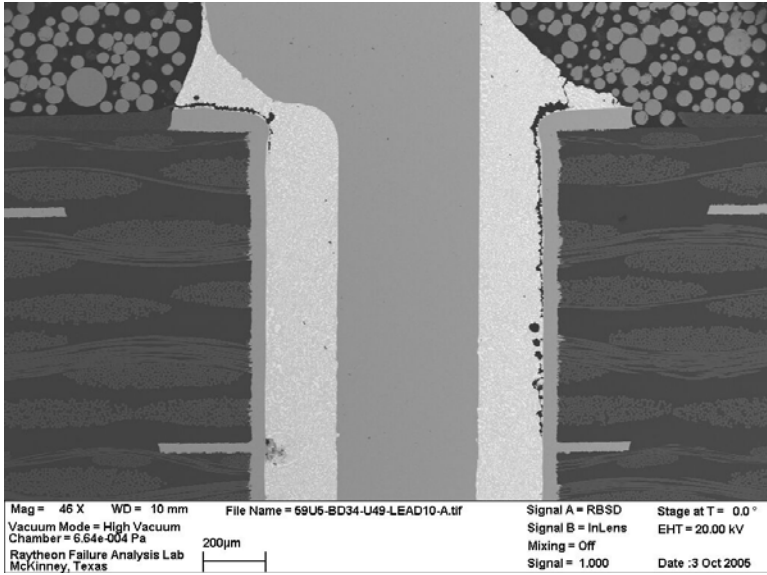


**Figure 20** SEM Micrograph of SnPb Soldered Sn PDIP-20 on Manufactured Test Vehicle (SN 34, U49, Lead 10) The cracks in the solder are near the board feedthrough interface.

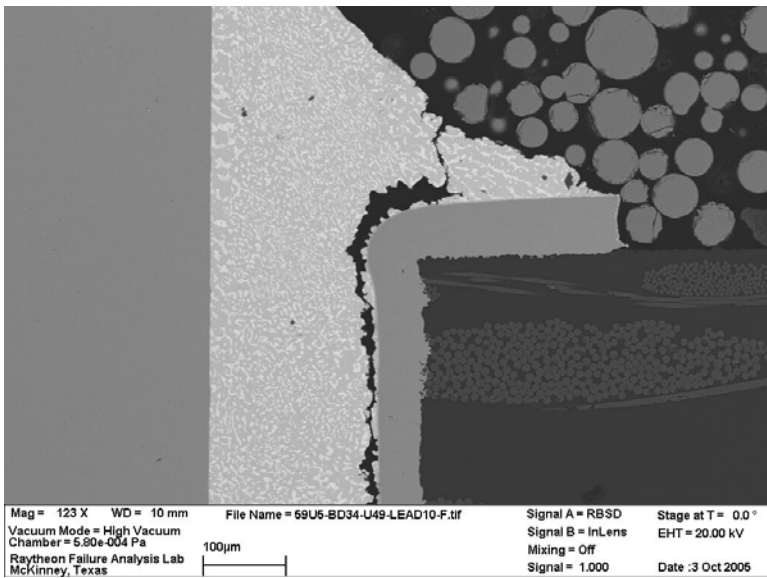


**Figure 21** SEM Micrograph of SnPb Soldered AuPdNi PDIP-20 on Manufactured Test Vehicle (SN 34, U49, Lead 10)

PLCC-20

**Table 4** Summary of Intermetallic Compound Thickness on Tin-Lead Solder Joints of PLCC-20 Components on Manufactured Test Vehicles

SN	REFDES	Lead Finish	Lead	IMC Thickness, Lead Side (um)	IMC Thickness, Board Side (um)	IMC at IC	IMC at PWB	Observations
32	U28	Sn	10	1.213 2.048	1.373 2.354	CuSn	CuSn	No cracks.
32	U28	Sn	16	1.008 2.575	1.153 2.210	CuSn	CuSn	Crack in solder near lead interface extends about $\frac{3}{4}$ of the way through the joint. Small crack near outer edge of fillet.
34	U27	Sn	16	1.415 2.937	1.336 3.073	CuSn	CuSn	Slightly cracked through solder.
34	U27	Sn	1	1.279 2.898	1.394 3.080	CuSn	CuSn	Minor crack through solder on PWB side.

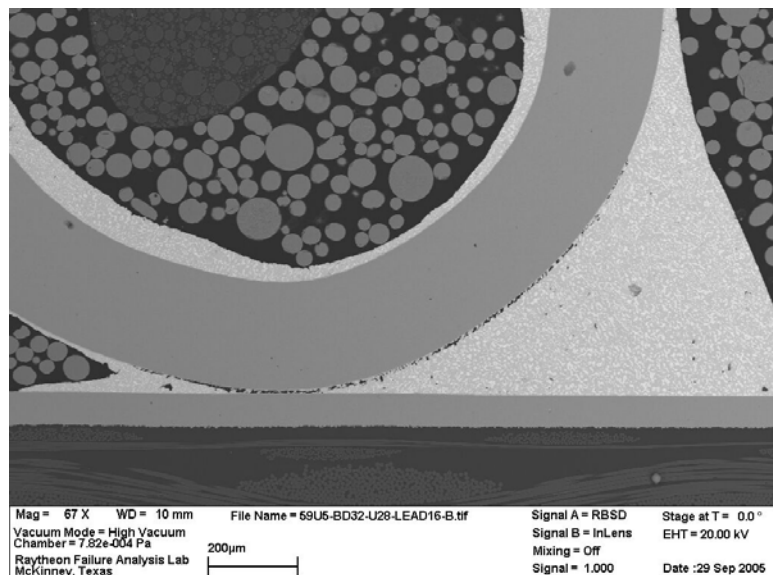


**Figure 22** SEM Micrograph of SnPb Soldered Sn PLCC-20 on Manufactured Test Vehicle (SN 32, U28, Lead 16) Crack in solder near the lead interface extends about  $\frac{3}{4}$  of the way through the joint, also a small crack near outer edge of fillet.

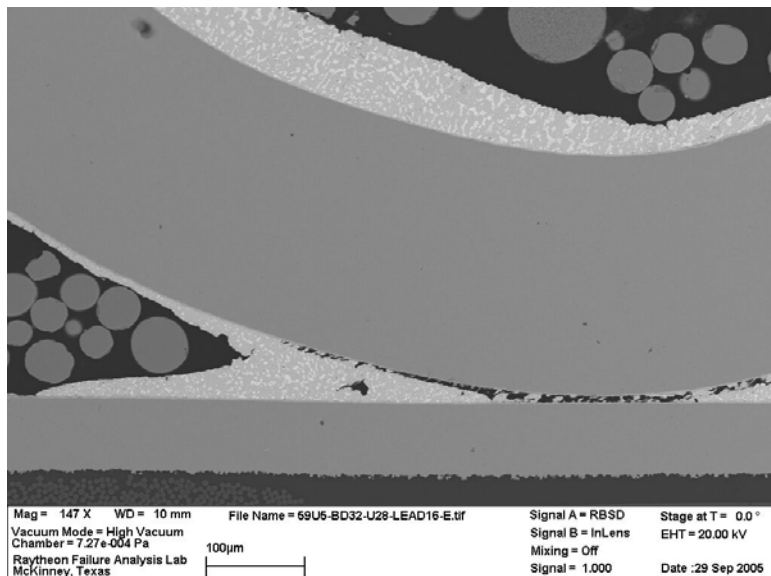


**Figure 23** SEM Micrograph of SnPb Soldered Sn PLCC-20 on Manufactured Test Vehicle (SN 32, U28, Lead 16) Closer view of crack near the lead interface.

*TQFP-144*

**Table 5** Summary of Intermetallic Compound Thickness on Tin-Lead Solder Joints of TQFP-144 Components on Manufactured Test Vehicles

SN	REFDES	Lead Finish	Lead	IMC Thickness, IC (um)	IMC Thickness, PWB (um)	IMC at IC	IMC at PWB	Observations
30	U1	Sn	Lead 144	643.7nm 2.974	1.457 2.331	CuSn	CuSn	Minor cracking in joint on underside of lead.
30	U1	Sn	Lead 37	1.048 3.669	949.2nm 2.413	CuSn	CuSn	Minor cracking in joint on underside of lead.
34	U1	Sn	Lead 144	1.240 4.592	1.236 2.474	CuSn	CuSn	Cracked all the way through solder on lead side.
34	U1	Sn	Lead 37	1.657 3.312	1.373 2.560	CuSn	CuSn	Cracked half way through solder joint on lead side at heel. Slightly cracked through solder at toe.

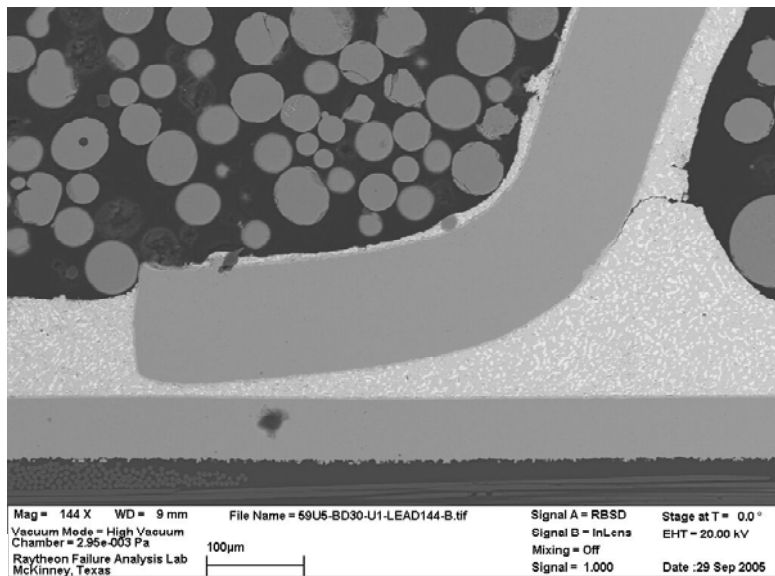


**Figure 24** SEM Micrograph of SnPb Soldered Sn TQFP-144 on Manufactured Test Vehicle (SN 30, U1, Lead 144) Cracking is present in the solder joint. The joint is not cracked all the way through the solder. See the EDS data in Figure 28 and Figure 29 providing elemental analysis information on this solder joint metallurgy.

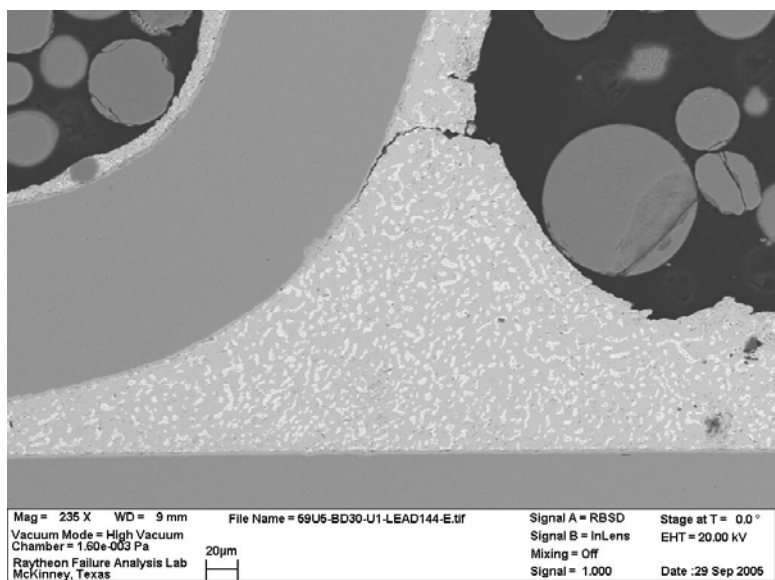


**Figure 25** SEM Micrograph of SnPb Soldered Sn TQFP-144 on Manufactured Test Vehicle (SN 30, U1, Lead 144) Heel region showing the partial solder crack.

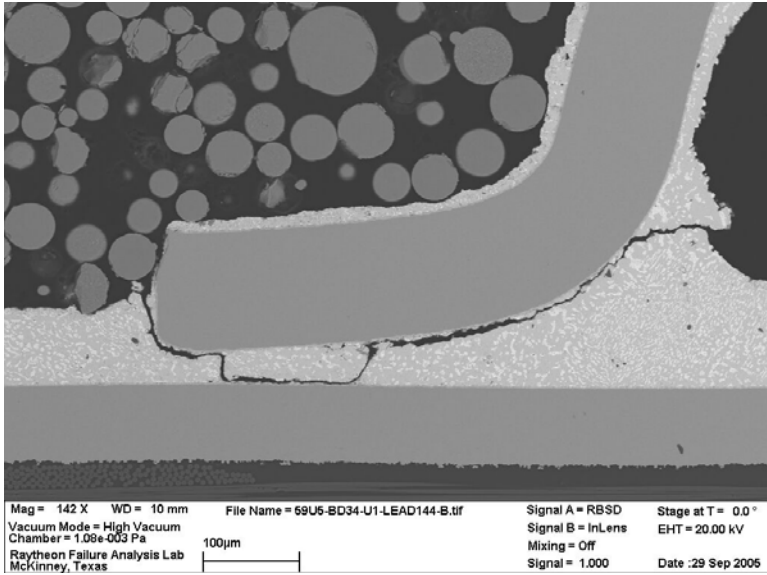


**Figure 26** SEM Micrograph of SnPb Soldered Sn TQFP-144 on Manufactured Test Vehicle (SN 34, U1, Lead 144) The solder joint is cracked through the solder.

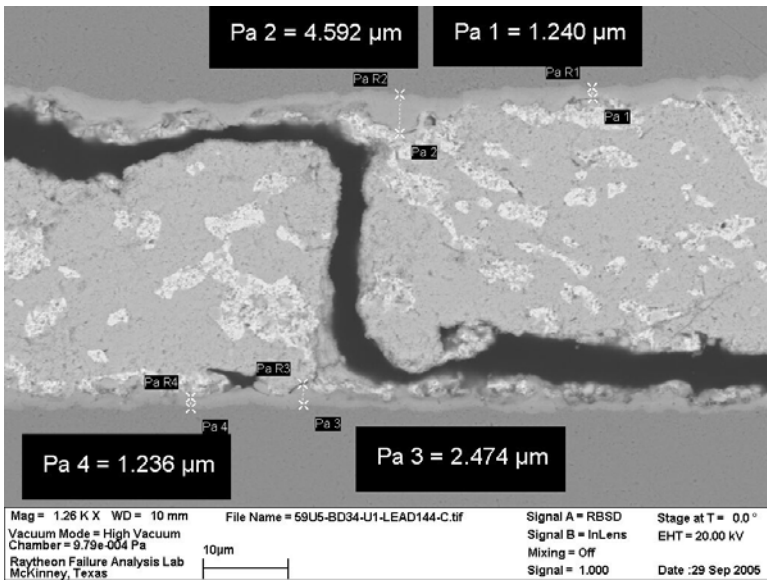


**Figure 27** SEM Micrograph of SnPb Soldered Sn TQFP-144 on Manufactured Test Vehicle (SN 34, U1, Lead 144) Intermetallic measurements at the component lead and board pad interfaces. The crack is through the solder not the intermetallic layer.

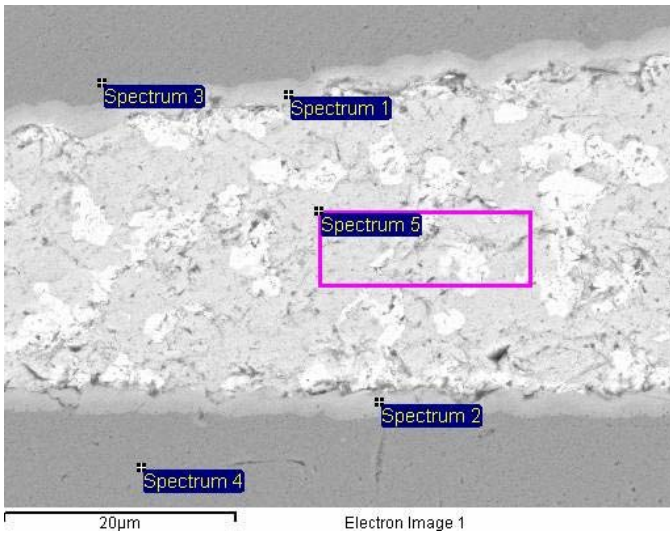


**Figure 28** SEM Micrograph of SnPb Soldered Sn TQFP-144 on Manufactured Test Vehicle (SN 30, U1, Lead 144) EDS elemental analysis indicates the lead and board pad are both copper (Cu). The intermetallic (IMC) layer at the component lead is CuSn; the board pad interface IMC is also CuSn. The solder was confirmed to be tin-lead (SnPb).

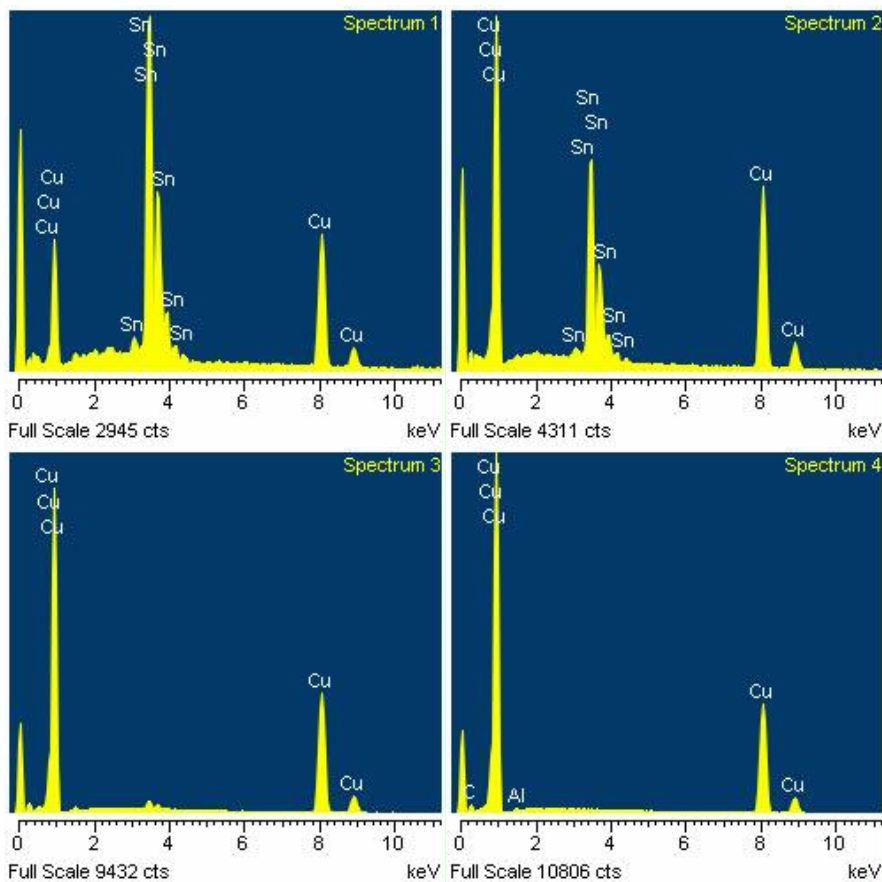


**Figure 29** EDS Spectra of SnPb Soldered Sn TQFP-144 on Manufactured Test Vehicle (SN 30, U1, Lead 144) EDS elemental analysis indicates the lead and board pad are both copper (Cu), however a thin Ni layer is present on the lead surface. The intermetallic layer at the component lead is nickel-tin (NiSn) and copper-tin (CuSn); the

board pad interface intermetallic layer is CuSn. The solder was confirmed to be tin-lead (SnPb). The presence of Cu at the lead interface is likely migrating from the board side.

*TQFP-208*

**Table 6** Summary of Intermetallic Compound Thickness on Tin-Lead Solder Joints of TQFP-208 Components on Manufactured Test Vehicles

SN	REFDES	Lead Finish	Lead	IMC Thickness, IC (um)	IMC Thickness, PWB (um)	IMC at IC	IMC at PWB	Observations
30	U57	AuPdNi	104	683.0nm 2.651	1.495 3.409	NiSn CuSn	CuSn	Crack extends about 1/3 of the way into the solder joint near the lead interface.
30	U57	AuPdNi	157	897.6nm 3.673	1.550 3.265	NiSn CuSn	CuSn	Crack extends about 1/3 of the way into the solder joint near the lead interface.
34	U3	AuPdNi	104	467.4nm 1.475	684.1nm 3.920	NiSn CuSn	CuSn	Crack through about 1/3 of solder joint on lead side.
34	U3	AuPdNi	167	1.083 2.782	1.064 3.682	NiSn CuSn	CuSn	Crack through about 1/3 of solder joint on lead side.

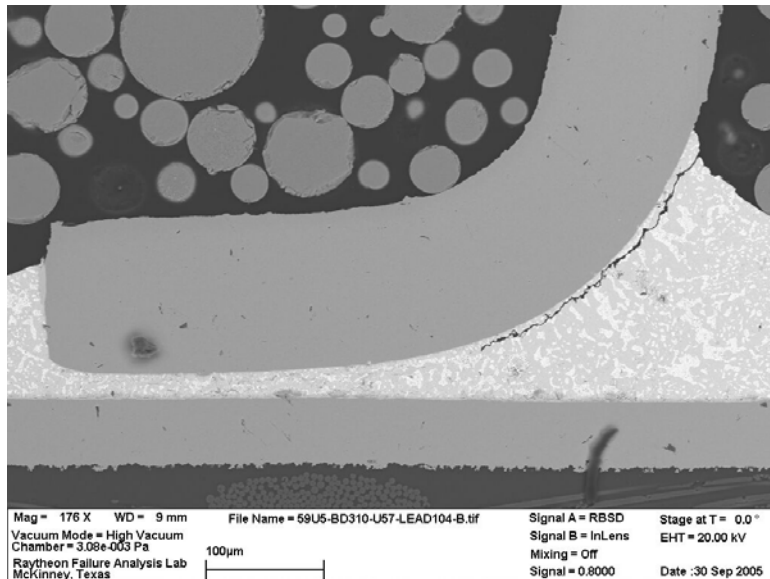


**Figure 30** SEM Micrograph of SnPb Soldered AuPdNi TQFP-208 on Manufactured Test Vehicle (SN 30, U57, Lead 104) A crack extends about one third of the way across the solder joint. Lead 157 is similar in appearance.

TSOP-50

**Table 7** Summary of Intermetallic Compound Thickness on Tin-Lead Solder Joints of TSOP-50 Components on Manufactured Test Vehicles

SN	REFDES	Lead Finish	Lead	IMC Thickness, IC (um)	IMC Thickness, PWB (um)	IMC at IC	IMC at PWB	Observations
31	U24	SnPb	1	<500nm	1.572 4.580	Ni/Sn	Cu/Sn	Crack extends all the way through the solder joint. Lead 60 similar in appearance.
32	U26	SnPb	Left Lead	201nm 1.766	1.858 3.114	NiSn **CuSn dispersed phases of SnAg in bulk solder	CuSn	Crack extends all the way through the solder joints. One side of the TSOP was sectioned in profile; the other side is a front view. Voiding was present on some of the solder bonds

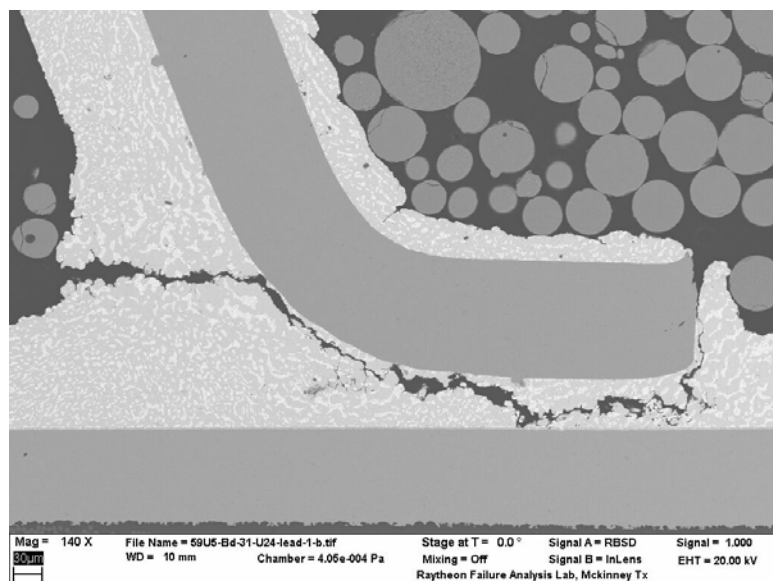


**Figure 31** SEM Micrograph of SnPb Soldered SnPb TSOP-50 on Manufactured Test Vehicle (SN 31, U24, Lead 1) Crack propagates all the way through the joint.

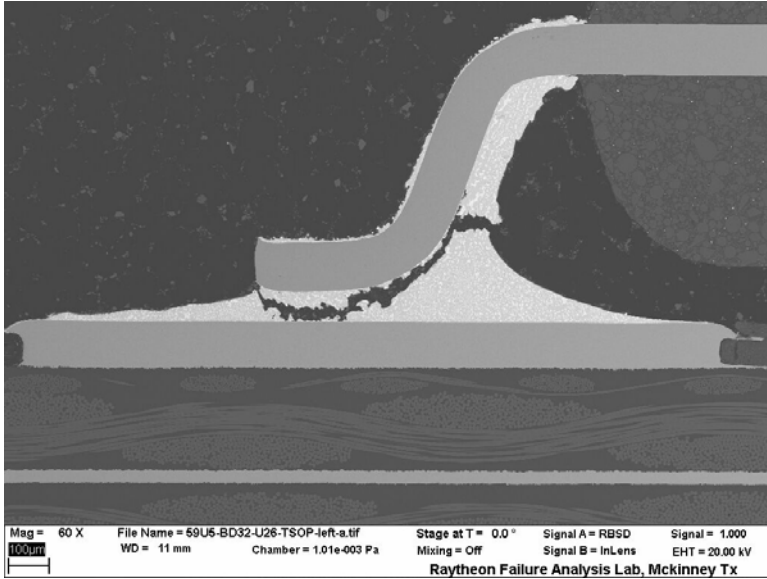


**Figure 32** SEM Micrograph of SnPb Soldered SnPb TSOP-50 on Manufactured Test Vehicle (SN 32 U26, left side) Solder is fractured all the way through.

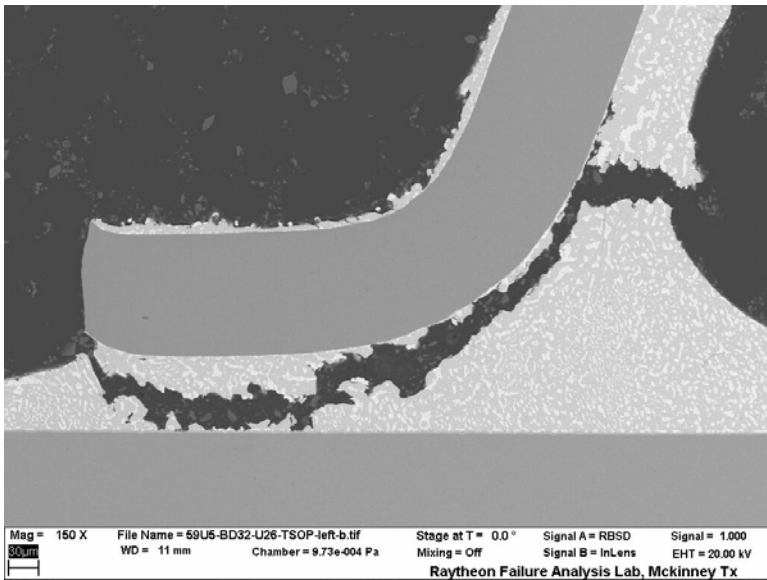


**Figure 33** SEM Micrograph of SnPb Soldered SnPb TSOP-50 on Manufactured Test Vehicle (SN 32 U26, left side) Solder is fractured all the way through.

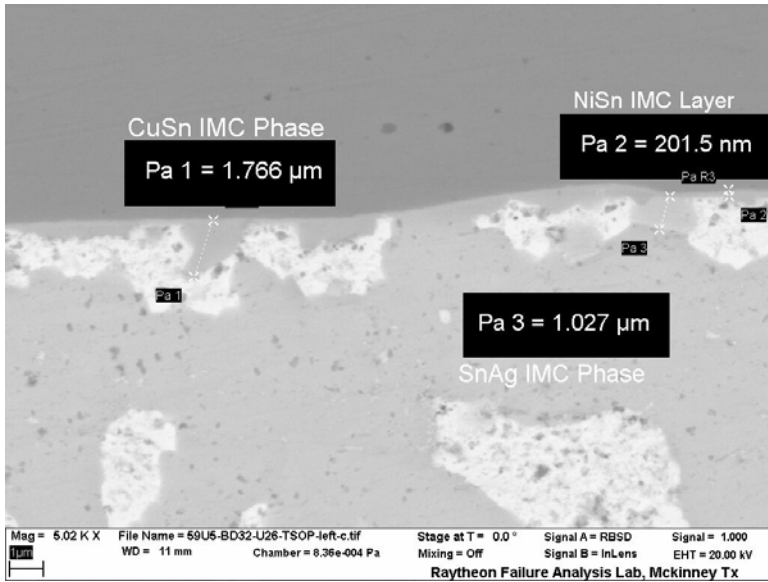


**Figure 34** SEM Micrograph of SnPb Soldered SnPb TSOP-50 on Manufactured Test Vehicle (SN 32 U26, left side) Lead side interface showing the intermetallic compounds present; NiSn, CuSn, and SnAg.

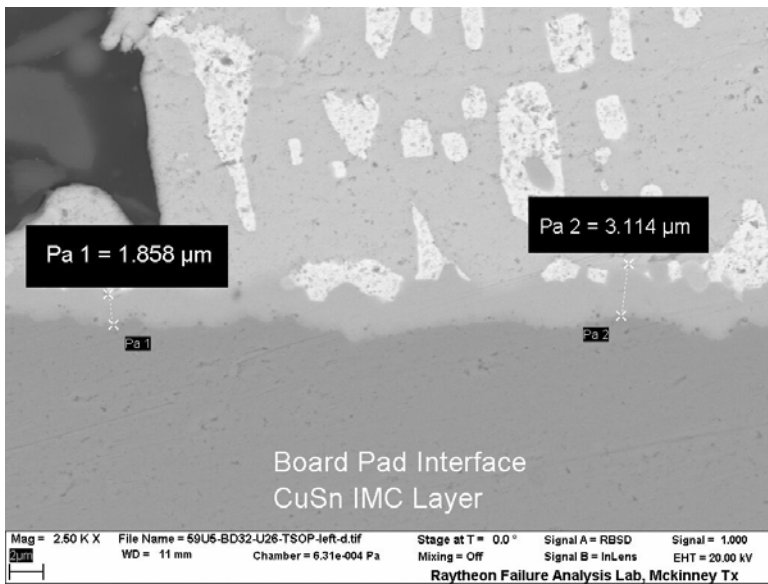


**Figure 35** SEM Micrograph of SnPb Soldered SnPb TSOP-50 on Manufactured Test Vehicle (SN 32 U26, left side) Board side interface showing the CuSn intermetallic layer.

***Tin-Silver-Copper Solder***

*BGA-225*

**Table 8** Summary of Intermetallic Compound Thickness on Tin-Silver-Copper Solder Joints of BGA-225 Components on Manufactured Test Vehicles

SN	REFDES	Lead Finish	Lead	IMC Thickness, IC (um)	IMC Thickness, PWB (um)	IMC at IC	IMC at PWB	Observations
100	U5	SnPb	15R	990nm 1.40	1.18 3.06	NiSn & *CuSn	CuSn	Crack at component interface completely through joint. Crack at PWB side approx. ½ distance across joint. Other bumps contain cracks as well, varying degrees of severity.
100	U5	SnPb	8R			NiSn & *CuSn	CuSn	Crack initiation top left corner near the component side interface.
100	U5	SnPb	1R	806nm 3.28	1.75 3.17	NiSn & *CuSn	CuSn	Minor cracks at corners on component side of joint.
101	U55	SnAgCu	15A	1.78 3.39	3.59	NiSn & *CuSn	CuSn	Cracks at corners, component side. Minor cracking lower left at PWB interface. Some bumps have cracks extending all the way through joint at component interface.
101	U55	SnAgCu	8A			NiSn & *CuSn	CuSn	No cracks in the solder
101	U55	SnAgCu	1A	1.87 4.82	3.03 6.79	NiSn & *CuSn	CuSn	Crack at component interface extends about ½ way through joint. Crack at PWB interface almost completely through.
102	U6	SnAgCu	15R	884nm 1.95	2.08 3.77	NiSn & *CuSn	CuSn	Crack completely through solder on PWB side. Crack present in solder at component interface. Other bumps similar in appearance.
102	U6	SnAgCu	8R			NiSn & *CuSn	CuSn	Crack initiation in the top right corner near the component side interface.
102	U6	SnAgCu	1R	1.41	1.51 3.48	NiSn & *CuSn	CuSn	Crack completely through solder on component side. Crack present in solder on PWB side.
102	U44	SnPb	15A	845nm 3.38	2.01 4.38	NiSn & *CuSn	CuSn	Minor cracking at component interface at corners.

SN	REFDES	Lead Finish	Lead	IMC Thickness, IC (um)	IMC Thickness, PWB (um)	IMC at IC	IMC at PWB	Observations
102	U44	SnPb	8A			NiSn & *CuSn	CuSn	No cracks in the solder
102	U44	SnPb	1A	650 5.90	2.11 3.80	NiSn & *CuSn	CuSn	Crack all the way through the solder near the component side interface.

\*The presence of Cu at the component side interface of the BGA's is the result of Cu migration from the board side interface and/or Cu from the SAC solder. The solder bonds to a nickel plating layer on the component side of the joint.

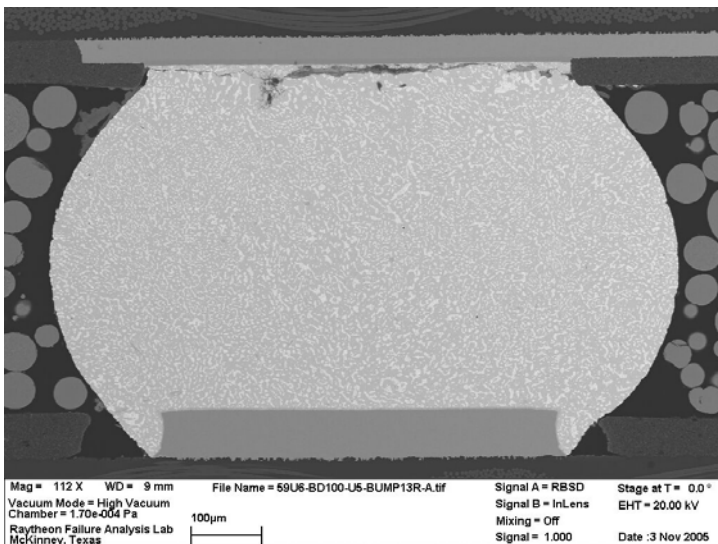


**Figure 36** SEM Micrograph of SnAgCu Soldered SnPb BGA-225 on Manufactured Test Vehicle (SN 100, U5, Bump 15R) Crack extends all the way through the solder joint at the component side of the joint.

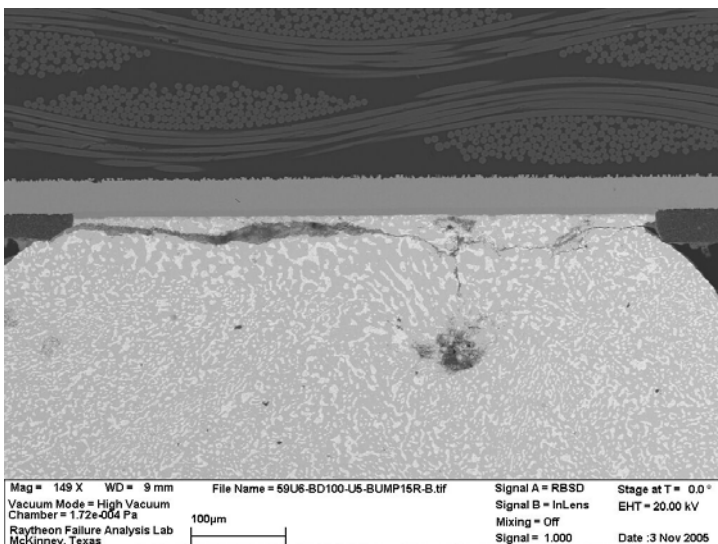


**Figure 37** SEM Micrograph of SnAgCu Soldered SnPb BGA-225 on Manufactured Test Vehicle (SN 100, U5, Bump 15R) Closer view of the crack through the solder joint at the component side of the joint.

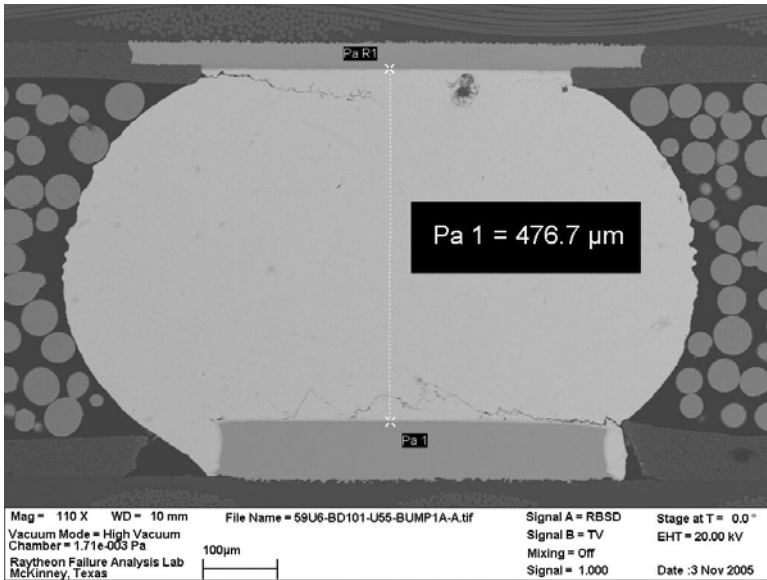


**Figure 38** SEM Micrograph of SnAgCu Soldered SnAgCu BGA-225 on Manufactured Test Vehicle (SN 101, U55, Bump 1A) Crack at component interface extends about ½ way through joint. Crack at PWB interface almost completely through.

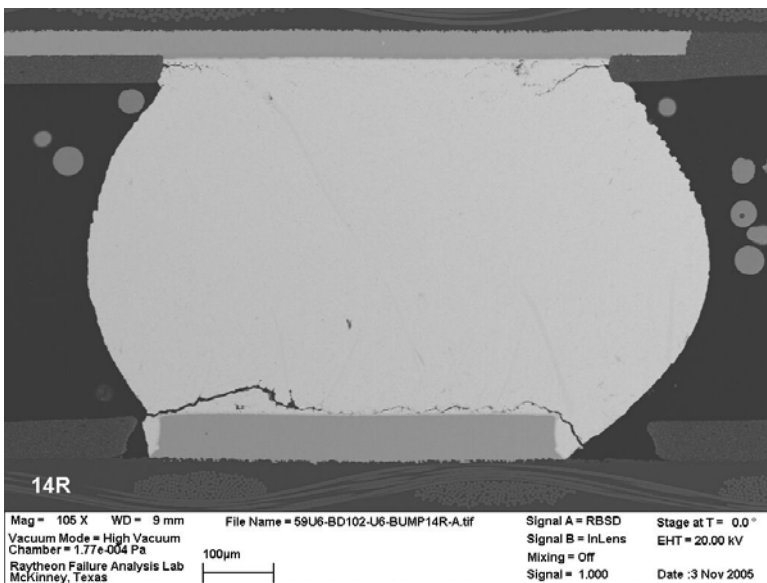


**Figure 39** SEM Micrograph of SnAgCu Soldered SnAgCu BGA-225 on Manufactured Test Vehicle (SN Board 102, U6, Bump 14R) Solder bump is cracked all the way through the solder at the board side interface. Partial cracks are present at the component side interface.

CLCC-20

**Table 9** Summary of Intermetallic Compound Thickness on Tin-Silver-Copper Solder Joints of CLCC-20 Components on Manufactured Test Vehicles

SN	REFDES	Lead Finish	Lead	IMC Thickness, IC (um)	IMC Thickness, PWB (um)	IMC at IC	IMC at PWB	Observations
99	U46	SnPb	15	1.91 3.96	1.33 2.79	*NiSn Low levels of Cu	CuSn	Crack extends through solder joint. Appears to be voiding in solder below component.
99	U46	SnPb	1	5.39 1.67	1.32 3.15	NiSn Low levels of Cu	CuSn	Crack extends through solder joint. Appears to be voiding in solder below component and in bulk solder.
101	U17	SnAgCu	15	---	893nm 2.87	NiSn Low levels of Cu	CuSn	Component missing due to fractured joint.
101	U17	SnAgCu	1	---	1.39 2.83	NiSn Low levels of Cu	CuSn	Component missing due to fractured joint.
102	U14	SnAgCu	15	---	683nm 3.04	NiSn Low levels of Cu	CuSn	Component missing due to fractured joint.
102	U14	SnAgCu	1	---	604nm 2.18	NiSn Low levels of Cu	CuSn	Component missing due to fractured joint.
103	U53	SnPb	15	1.18 4.17	1.51 4.19	NiSn Low levels of Cu	CuSn	Crack extends completely through joint.

\*Solder bond on the component side is made to a Ni plating layer. Presence of Cu is from the SAC solder or due to migration from the board side interface.

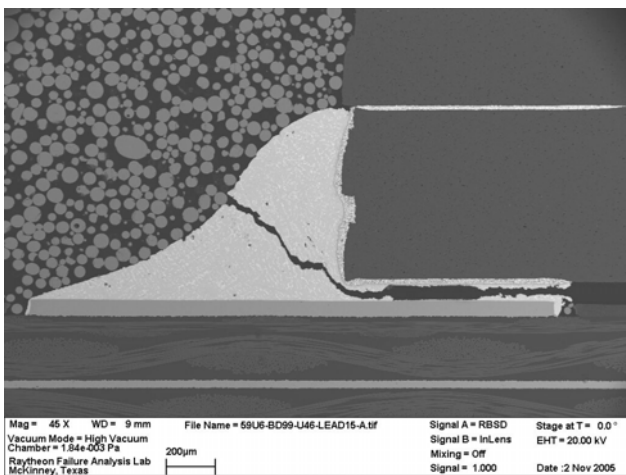


**Figure 40** SEM Micrograph of SnAgCu Soldered SnPb CLCC-20 on Manufactured Test Vehicle (SN 99, U46, Lead 25) Crack extends completely through joint. Some voiding is present below component.

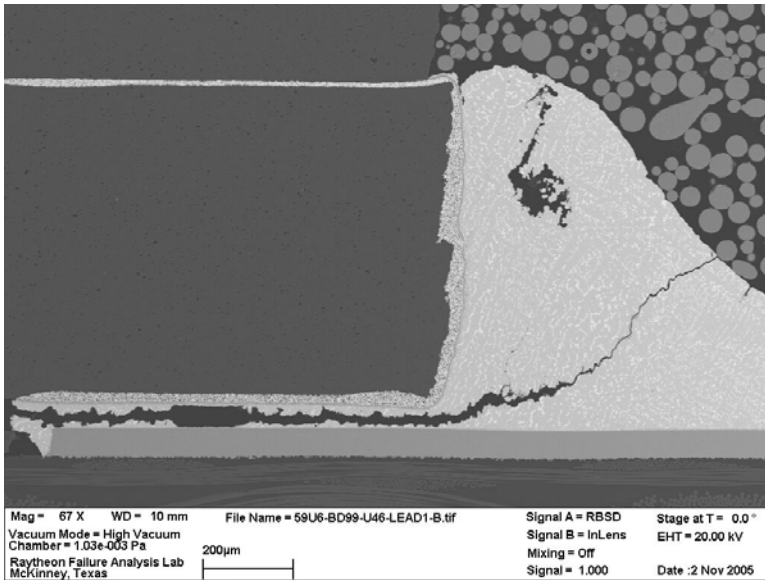


**Figure 41** SEM Micrograph of SnAgCu Soldered SnPb CLCC-20 on Manufactured Test Vehicle (SN 99, U46, Lead 1) Crack extends completely through joint. Voids are present below component and in bulk solder.

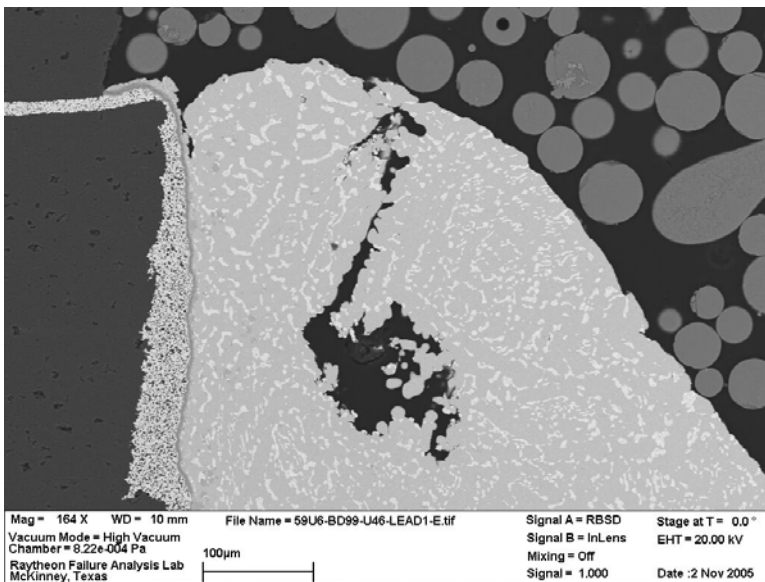


**Figure 42** SEM Micrograph of SnAgCu Soldered SnPb CLCC-20 on Manufactured Test Vehicle (SN 99, U46, Lead 1) The CLCC-20 device U46 on board SN 99 should have a tin-lead finish and tin-silver-copper solder joint. In this high magnification view, the appearance of the solder resembles tin-lead solder. The image was taken in backscatter mode, which indicates atomic number information. The bright phases are lead-rich phases and the medium gray phases are the tin-rich phases. This could indicate a good mix between the tin-silver-copper solder and the tin-lead finish on the component. However, there appears to be a lot of lead present to be solely from the tinned finish.

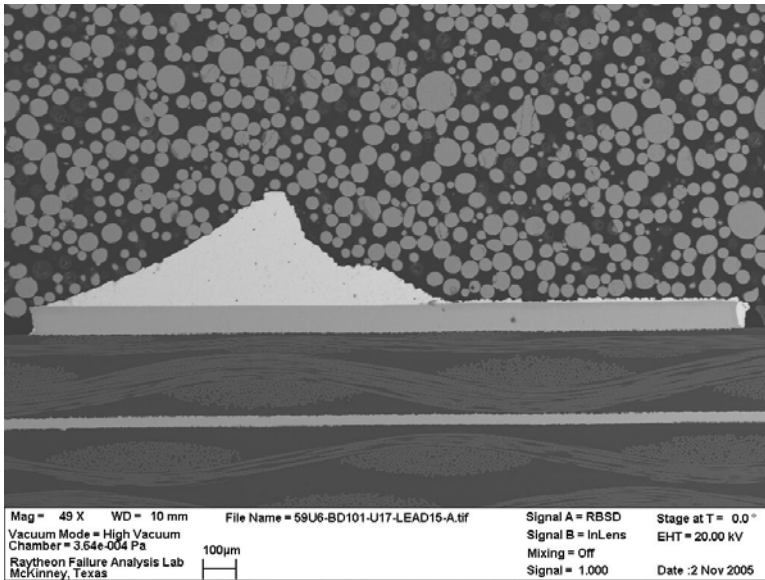


**Figure 43** SEM Micrograph of SnAgCu Soldered SnAgCu CLCC-20 on Manufactured Test Vehicle (SN 101, U17, Lead 15) Component missing as a result of the fractured solder joint.

*PDIP-20*

**Table 10** Summary of Intermetallic Compound Thickness on Tin-Silver-Copper Solder Joints of PDIP-20 Components on Manufactured Test Vehicles

SN	REFDES	Lead Finish	Lead	IMC Thickness, IC (um)	IMC Thickness, PWB (um)	IMC at IC	IMC at PWB	Observations
99	U23	AuPdNi	15	752nm 441nm	1.18 1.86	NiSnCu	AgSnCu	Crack in solder on both sides of lead near PWB interface. Crack on left side of lead on other side of board. Other leads also have cracks. Some voiding.
99	U23	AuPdNi	1	328nm 751nm	1.35 2.07	NiSnCu	AgSnCu	No cracks.
99	U11	Sn	15	1.17 3.70	1.09 1.62	NiSnCu	AgSnCu	Crack in solder on both sides of lead and board. Cracks near lead interface and PWB interface.
99	U11	Sn	1	993nm 2.19	1.16 1.67	NiSnCu	AgSnCu	Crack in solder on both sides of lead and board. Cracks near lead interface and PWB interface.

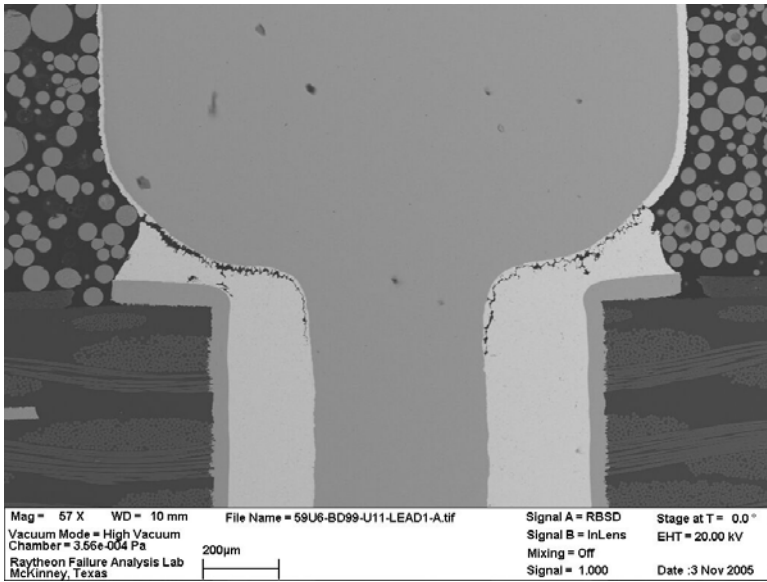


**Figure 44** SEM Micrograph of SnAgCu Soldered Sn PDIP-20 on Manufactured Test Vehicle (SN 99, U11, Lead 1) Cracks in solder on both sides of lead near lead interface. EDS data in Figure 46 and Figure 47 provide the metallurgical solder joint data.

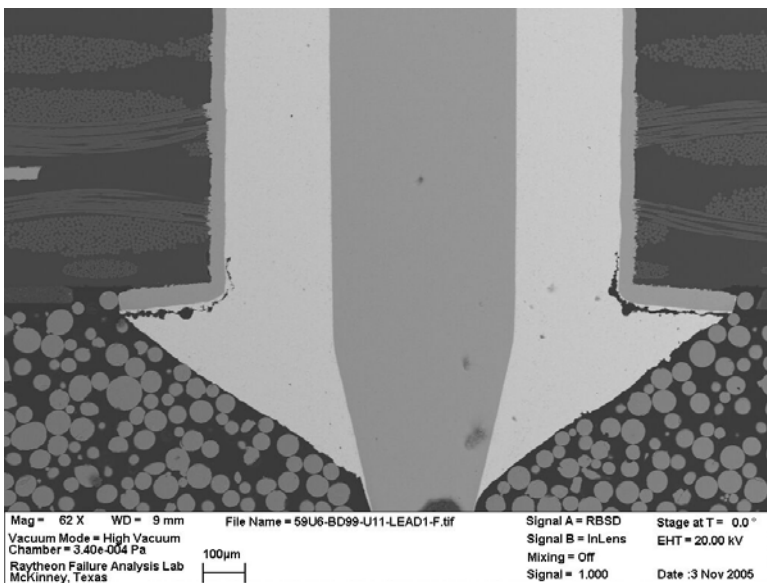


**Figure 45** SEM Micrograph of SnAgCu Soldered Sn PDIP-20 on Manufactured Test Vehicle (SN 99, U11, Lead 1) Cracks also present on opposite side of board near PWB interface.

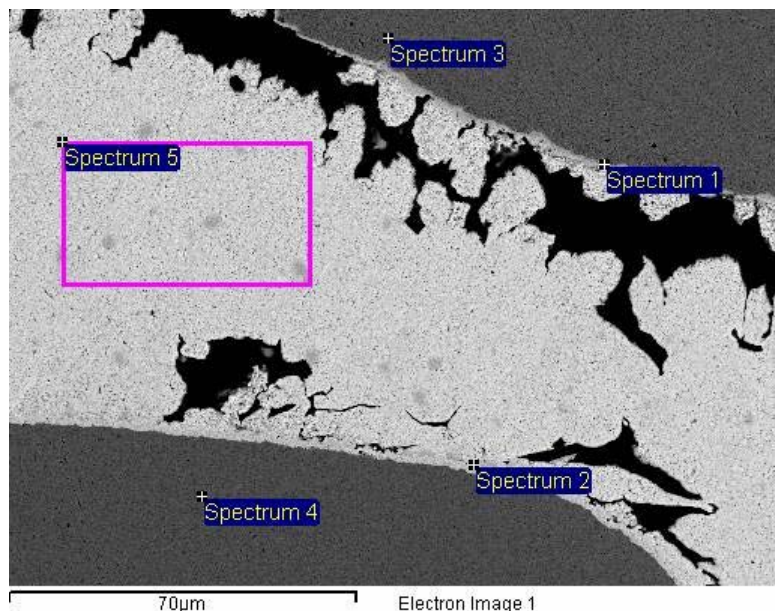


**Figure 46** SEM Micrograph of SnAgCu Soldered Sn PDIP-20 on Manufactured Test Vehicle (SN 99, U11, Lead 1) The board base metallization is Cu plated with immersion Ag. The intermetallic layer is mainly AgSn with low levels of Cu. The lead is Cu with a Ni plating on the surface. The intermetallic layer is NiSnCu.

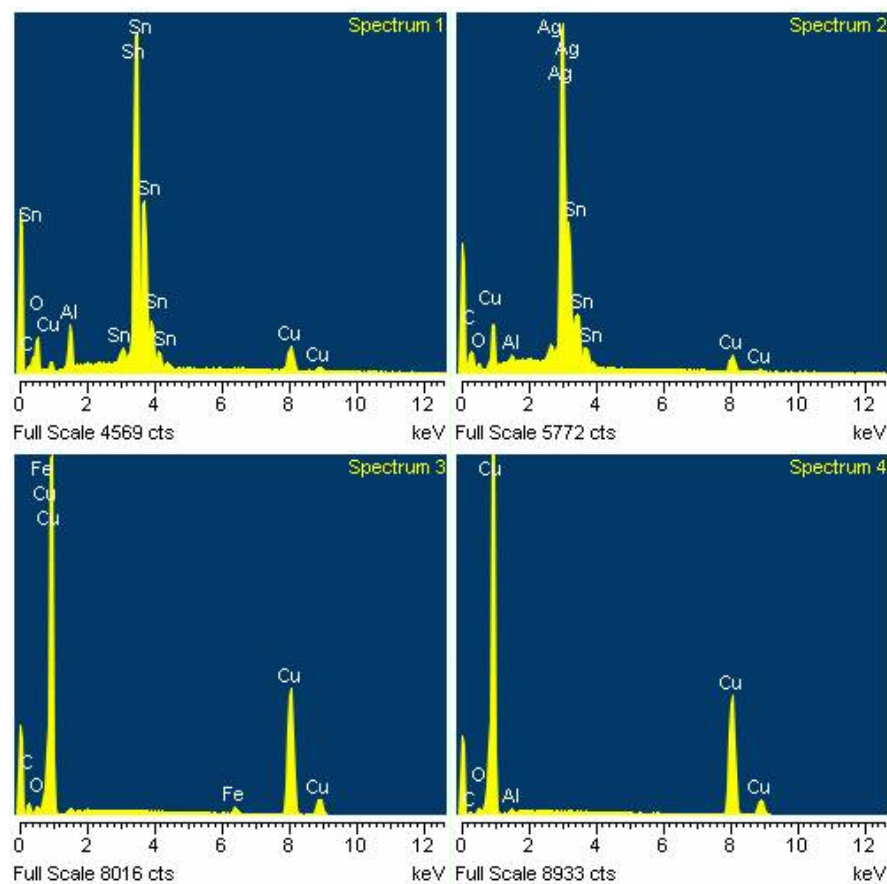


**Figure 47** EDS Spectra of SnAgCu Soldered Sn PDIP-20 on Manufactured Test Vehicle (SN 99, U11, Lead 1)

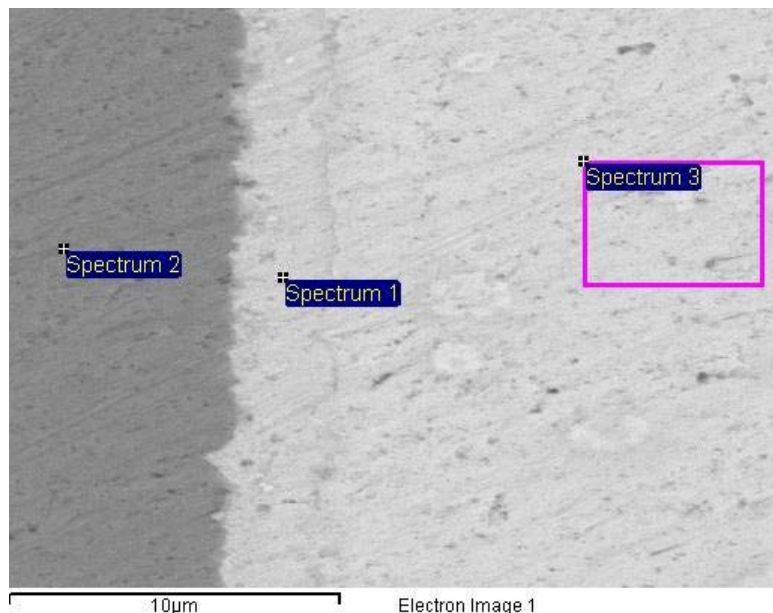


**Figure 48** SEM Micrograph of SnAgCu Soldered AuPdNi PDIP-20 on Manufactured Test Vehicle (SN 99, U23, Lead 1) Board side interface and IMC layer.

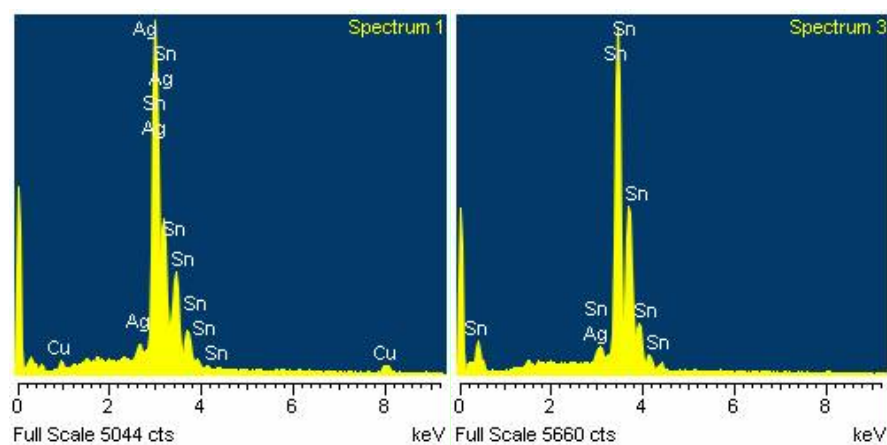


**Figure 49** EDS Spectra of SnAgCu Soldered AuPdNi PDIP-20 on Manufactured Test Vehicle (SN 99, U23, Lead 1) The board metallization is Cu (spectrum not shown) plated with immersion Ag, the intermetallic layer is mainly AgSn with low levels of Cu (Spectrum 1), solder is SnAgCu (Spectrum 3).

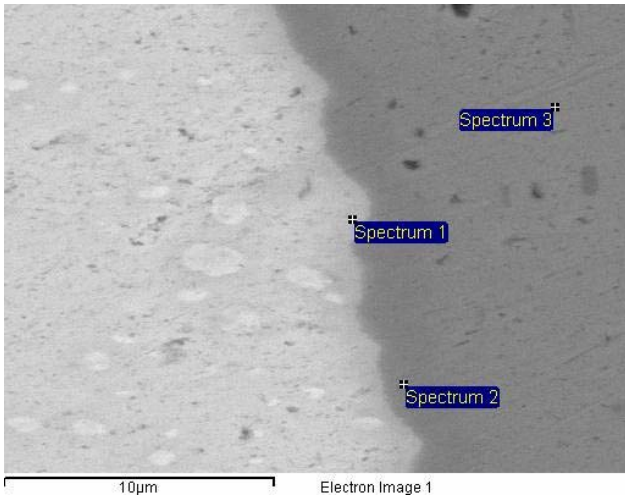


**Figure 50** SEM Micrograph of SnAgCu Soldered AuPdNi PDIP-20 on Manufactured Test Vehicle (SN 99, U23, Lead 1) Component lead side interface and IMC layer

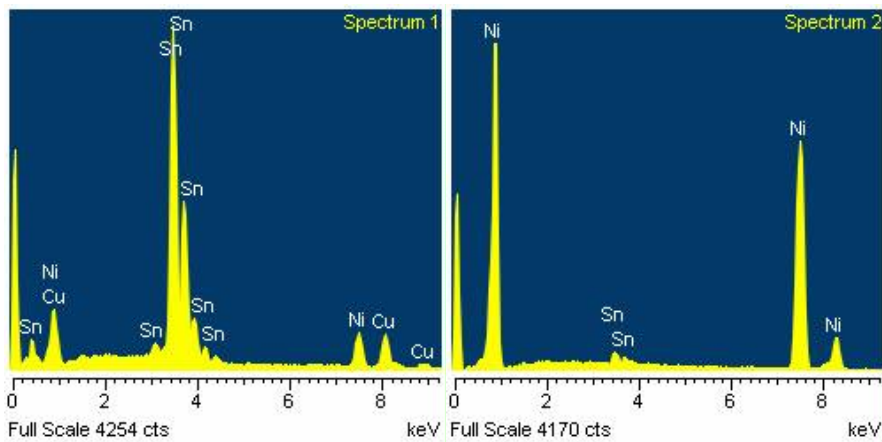


**Figure 51** EDS Spectra of SnAgCu Soldered AuPdNi PDIP-20 on Manufactured Test Vehicle (SN 99, U23, Lead 1) The lead is Cu with a Ni plating on the surface. The intermetallic layer is NiSnCu. Spectrum 1 = IMC, Spectrum 2 = Ni layer, Spectrum 3 = Cu base (spectrum not shown)

*PLCC-20*

**Table 11** Summary of Intermetallic Compound Thickness on Tin-Silver-Copper Solder Joints of PLCC-20 Components on Manufactured Test Vehicles

SN	REFDES	Lead Finish	Lead	IMC Thickness, IC (um)	IMC Thickness, PWB (um)	IMC at IC	IMC at PWB	Observations
102	U47	Sn	15	1.31 2.67	2.03 3.98	CuSn	CuSn	Minor voiding in joint.

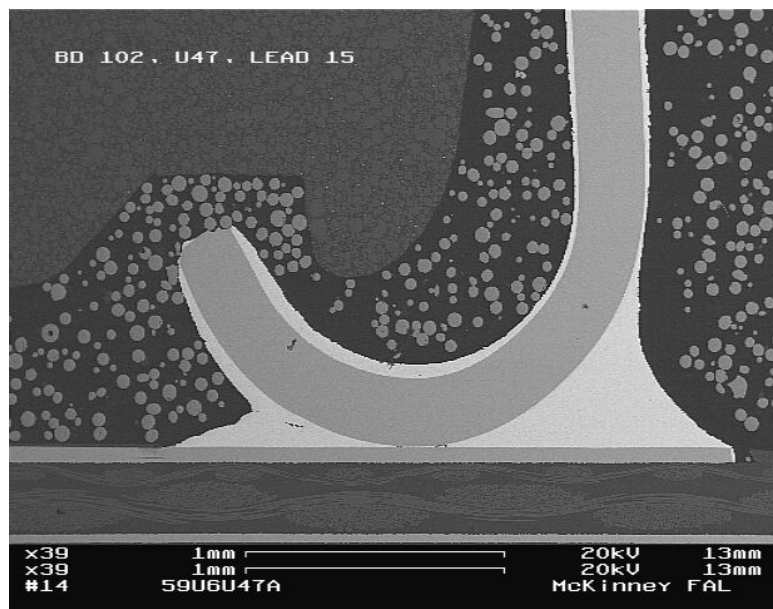


**Figure 52** SEM Micrograph of SnAgCu Soldered Sn PLCC-20 on Manufactured Test Vehicle (SN 102, U47, Lead 15) Minor voiding in joint.

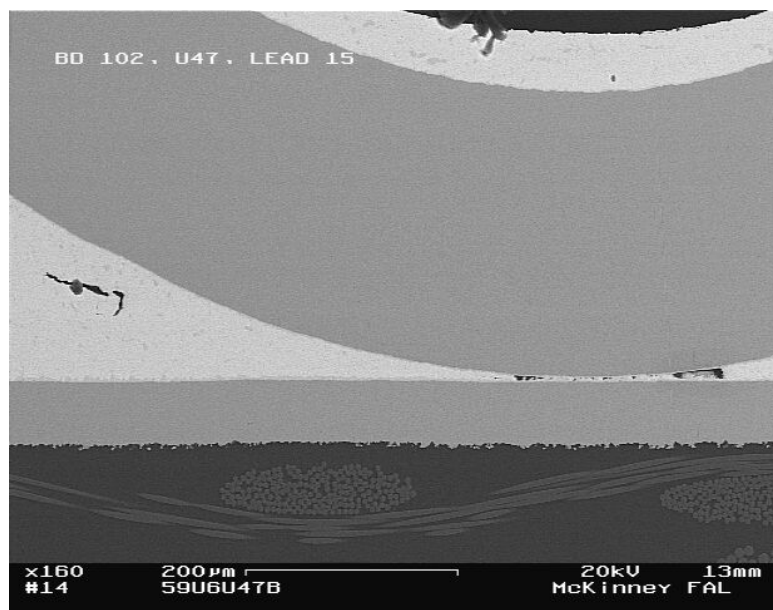


**Figure 53** SEM Micrograph of SnAgCu Soldered Sn PLCC-20 on Manufactured Test Vehicle (SN 102, U47, Lead 15) High magnification view of joint seen above.

TQFP-144

**Table 12** Summary of Intermetallic Compound Thickness on Tin-Silver-Copper Solder Joints of TQFP-144 Components on Manufactured Test Vehicles

SN	REFDES	Lead Finish	Lead	IMC Thickness, IC (um)	IMC Thickness, PWB (um)	IMC at IC	IMC at PWB	Observations
101	U58	Sn	144	1.08 5.53	844nm 2.83	CuSn	CuSn	Crack extends ¼ of way into joint. Initiates on inside of joint near lead interface.
101	U58	Sn	37	1.29 6.95	910nm 2.87	CuSn	CuSn	Cracks initiating on inside of joint.
102	U7	Sn	72	1.07 3.74	1.07 3.92	CuSn	CuSn	Crack extends completely through joint.
102	U7	Sn	104	1.96 4.37	981nm 2.67	CuSn	CuSn	Crack present in solder initiating on inside of joint on underside of lead.

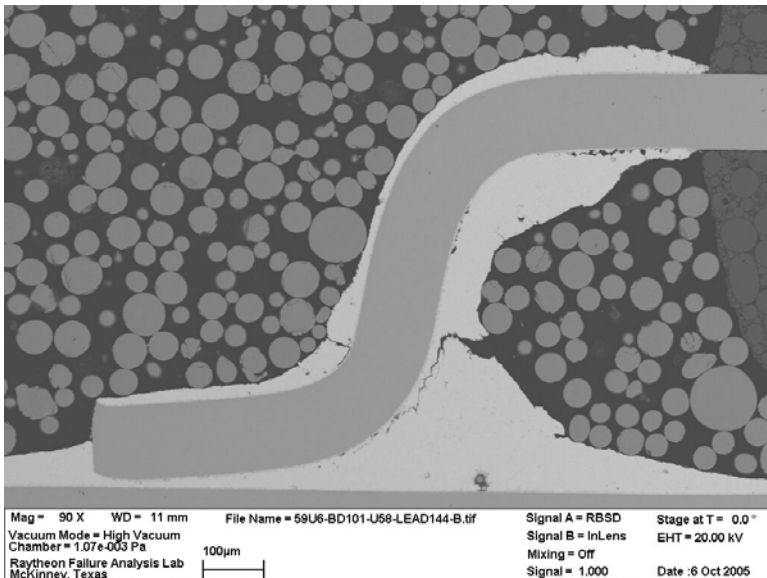


**Figure 54** SEM Micrograph of SnAgCu Soldered Sn TQFP-144 on Manufactured Test Vehicle (SN 101, U58, Lead 144) Crack extends ¼ of way into joint. Initiates on inside of joint near lead interface.

TQFP-208

**Table 13** Summary of Intermetallic Compound Thickness on Tin-Silver-Copper Solder Joints of TQFP-208 Components on Manufactured Test Vehicles

Sn	REFDES	Lead Finish	Lead	IMC Thickness, IC (um)	IMC Thickness, PWB (um)	IMC at IC	IMC at PWB	Observations
101	U3	AuPdNi	105	1.13 5.00	1.01 2.67	*NiSnCu	CuSn	Crack extends ¼ of way into joint. Initiates on inside of joint near lead interface.
101	U3	AuPdNi	157	1.30 6.29	960nm 2.35	*NiSnCu	CuSn	Crack extends ¼ of way into joint. Initiates on inside of joint near lead interface.
102	U31	AuPdNi	208	1.23 6.41	2.02 4.89	*NiSnCu	CuSn	Crack extends about ½ way through joint initiating on inside joint near component body.
102	U31	AuPdNi	53	1.23 6.41		*NiSnCu	CuSn	Crack extends about ½ way through joint initiating on inside joint near component body.

\*Solder bond is made to AuPdNi finish on the component lead, forming a NiSnCu IMC. The Cu is either migrating from the board side or is from the SAC solder.

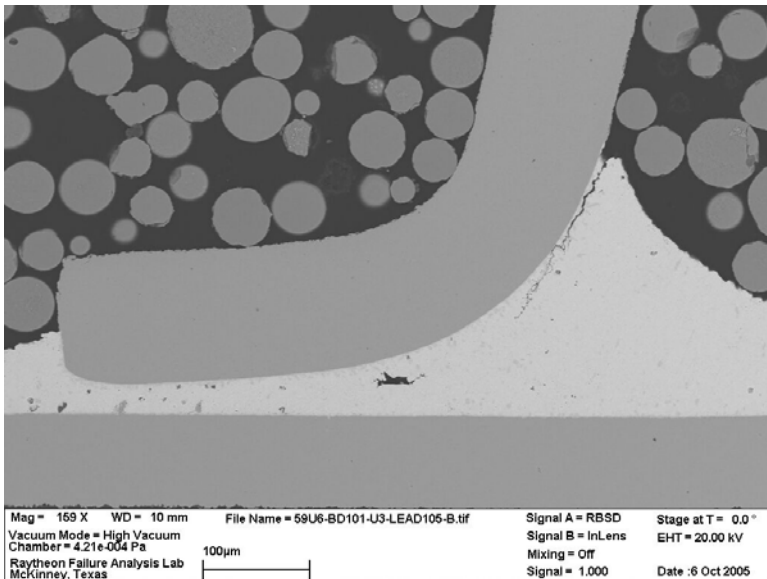


**Figure 55** SEM Micrograph of SnAgCu Soldered AuPdNi TQFP-208 on Manufactured Test Vehicle (SN 101, U3, Lead 105) Crack extends about ¼ of the way into the joint at the lead interface. The crack is initiating on the inside portion of the joint. A small void is present in the joint. EDS data for the joint metallurgy for this device can be observed in Figure 57, Figure 58, Figure 59, and Figure 60.

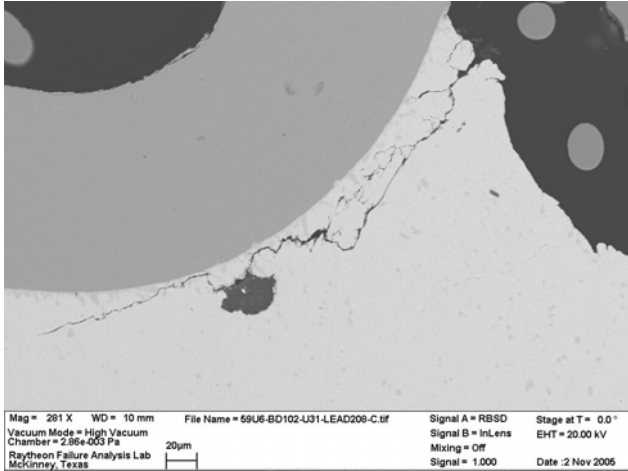


**Figure 56** SEM Micrograph of SnAgCu Soldered AuPdNi TQFP-208 on Manufactured Test Vehicle (SN 103, U31, Lead 208) Crack extends approximately 1/2 of the way into the joint.

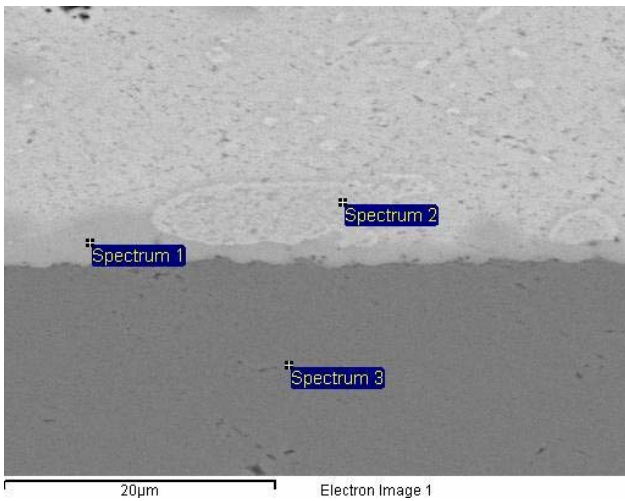


**Figure 57** SEM Micrograph of SnAgCu Soldered AuPdNi TQFP-208 on Manufactured Test Vehicle (SN 101, U3, Lead 105) Board side solder interface.

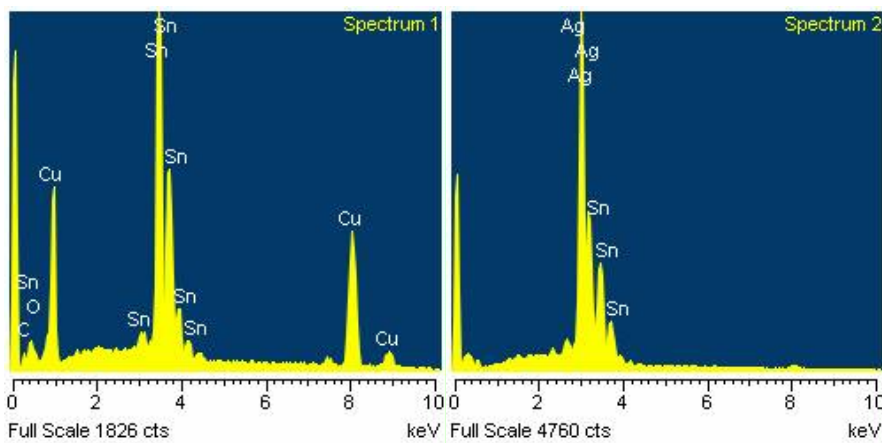


**Figure 58** EDS Spectra of SnAgCu Soldered AuPdNi TQFP-208 on Manufactured Test Vehicle (SN 101, U3, Lead 105) The base material is Cu (Spectrum 3), the IMC layer is CuSn (Spectrum 1), Spectrum 2 indicates a AgSn IMC phases near the board interface.

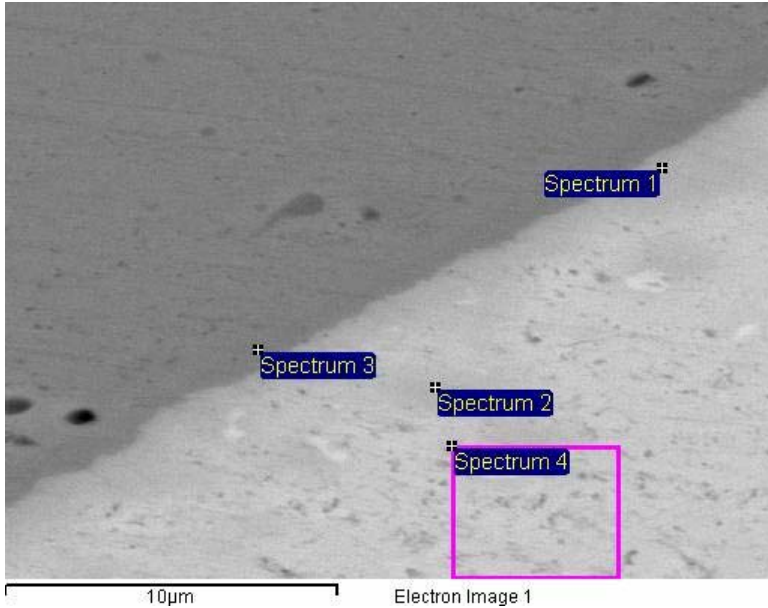


**Figure 59** SEM Micrograph of SnAgCu Soldered AuPdNi TQFP-208 on Manufactured Test Vehicle (SN 101, U3, Lead 105) Component side solder interface.

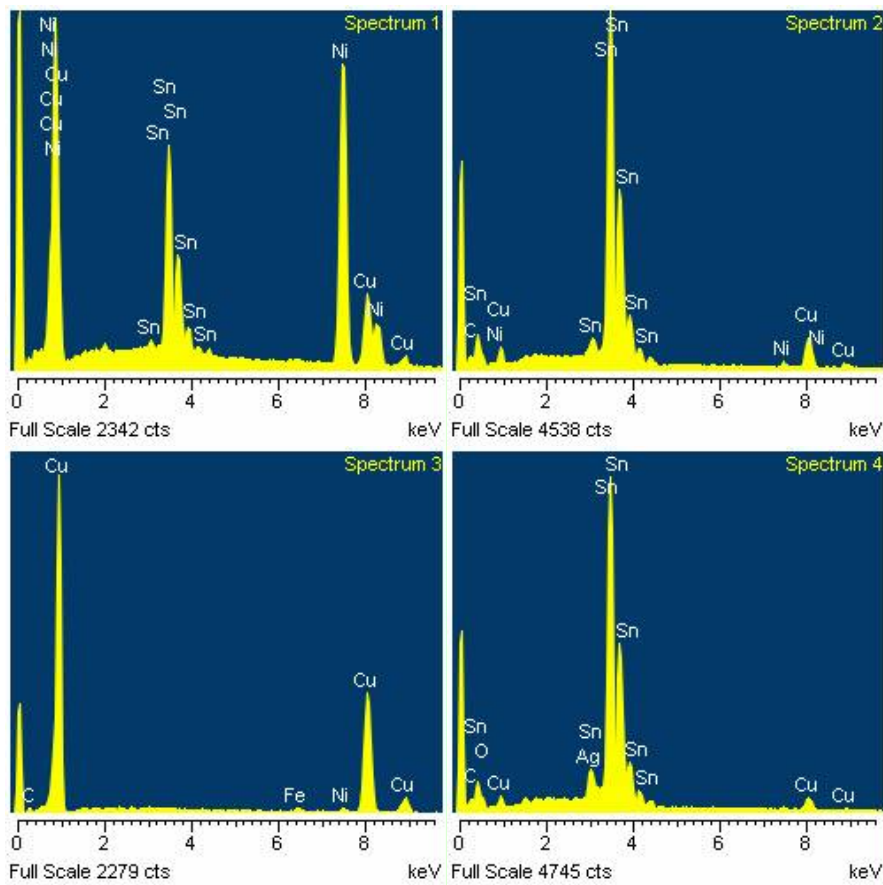


**Figure 60** SEM Micrograph of SnAgCu Soldered AuPdNi TQFP-208 on Manufactured Test Vehicle (SN 101, U3, Lead 105) Intermetallic layer is NiSnCu (Spectrum 1), CuSn intermetallic likely migrating from the board side interface (Spectrum 2), lead is Cu with a Ni plating (Spectrum 3), solder is SnAgCu (Spectrum 4).

TSOP-50

**Table 14** Summary of Intermetallic Compound Thickness on Tin-Silver-Copper Solder Joints of TSOP-50 Components on Manufactured Test Vehicles

SN	REFDES	Lead Finish	Lead	IMC Thickness, IC (um)	IMC Thickness, PWB (um)	IMC at IC	IMC at PWB	Observations
99	U16	SnPb	25	1.16	993nm 3.76um	NiSn & *CuSn	CuSn	Crack extends completely through joint.
99	U16	SnPb	26	227nm	1.48um 3.25um	NiSn & *CuSn	CuSn	Crack extends completely through joint.
100	U39	SnCu	1	261nm	1.35 3.37	NiSn & *CuSn	CuSn	Crack extends completely through solder joint.
100	U39	SnCu	50	223nm	1.45 2.78	NiSn & *CuSn	CuSn	Crack extends completely through solder joint.
101	U62	SnPb	15	102nm 226nm	870nm 4.00	NiSn & *CuSn	CuSn	Crack extends from outside of the joint inward on both sides of joint. Crack almost completely through joint. Voiding present.
101	U62	SnPb	1	161nm	773nm 3.86	NiSn & *CuSn	CuSn	Crack extends from outside of the joint inwards on both sides of joint. Crack almost completely through joint.
102	U12	SnCu	25	225nm	753nm 1.43	NiSn & *CuSn	CuSn	Crack extends completely through joint.
102	U12	SnCu	26	201nm	1.39 3.48	NiSn & *CuSn	CuSn	Crack extends completely through joint.

\*The presence of Cu at the Component side interface of the TSOP is the result of Cu migration from the board side interface and/or Cu from the SAC solder. The solder bond at the component side is made to a Ni layer interface.

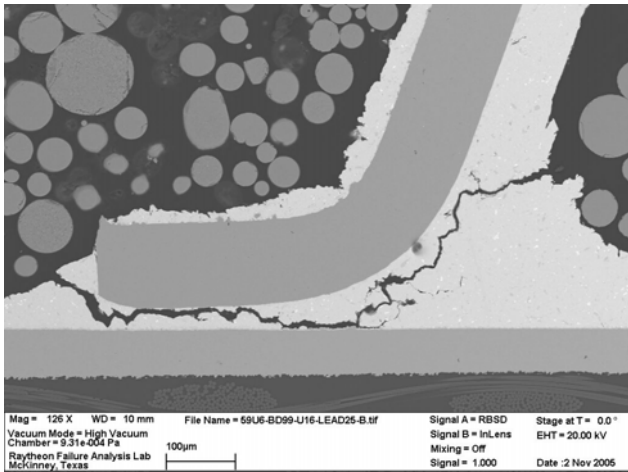


**Figure 61** SEM Micrograph of SnAgCu Soldered SnPb TSOP-50 on Manufactured Test Vehicle (SN 99, U16, Lead 25) Crack extends completely through joint.

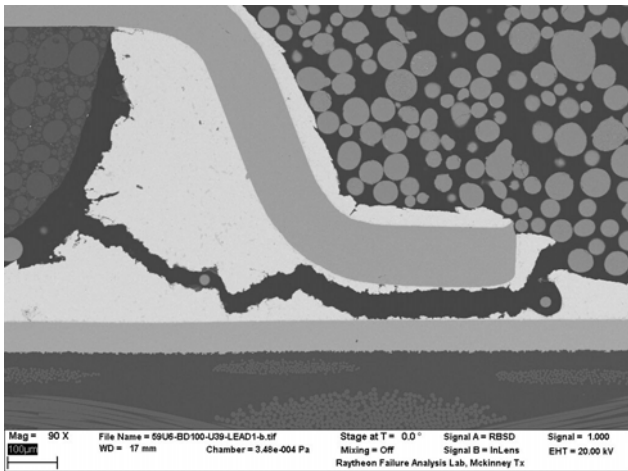


**Figure 62** SEM Micrograph of SnAgCu Soldered SnCu TSOP-50 on Manufactured Test Vehicle (SN 100, U39, Lead 1) Crack extends all the way through the joint.

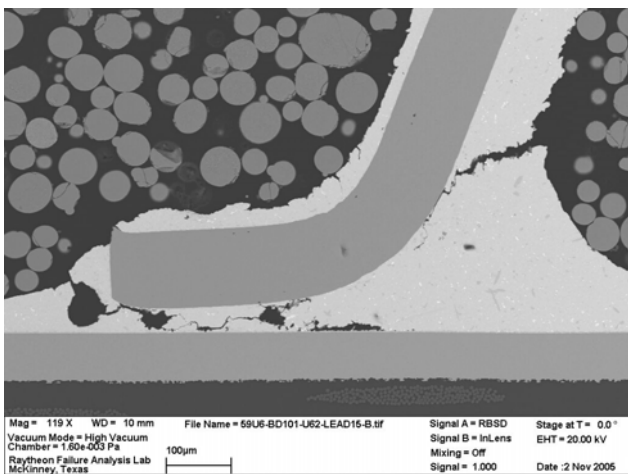


**Figure 63** SEM Micrograph of SnAgCu Soldered SnPb TSOP-50 on Manufactured Test Vehicle (SN 101, U62, Lead 15) Crack extends from outside of the joint inward on both sides of joint. Crack is almost completely through joint. Some voids are present.

***Tin-Silver-Copper-Bismuth Solder***

*BGA-225*

**Table 15** Summary of Intermetallic Compound Thickness on Tin-Silver-Copper-Bismuth Solder Joints of BGA-225 Components on Manufactured Test Vehicles

SN	REFDES	Lead Finish	Lead	IMC Thickness, IC (um)	IMC Thickness, PWB (um)	IMC at IC	IMC at PWB	Observations
113	U4	SnAgCu	15R	1.08 1.67	916nm 3.23	NiSn & *CuSn	CuSn	Crack at board interface completely through joint. Crack initiations in the corners at component interface
113	U4	SnAgCu	1R	482nm 1.40	1.85 3.45	NiSn & *CuSn	CuSn	Crack at component interface completely through joint. Crack at board interface approx. 3/4 through solder.
113	U4	SnAgCu	7R	476nm 2.30	1.23 3.70	NiSn & *CuSn	CuSn	No cracks.
141	U56	SnPb	1A	1.08 3.67	2.14 2.31	NiSn & *CuSn	CuSn	Crack at board interface almost completely through joint.
141	U56	SnPb	1R	1.05 3.47	2.08 3.53	NiSn & *CuSn	CuSn	Crack at component interface completely through joint. Void in solder
142	U55	SnAgCu	15A	1.66 2.61	2.80 4.74	NiSn & *CuSn	CuSn	Cracks completely through the solder joint at both board and component interfaces. This component failed after only one cycle. The cause of the failure is likely due to something other than the solder since the solder was fractured due to fatigue.
142	U55	SnAgCu	1A	1.37 2.26	2.70 5.40	NiSn & *CuSn	CuSn	Crack at board interface completely through joint. Crack at component side interface almost through the entire joint. A large void stopped the crack.
142	U55	SnAgCu	7A	1.77 4.60	2.36 4.92	NiSn & *CuSn	CuSn	Crack initiation top right corner at component interface.
142	U2	SnPb	R15	772nm 3.39	1.41 3.37	NiSn & *CuSn	CuSn	Cracks completely through the solder joint at both board and component interfaces.
142	U2	SnPb	R1	638nm 2.25	1.23 4.11	NiSn & *CuSn	CuSn	Crack at component interface completely through joint. Crack initiations in solder near board side interface.

SN	REFDES	Lead Finish	Lead	IMC Thickness, IC (um)	IMC Thickness, PWB (um)	IMC at IC	IMC at PWB	Observations
142	U2	SnPb	R7	763nm 3.26	1.65 3.25	NiSn & *CuSn	CuSn	Crack at component interface completely through joint.

\*The presence of Cu at the component side interface of the BGA's is the result of Cu migration from the board side interface and/or Cu from the SAC solder. The solder bond at the component side is made to a Ni layer interface.

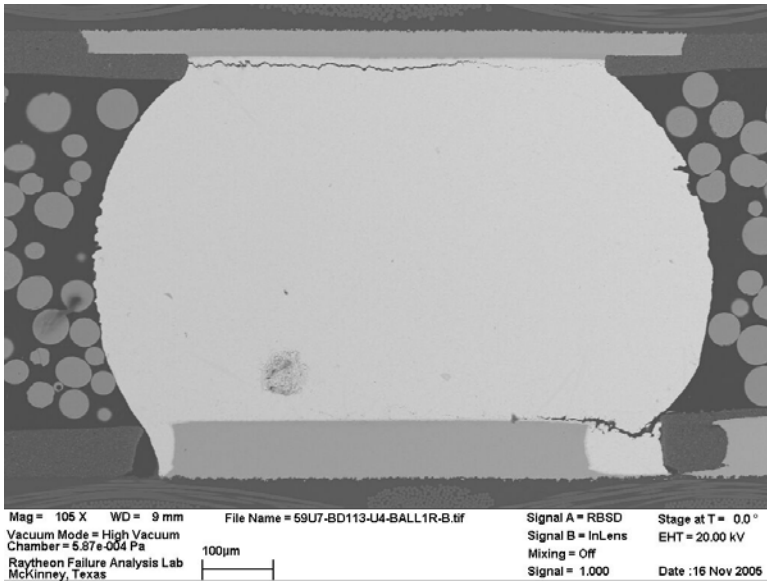


**Figure 64** SEM Micrograph of SnAgCuBi Soldered SnAgCu BGA-225 on Manufactured Test Vehicle (SN 113, U4, Bump 1R) Solder cracked at both interfaces, crack extends completely through the solder joint at the component side interface.

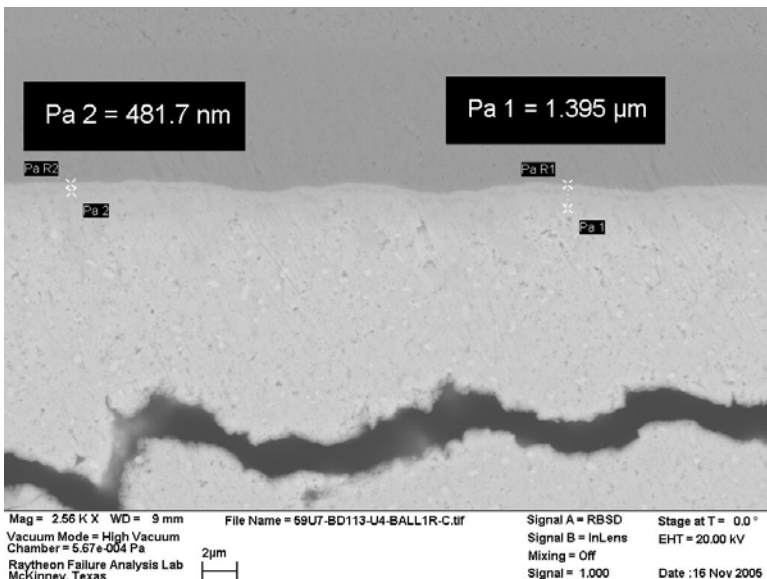


**Figure 65** SEM Micrograph of SnAgCuBi Soldered SnAgCu BGA-225 on Manufactured Test Vehicle (SN 113, U4, Bump 1R) Component side interface, intermetallic layer measurements are shown.

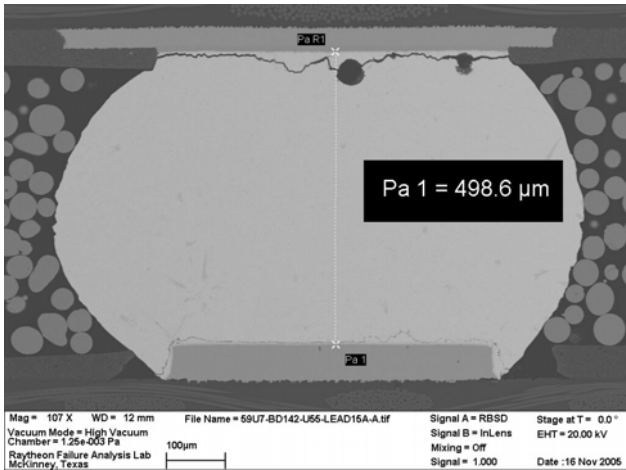


**Figure 66** SEM Micrograph of SnAgCuBi Soldered SnAgCu BGA-225 on Manufactured Test Vehicle (SN 142, U55, Bump 15A) Solder completely cracked through the joint at both interfaces.

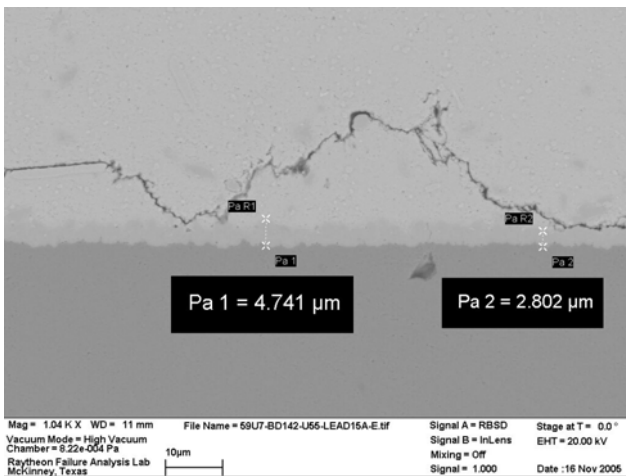


**Figure 67** SEM Micrograph of SnAgCuBi Soldered SnAgCu BGA-225 on Manufactured Test Vehicle (SN 142, U55, Bump 15A) Solder completely cracked through the joint at both interfaces. Closer view of board side interface shows the CuSn intermetallic layer and that the crack is through the solder.

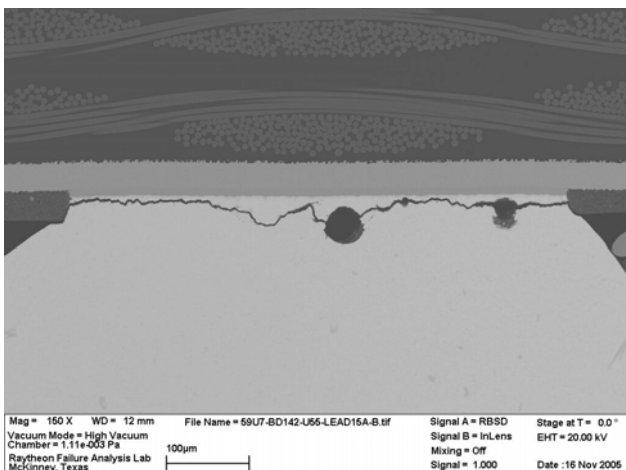


**Figure 68** SEM Micrograph of SnAgCuBi Soldered SnAgCu BGA-225 on Manufactured Test Vehicle (SN 142, U55, Bump 15A) Closer view of component side interface.

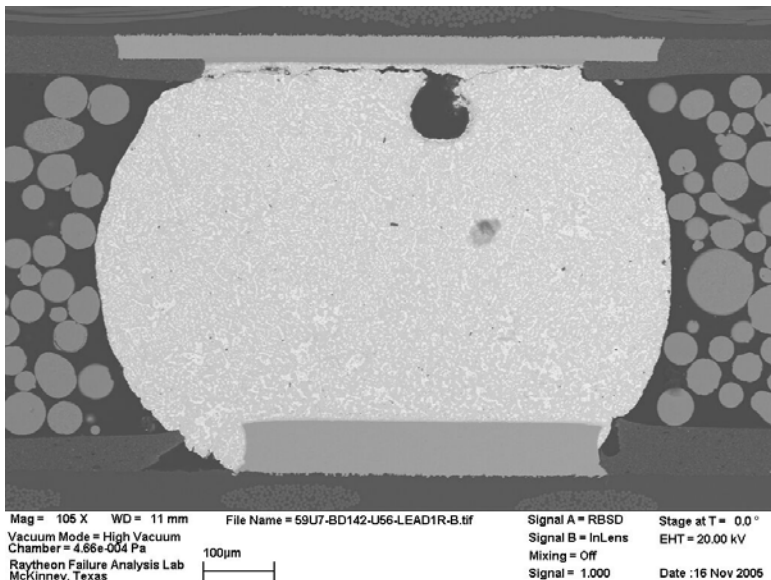


**Figure 69** SEM Micrograph of SnAgCuBi Soldered SnPb BGA-225 on Manufactured Test Vehicle (SN 142, U56, Bump 1R)

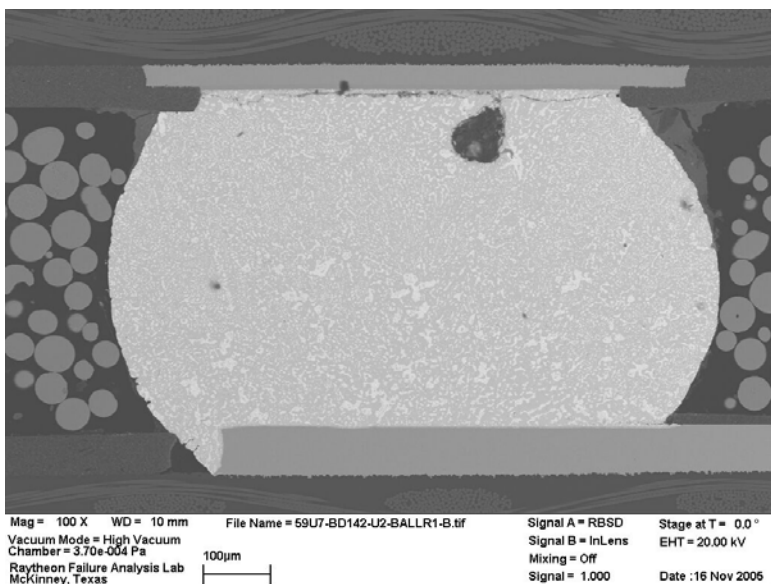


**Figure 70** SEM Micrograph of SnAgCuBi Soldered SnPb BGA-225 on Manufactured Test Vehicle (SN 142, U2, Bump 1R)

CLCC-20

**Table 16** Summary of Intermetallic Compound Thickness on Tin-Silver-Copper-Bismuth Solder Joints of CLCC-20 Components on Manufactured Test Vehicles

SN	REFDES	Lead Finish	Lead	IMC Thickness, IC (um)	IMC Thickness, PWB (um)	IMC at IC	IMC at PWB	Observations
113	U9	SnPb	11	1.12 4.54	1.01 2.44	NiSn *CuSn	CuSn	Crack extends through solder joint. Appears to be voiding in solder below component.
113	U9	SnPb	5	903nm 5.28	1.23 2.62	NiSn *CuSn	CuSn	Crack extends through solder joint. Appears to be voiding in solder below component.
141	U45	SnAgCuBi	15	790nm 3.27	760nm 3.09	NiSn *CuSn	CuSn	Crack extends through solder joint. Appears to be voiding in solder below component.
141	U45	SnAgCuBi	1	764nm 4.02	468nm 3.04	NiSn *CuSn	CuSn	Minor cracking and voiding in solder. Crack extends into the tungsten (W) thick-film on the component metallurgy. Crack is not all the way through the joint.
141	U46	SnPb	11	811nm 2.30	1.17 1.69	NiSn *CuSn	CuSn	Crack and voiding in solder below component. Crack is not all the way through the solder fillet.
141	U46	SnPb	5	1.35 3.72	1.42 3.20	NiSn *CuSn	CuSn	Crack extends through solder joint. Appears to be voiding in solder below component.
142	U17	SnAgCuBi	11	724nm 3.25	779nm 4.83	NiSn *CuSn	CuSn	Crack extends through solder joint. Appears to be voiding in solder below component.
142	U17	SnAgCuBi	5	564nm 3.28	1.24 2.65	NiSn *CuSn	CuSn	Crack extends through solder joint. Appears to be voiding in solder below component. This component failed after only one cycle. The cause of the failure is likely due to something other than the solder since the solder was fractured due to fatigue.

\*Solder bond on the component side is made to a Ni layer. Presence of Cu is from the SnAgCuBi solder or due to migration from the board side interface.

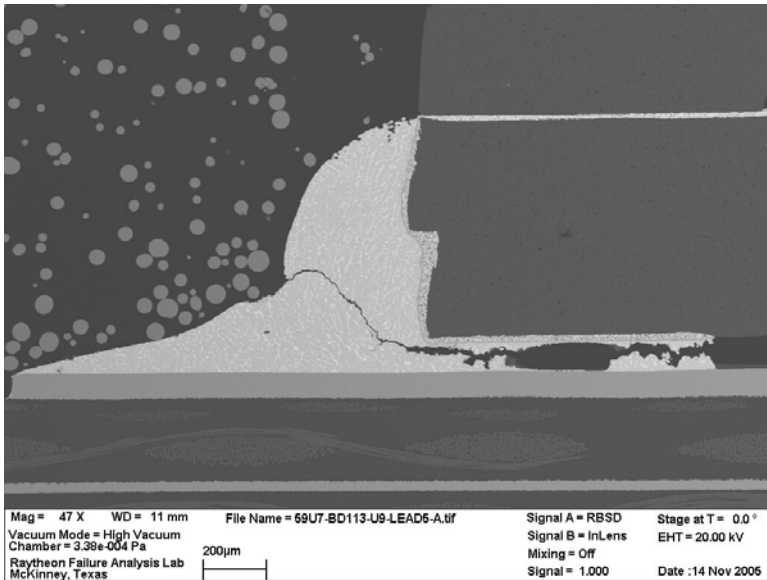


**Figure 71** SEM Micrograph of SnAgCuBi Soldered SnPb CLCC-20 on Manufactured Test Vehicle (SN 113, U9, Lead 5) Crack extends through the solder joint, it appears the solder was voided below the component.

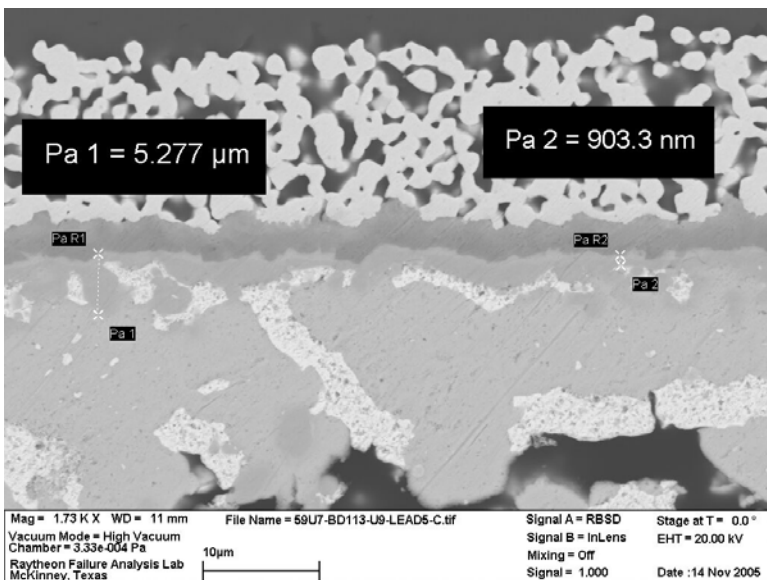


**Figure 72** SEM Micrograph of SnAgCuBi Soldered SnPb CLCC-20 on Manufactured Test Vehicle (SN 113, U9, Lead 5) Solder to component interface showing measurements of the NiSn IMC layer. The metallurgy on the component is a W thick-film followed by a Ni layer. The solder bonds to the Ni and forms a NiSn IMC. Some CuSn is also present near the component interface due to Cu migrating from the board side interface.

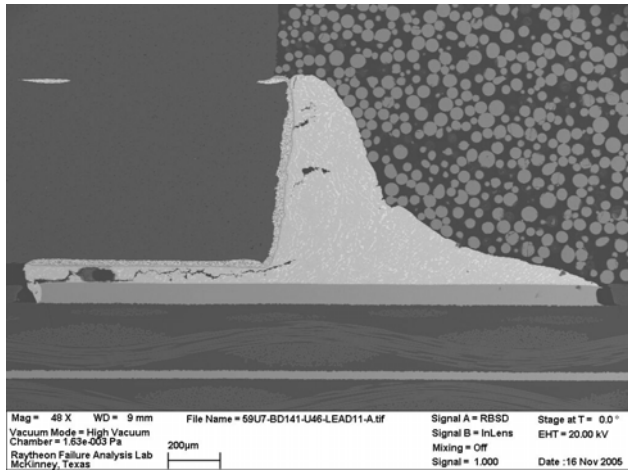


**Figure 73** SEM Micrograph of SnAgCuBi Soldered SnPb CLCC-20 on Manufactured Test Vehicle (SN 141, U46, Lead 11) Crack below the component, crack does not extend all the way through the solder fillet.

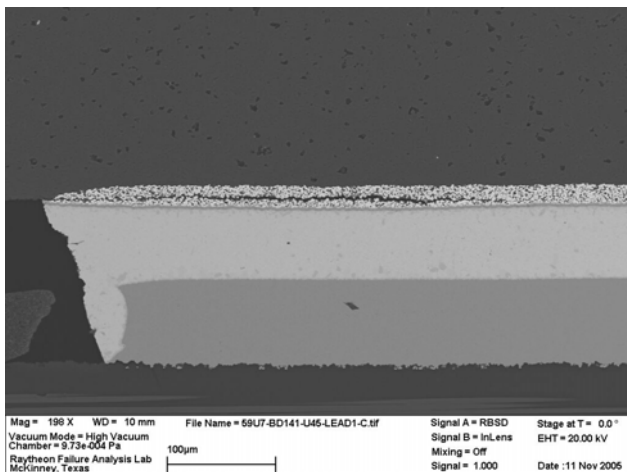


**Figure 74** SEM Micrograph of SnAgCuBi Soldered SnAgCuBi CLCC-20 on Manufactured Test Vehicle (SN 141, U45, Lead 1) Crack in the W thick-film at the component.

*PLCC-20*

**Table 17** Summary of Intermetallic Compound Thickness on Tin-Silver-Copper-Bismuth Solder Joints of PLCC-20 Components on Manufactured Test Vehicles

SN	REDES	Lead Finish	Lead	IMC Thickness, IC (um)	IMC Thickness, PWB (um)	IMC at IC	IMC at PWB	Observations
140	U54	Sn	10	553nm 3.02	1.39 5.20	CuSn	CuSn	Small isolated cracks near lead interface, solder not cracked all the way through.
140	U54	Sn	16	589nm 2.94	1.02 5.67	CuSn	CuSn	No cracks.

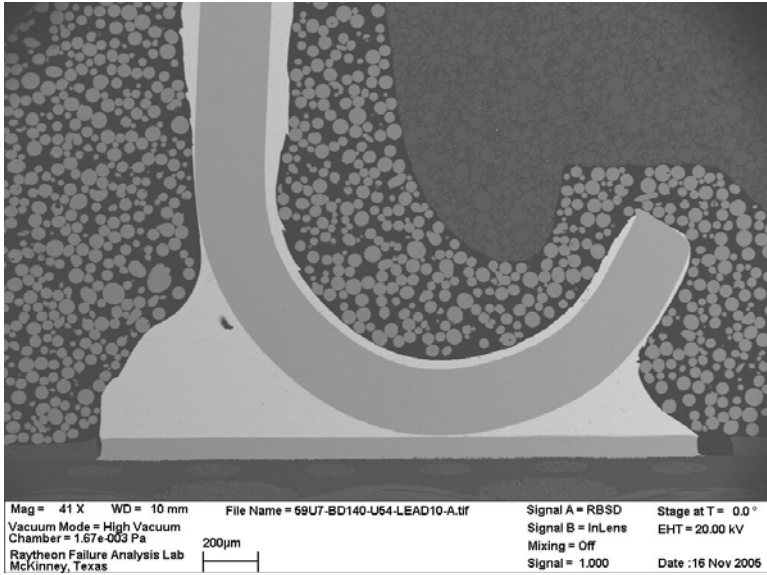


**Figure 75** SEM Micrograph of SnAgCuBi Soldered Sn PLCC-20 on Manufactured Test Vehicle (SN 140, U54, Lead 10)

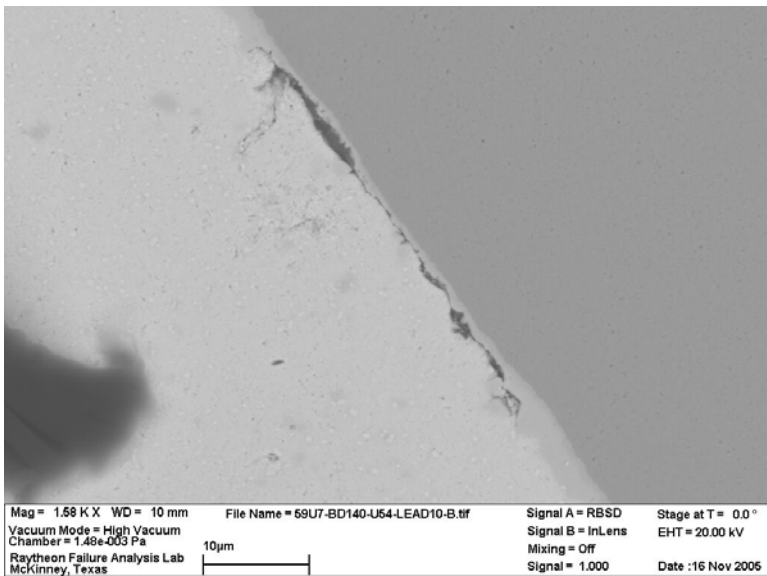


**Figure 76** SEM Micrograph of SnAgCuBi Soldered Sn PLCC-20 on Manufactured Test Vehicle (SN 140, U54, Lead 10) Small crack near lead intermetallic interface. EDS data of solder joint indicates metallurgy in Figure 77 and Figure 78.

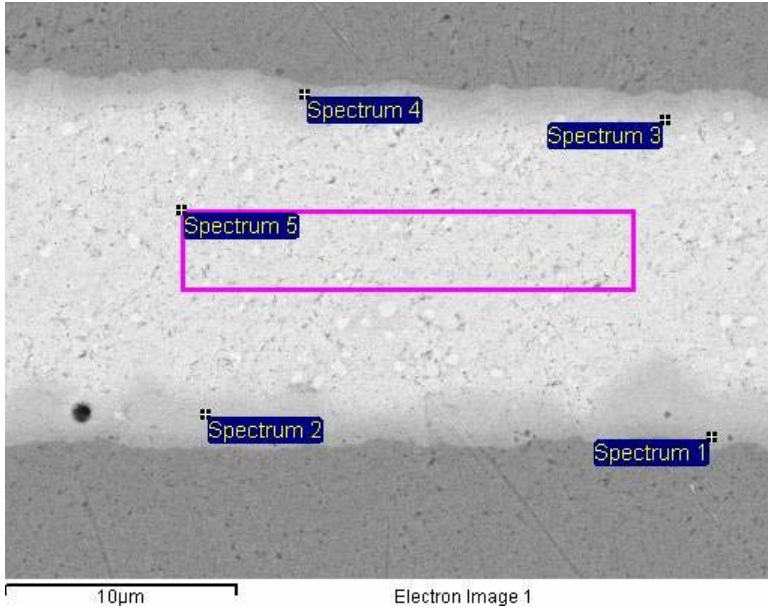


**Figure 77** SEM Micrograph of SnAgCuBi Soldered Sn PLCC-20 on Manufactured Test Vehicle (SN 140, U54, Lead 10) Image shows intermetallic layer at lead (top) and board (bottom) interfaces.

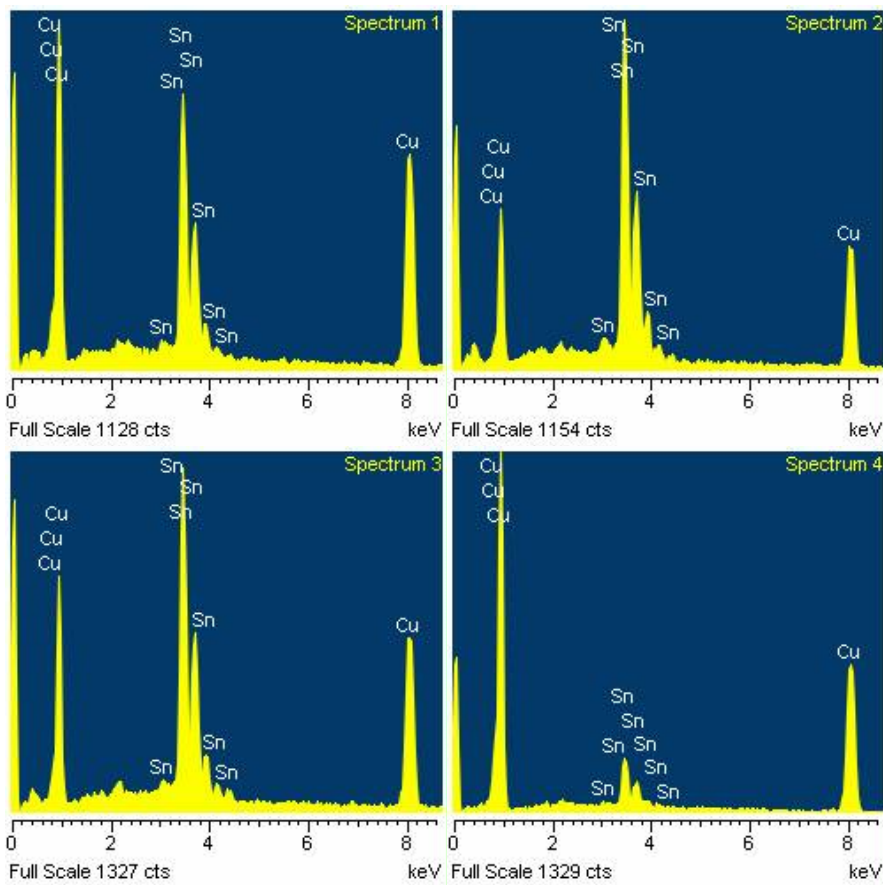


**Figure 78** EDS Spectra of SnAgCuBi Soldered Sn PLCC-20 on Manufactured Test Vehicle (SN 140, U54, Lead 10) Intermetallic layer at both interfaces is CuSn.

TQFP-144

**Table 18** Summary of Intermetallic Compound Thickness on Tin-Silver-Copper-Bismuth Solder Joints of TQFP-144 Components on Manufactured Test Vehicles

SN	REFDES	Lead Finish	Lead	IMC Thickness, IC (um)	IMC Thickness, PWB (um)	IMC at IC	IMC at PWB	Observations
139	U1	Sn	109	603nm 3.60	1.01 5.48	CuSn	CuSn	Crack extends all the way through solder joint along the lead interface. Small voids in solder
139	U1	Sn	72	1.03 3.30	906nm 5.01	CuSn	CuSn	Crack extends approximately ¾ through solder joint near the lead interface. Small voids in solder
142	U58	Sn	36	891nm 4.10um	891nm 3.03um	CuSn	CuSn	Crack in solder initiating from the inside of the lead extends about half way in. Crack is at the solder to IMC interface.
142	U58	Sn	73	1.16 4.28	1.25 4.55	CuSn	CuSn	Similar to Lead 36.

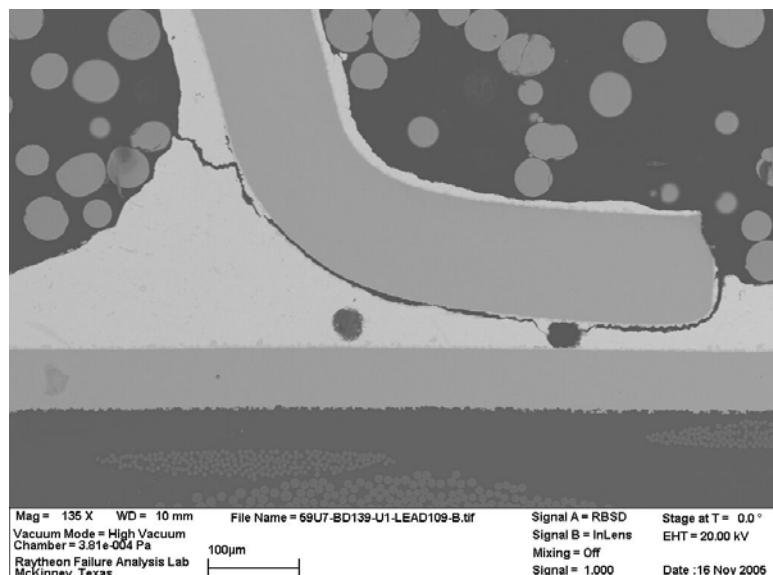


**Figure 79** SEM Micrograph of SnAgCuBi Soldered Sn TQFP-144 on Manufactured Test Vehicle (SN 139, U1, Lead 109) Crack extends through the solder, along the lead interface after the crack gets through the heel solder fillet.

TQFP-208

**Table 19** Summary of Intermetallic Compound Thickness on Tin-Silver-Copper-Bismuth Solder Joints of TQFP-208 Components on Manufactured Test Vehicles

SN	REFDES	Lead Finish	Lead	IMC Thickness, IC (um)	IMC Thickness, PWB (um)	IMC at IC	IMC at PWB	Observations
139	U57	AuPdNi	104	1.23 6.25	928nm 3.90	*NiSnCu	CuSn	Crack extends approximately ½ through solder joint near the lead interface. Small voids in solder
139	U57	AuPdNi	157	1.19 9.28	1.01 4.44	*NiSnCu	CuSn	Crack extends approximately ½ through solder joint near the lead interface. Small voids in solder
142	U31	AuPdNi	125	1.00 3.87	979nm 5.23	*NiSnCu	CuSn	Crack extends approximately ½ through solder along the lead IMC to solder interface.
142	U31	AuPdNi	52	858nm 3.28	548nm 2.90	*NiSnCu	CuSn	Crack extends approximately ½ through solder along the lead IMC to solder interface.

\*Solder bond is made to AuPdNi plating at the lead interface forming a NiSn IMC, CuSn IMC is also present. Cu is either from SnAgCuBi solder or migrated from the board side interface.

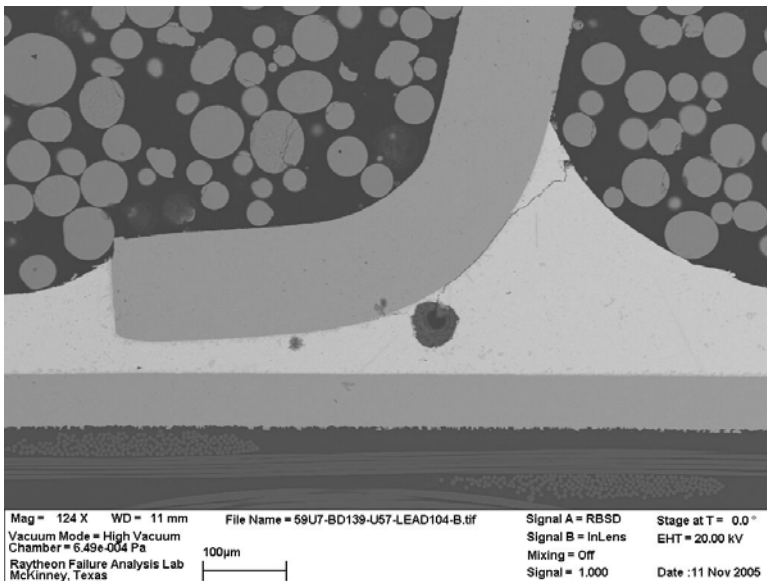


**Figure 80** SEM Micrograph of SnAgCuBi Soldered AuPdNi TQFP-208 on Manufactured Test Vehicle (SN 139, U57, Lead 104) Partial crack through the solder at the lead to IMC interface.

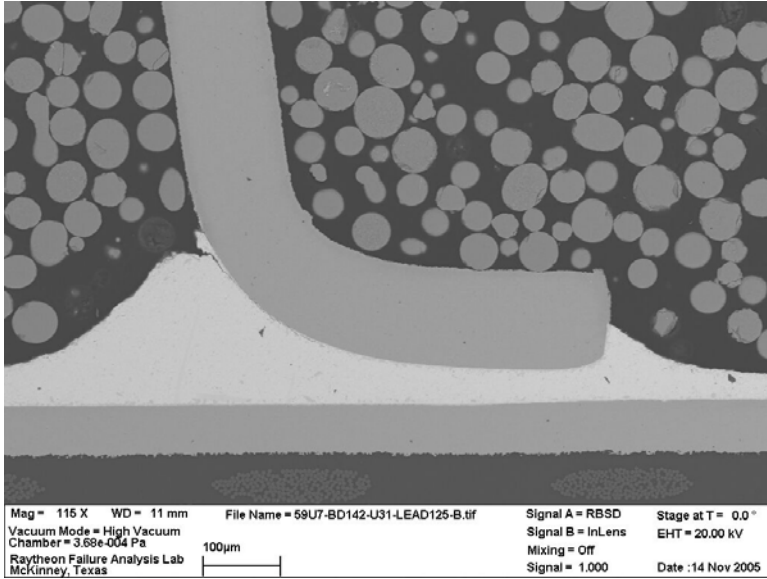


**Figure 81** SEM Micrograph of SnAgCuBi Soldered AuPdNi TQFP-208 on Manufactured Test Vehicle (SN 142, U31, Lead 125) Crack approximately 1/2 through the solder along the lead IMC to solder interface.

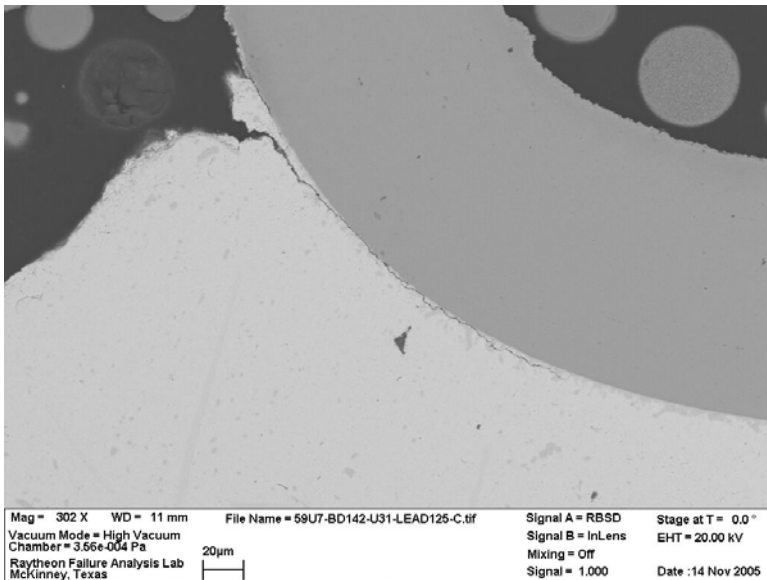


**Figure 82** SEM Micrograph of SnAgCuBi Soldered AuPdNi TQFP-208 on Manufactured Test Vehicle (SN 142, U31, Lead 125) Crack approximately 1/2 through the solder along the lead IMC to solder interface.

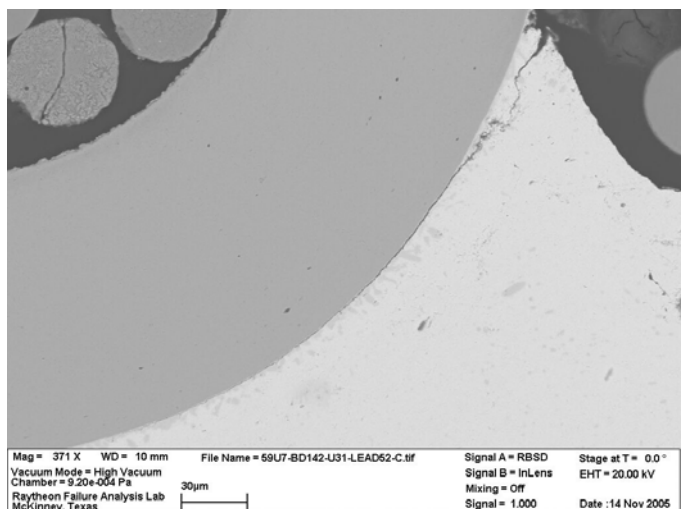


**Figure 83** SEM Micrograph of SnAgCuBi Soldered AuPdNi TQFP-208 on Manufactured Test Vehicle (SN 142, U31, Lead 52)

TSOP-50

**Table 20** Summary of Intermetallic Compound Thickness on Tin-Silver-Copper-Bismuth Solder Joints of TSOP-50 Components on Manufactured Test Vehicles

SN	REFDES	Lead Finish	Lead	IMC Thickness, IC (um)	IMC Thickness, PWB (um)	IMC at IC	IMC at PWB	Observations
141	U24	SnPb	1	---	1.17 3.62	NiSn & *CuSn	CuSn	Component missing, came off board during testing.
141	U24	SnPb	50	---	850nm 5.03	NiSn & *CuSn	CuSn	Component missing, came off board during testing.
142	U29	SnCu	1	---	676nm 3.84	NiSn & *CuSn	CuSn	Component missing, came off board during testing.
142	U29	SnCu	50	---	1.62 3.97	NiSn & *CuSn	CuSn	Component missing, came off board during testing.
142	U25	SnCu	25	279nm 1.72	1.17 2.77	NiSn & *CuSn	CuSn	Crack extends all the way through solder. Large void in solder.
142	U25	SnCu	26	269nm	1.26 3.14	NiSn & *CuSn	CuSn	Crack extends all the way through solder.
142	U24	SnPb	2		1.21 3.27	NiSn & *CuSn	CuSn	Component missing, came off board during testing.
142	U24	SnPb	49		1.49 3.45	NiSn & *CuSn	CuSn	Component missing, came off board during testing.

\*The presence of Cu at the Component side interface of the TSOP is the result of Cu migration from the board side interface and/or Cu from the SAC solder. The solder bond at the component side is made to a Ni layer interface.

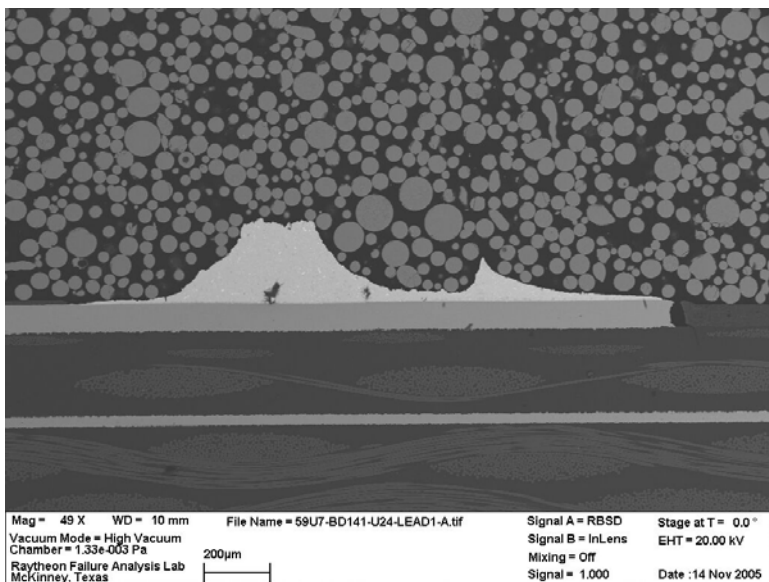


**Figure 84** SEM Micrograph of SnAgCuBi Soldered SnPb TSOP-50 on Manufactured Test Vehicle (SN 141, U24, Lead 1) Component missing, came off during testing.

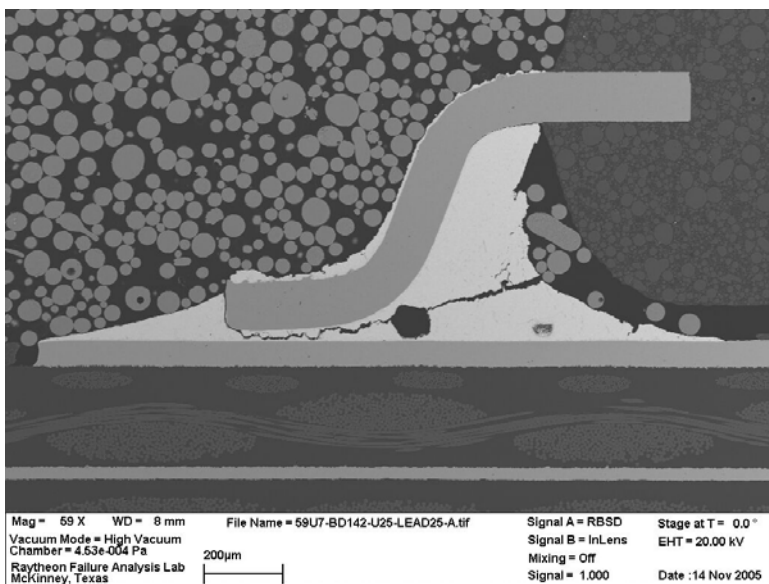


**Figure 85** SEM Micrograph of SnAgCuBi Soldered SnCu TSOP-50 on Manufactured Test Vehicle (SN 142, U25, Lead 25) Crack through the solder, also a void in the solder. EDS data of joint present in Figure 86 and Figure 87.

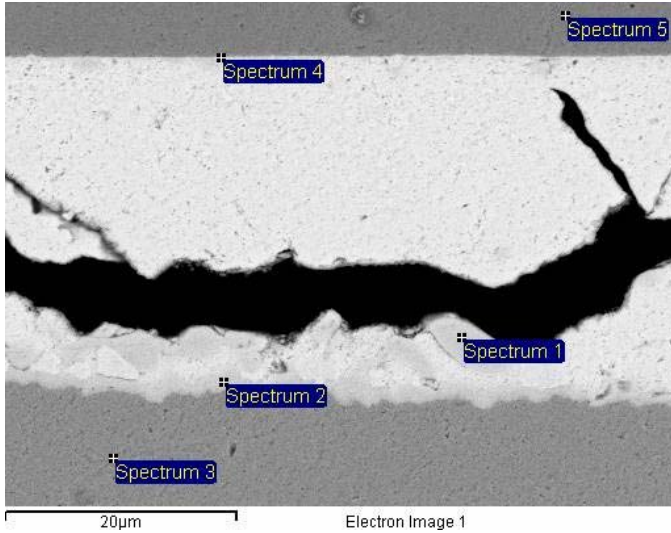


**Figure 86** SEM Micrograph of SnAgCuBi Soldered SnCu TSOP-50 on Manufactured Test Vehicle (SN 142, U25, Lead 25) Lead to solder to board metallurgy.

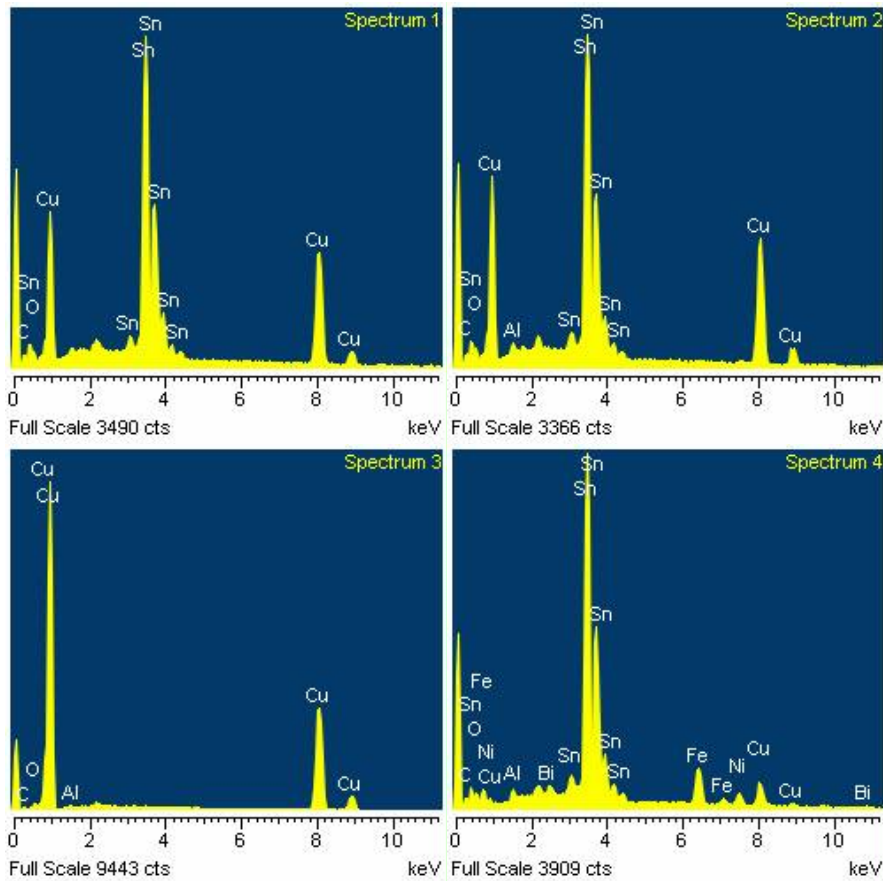


**Figure 87** EDS Spectra of SnAgCuBi Soldered SnCu TSOP-50 on Manufactured Test Vehicle (SN 142, U25, Lead 25) IMC at board CuSn (Spectra 1 and 2), board pad is Cu (Spectrum 3), IMC at component lead is NiSn and CuSn, solder bonds to alloy 42 (Ni-Fe) lead, presence of Cu at this interface is the result of Cu migration from the board or Cu from the SnAgCuBi solder.

**Tin-Copper Solder**

*PDIP-20*

**Table 21** Summary of Intermetallic Compound Thickness on Tin-Copper Solder Joints of PDIP-20 Components on Manufactured Test Vehicles

SN	REDES	Lead Finish	Lead	IMC Thickness, IC (um)	IMC Thickness, PWB (um)	IMC at IC	IMC at PWB	Observations
140	U51	Sn	10	776nm 2.44	655 2.08	CuSn	AgSnCu	Cracks in solder on both sides of lead near lead interface.
140	U51	Sn	1	655nm 1.34	1.30 3.33	CuSn	AgSnCu	Cracks in solder on both sides of lead near lead interface.
142	U35	AuPdNi	10	583nm 1.09	1.66 2.30	CuSn	AgSnCu	Cracks are in PWB near the PTH plating interface. Cracks extend down hole along Cu plating interface. Solder did not crack PWB cracked.
142	U35	AuPdNi	1	1.07 2.94		CuSn	AgSnCu	Solder did not crack. Small isolated cracks in the PWB near the bottom of the PTH.

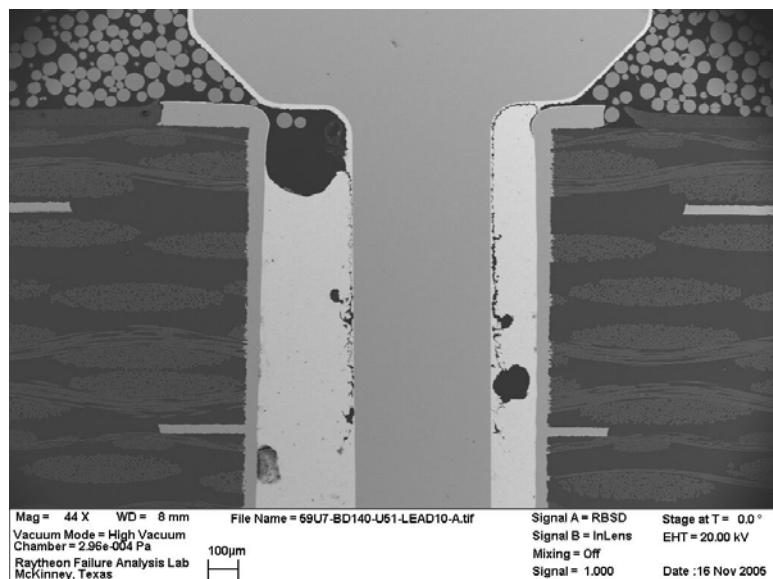


**Figure 88** SEM Micrograph of SnCu Soldered Sn PDIP-20 on Manufactured Test Vehicle (SN 140, U51, Lead 10) Cracks in solder on both side of the lead. The metallurgy was examined by EDS in Figure 91, Figure 92, Figure 93 and Figure 94.

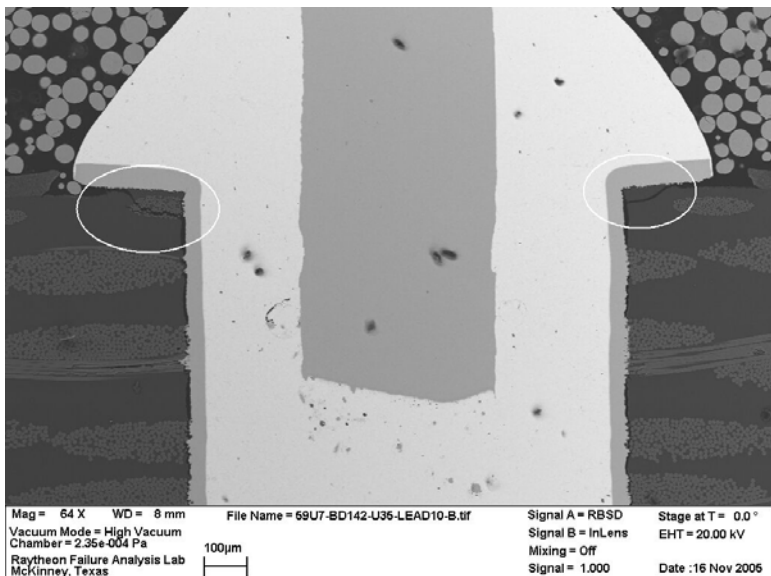


**Figure 89** SEM Micrograph of SnCu Soldered AuPdNi PDIP-20 on Manufactured Test Vehicle (SN 142, U35, Lead 10) Cracks in the PWB, top corners and extending into the PWB along the Cu plating interface.

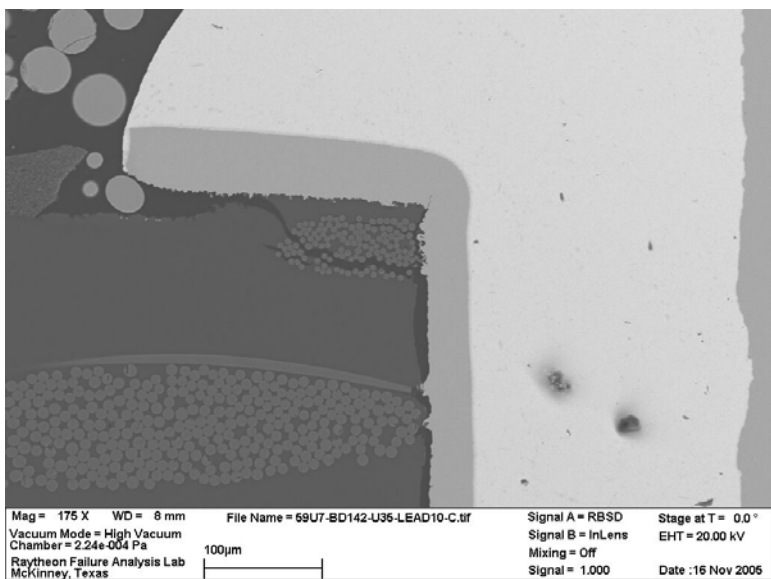


**Figure 90** SEM Micrograph of SnCu Soldered AuPdNi PDIP-20 on Manufactured Test Vehicle (SN 142, U35, Lead 10) Crack in the PWB.

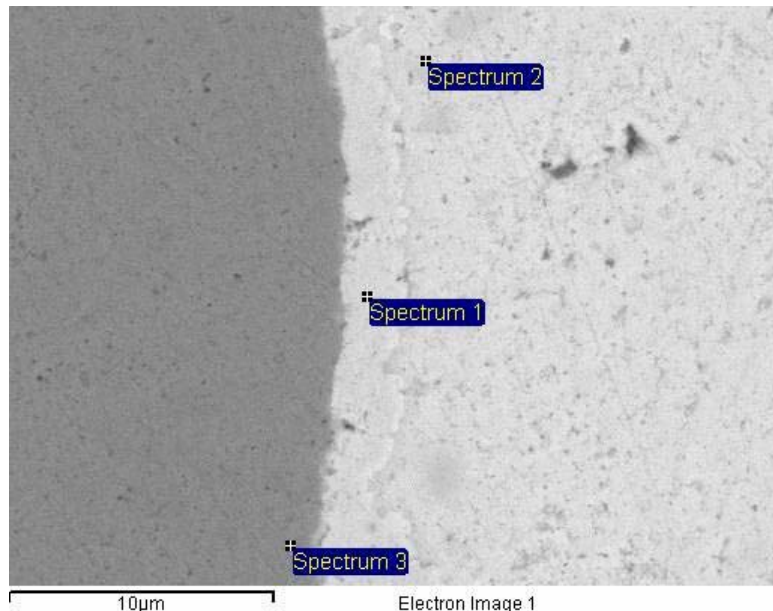


**Figure 91** SEM Micrograph of SnCu Soldered Sn PDIP-20 on Manufactured Test Vehicle (SN 140, U51) Board Interface.

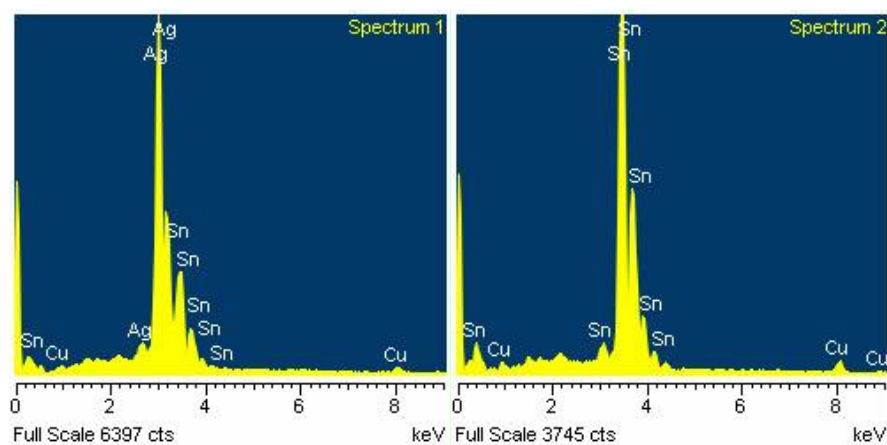


**Figure 92** EDS Spectra of SnCu Soldered Sn PDIP-20 on Manufactured Test Vehicle (SN 140, U51) The IMC layer is AgSnCu (Spectrum 1); the solder is SnAgCuBi (Spectrum 2). The board metal is Cu, spectrum not shown. The Ag is from the immersion Ag finish on the board.

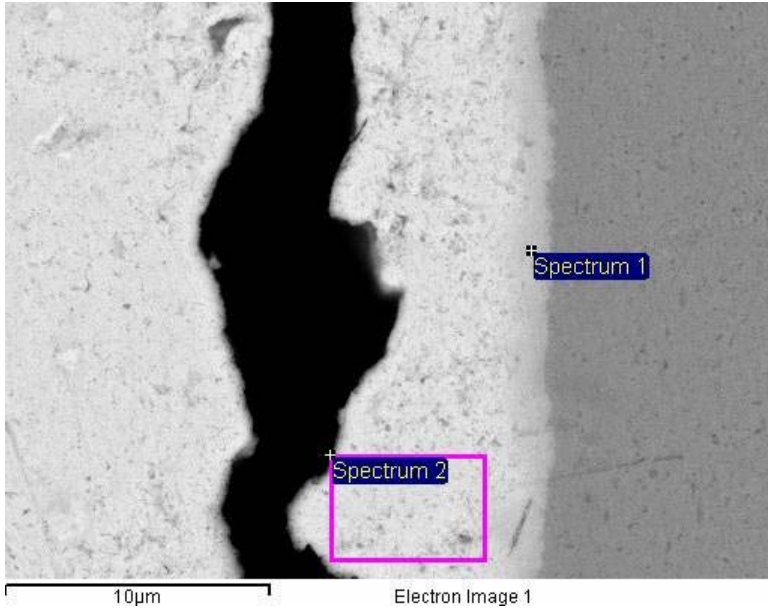


Figure 93 SEM Micrograph of SnCu Soldered Sn PDIP-20 on Manufactured Test Vehicle (SN 140, U51) Lead Interface.

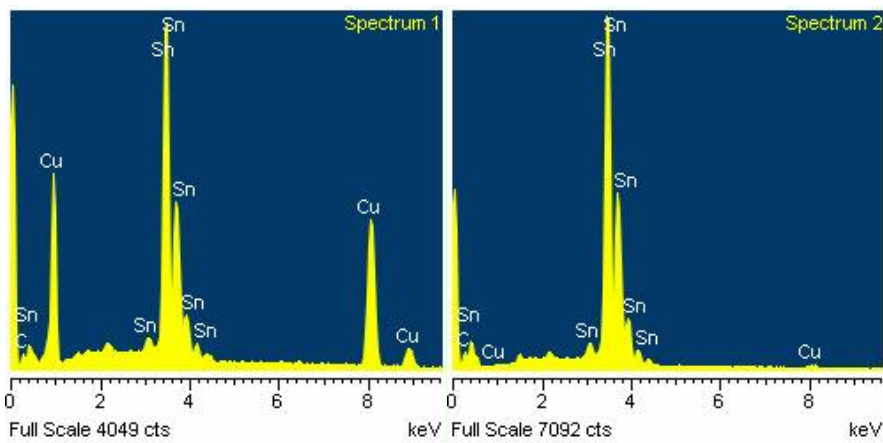


Figure 94 EDS Spectra of SnCu Soldered Sn PDIP-20 on Manufactured Test Vehicle (SN 140, U51) IMC layer at board interface is CuSn.

### Rework Test Vehicle Results and Discussion

The rework test vehicles were tested for 550 cycles. The HALT chamber experienced an over temperature condition during cycle 537. The failure data were truncated at 536 cycles and failures detected during cycle 537 and higher were excluded from analysis. Due to the over temperature condition, a larger number of components were missing from the test vehicles at the conclusion of the test than was experienced with the manufacture test vehicles.

Raytheon Materials & Process Engineering selected a number of reworked components to be microsectioned and is tabulated in Table 30 on page 101. Due to the over temperature condition, only the reworked TQFP-208 devices soldered with tin-silver-copper-bismuth soldered were analyzed with the SEM/EDS and presented in the following section.

***Tin-Silver-Copper-Bismuth Solder***

*TQFP-208*

**Table 22** Summary of Intermetallic Compound Thickness on Reworked TQFP-208 Soldered with Tin-Silver-Copper-Bismuth Solder Alloy on Rework Test Vehicles

SN	REFDES	Lead Finish	Lead	IMC Thickness, IC (um)	IMC Thickness, PWB (um)	IMC at IC	IMC at PWB	Observations
200	U57	AuPdNi	Left	287 nm 1.13	1.45 3.75	NiSnCu Low levels of Au also detected	CuSn Low levels of Au and Ni also sometimes detected	Separation between lead IMC and solder. Separation not occurring through the solder as seen in other joints in this study. Some voiding present between the solder and IMC on the board side. Microcracks in solder below lead. Cracks present in solder mask and board below component.
200	U57	AuPdNi	Right	277 nm 1.06	1.25 2.51	NiSnCu Low levels of Au also detected	CuSn Low levels of Au and Ni also sometimes detected	Separation occurring between lead IMC and solder extending about ¼ of the way into joint. Some voiding present at interface at the lead toe.
201	U3	AuPdNi	20	---	2.02 2.24 3.30 6.86	NiSnCu Low levels of Au also detected	CuSn Low levels of Au and Ni also sometimes detected	Component missing due to fractured solder. Microcracks present in the solder. Voiding at the solder to IMC interface. It appears the solder did not wet well to the board pad at the time of rework.
201	U3	AuPdNi	53	---	1.90 2.23	NiSnCu Low levels of Au also detected	CuSn Low levels of Au and Ni also sometimes detected	Component missing. Similar in appearance to Lead 20.
203	U3	AuPdNi	Left	---	2.01 3.13	NiSnCu Low levels of Au also detected	CuSn Low levels of Au and Ni also sometimes detected	Component missing. Microcracks present in the solder. Separation at solder to IMC interface result of poor wetting of the solder.

SN	REFDES	Lead Finish	Lead	IMC Thickness, IC (um)	IMC Thickness, PWB (um)	IMC at IC	IMC at PWB	Observations
203	U3	AuPdNi	Right	---	2.08	NiSnCu Low levels of Au also detected	CuSn Low levels of Au and Ni also sometimes detected	Component missing. Separation result of poor wetting of the solder.
204	U57	AuPdNi	105	558 nm 781 nm	2.12 4.02	NiSnCu Low levels of Au also detected	CuSn Low levels of Au and Ni also sometimes detected	Crack extends completely through joint at lead to solder interface. There is not an even dispersion of PbBi phases. These phases have a heavier concentration in the solder fillet as opposed to below the lead.
204	U57	AuPdNi	53	520 nm 1.00	1.31 2.97	NiSnCu Low levels of Au also detected	CuSn Low levels of Au and Ni also sometimes detected	Crack extends completely through joint at lead to solder interface. Separation at solder to board interface. This could be the result of poor wetting of the solder. Cracks in solder mask and board below component.

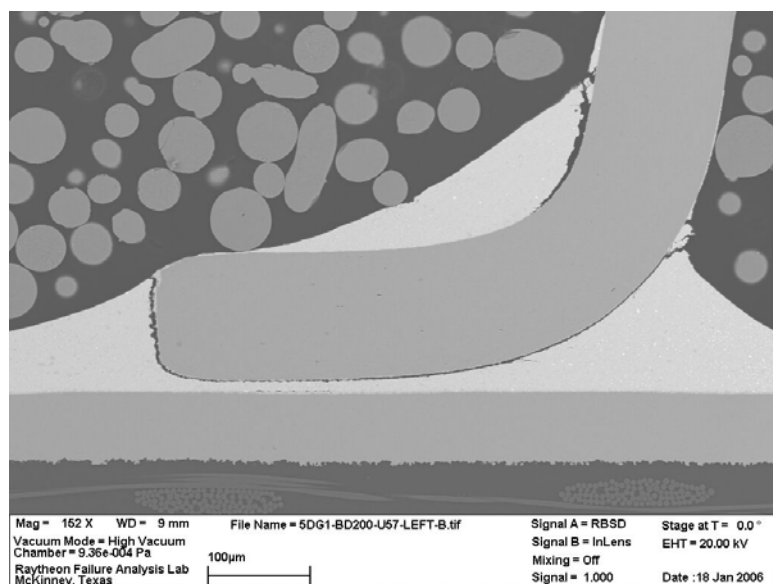


**Figure 95** SEM Micrograph of Reworked AuPdNi TQFP-208 Soldered with Tin-Silver-Copper-Bismuth Solder Alloy on Rework Test Vehicles (SN 200, U57, Lead Left) Separation present between lead and solder extending

completely through joint. Separation is not occurring through the solder as seen in other joints in this study. Separation is also present on the top of the lead at the interface.

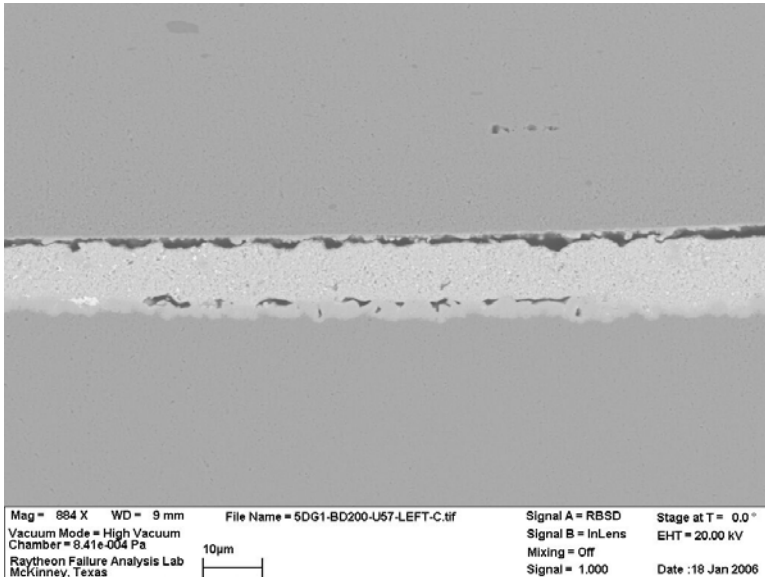


**Figure 96** SEM Micrograph of Reworked AuPdNi TQFP-208 Soldered with Tin-Silver-Copper-Bismuth Solder Alloy on Rework Test Vehicles (SN 200, U57, Lead Left) Some voiding present between the solder and intermetallic layer on the board side.

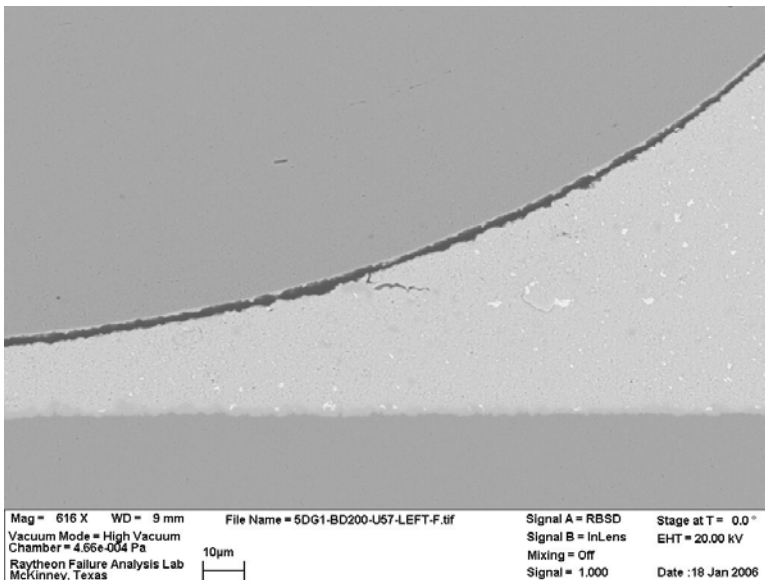


**Figure 97** SEM Micrograph of Reworked AuPdNi TQFP-208 Soldered with Tin-Silver-Copper-Bismuth Solder Alloy on Rework Test Vehicles (SN 200, U57, Lead Left) Microcracks in solder below lead.

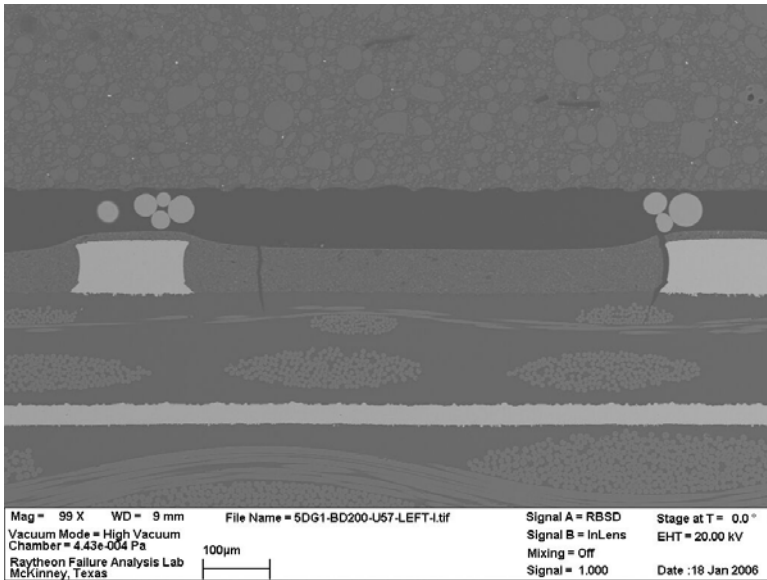


**Figure 98** SEM Micrograph of Reworked AuPdNi TQFP-208 Soldered with Tin-Silver-Copper-Bismuth Solder Alloy on Rework Test Vehicles (SN 200, U57, Lead Left) Cracks present in solder mask and board below component.

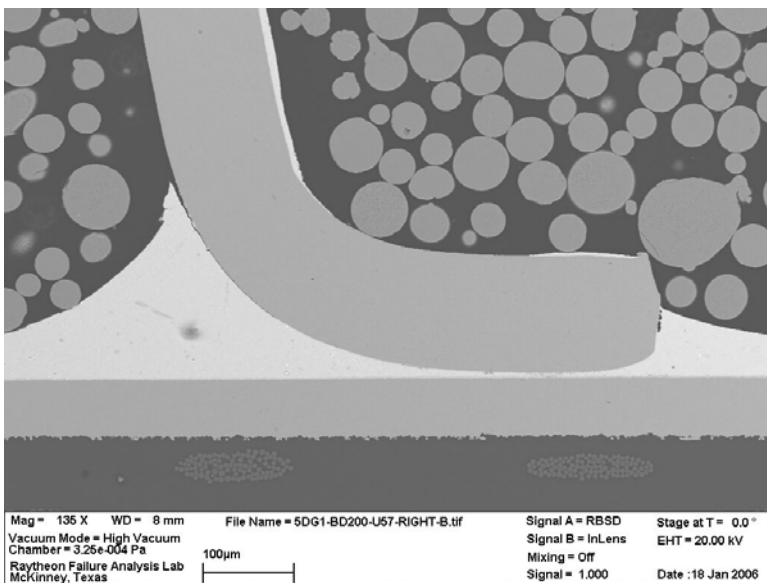


**Figure 99** SEM Micrograph of Reworked AuPdNi TQFP-208 Soldered with Tin-Silver-Copper-Bismuth Solder Alloy on Rework Test Vehicles (SN 200, U57, Lead Right) Separation occurring between lead intermetallic layer and solder extending about 1/4 of the way into joint.

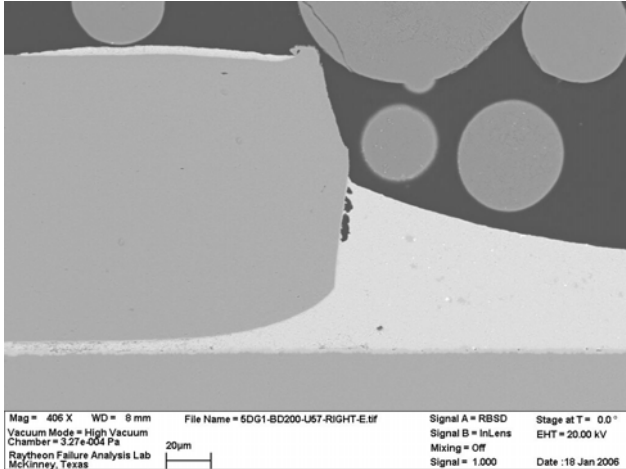


**Figure 100** SEM Micrograph of Reworked AuPdNi TQFP-208 Soldered with Tin-Silver-Copper-Bismuth Solder Alloy on Rework Test Vehicles (SN 200, U57, Lead Right) Some voiding is present at interface at the lead toe.

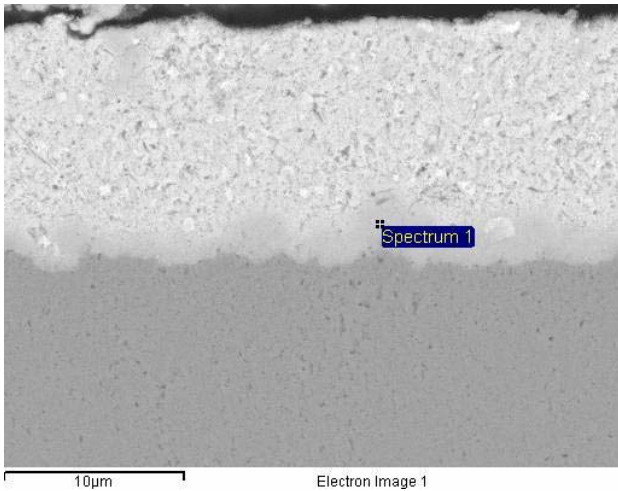


**Figure 101** SEM Micrograph of Reworked AuPdNi TQFP-208 Soldered with Tin-Silver-Copper-Bismuth Solder Alloy on Rework Test Vehicles (SN 200, U57, left side lead, board interface)

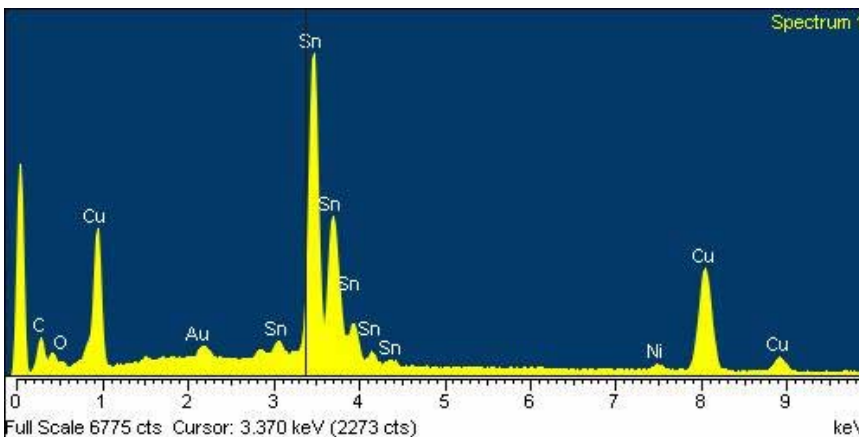


**Figure 102** EDS Spectra of Reworked AuPdNi TQFP-208 Soldered with Tin-Silver-Copper-Bismuth Solder Alloy on Rework Test Vehicles (SN 200, U57, left side lead, board interface) The intermetallic layer is CuSn however, low levels of Ni and Au are also present.

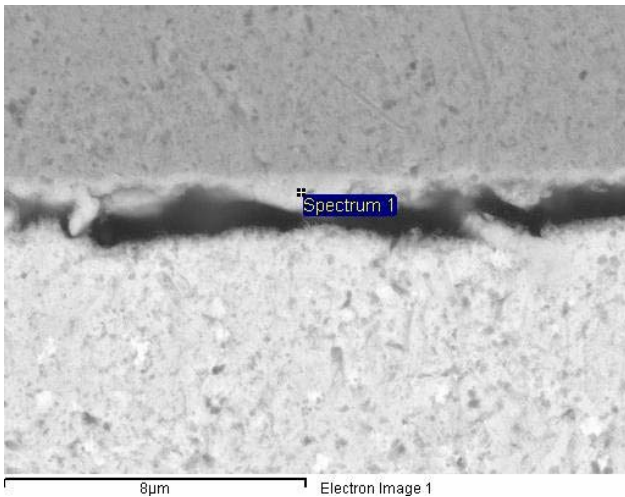


**Figure 103** SEM Micrograph of Reworked AuPdNi TQFP-208 Soldered with Tin-Silver-Copper-Bismuth Solder Alloy on Rework Test Vehicles (SN 200, U57, left side lead, component interface) The fracture is at the lead IMC to solder interface.

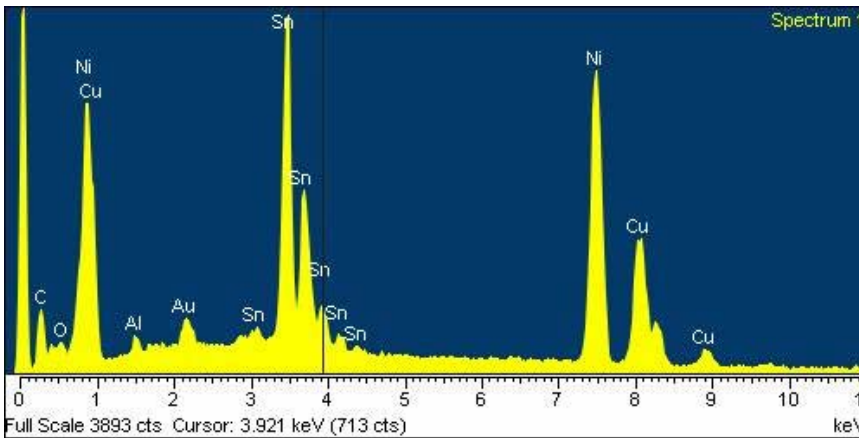


**Figure 104** EDS Spectra of Reworked AuPdNi TQFP-208 Soldered with Tin-Silver-Copper-Bismuth Solder Alloy on Rework Test Vehicles (SN 200, U57, left side lead, component interface) IMC is NiSnCu.

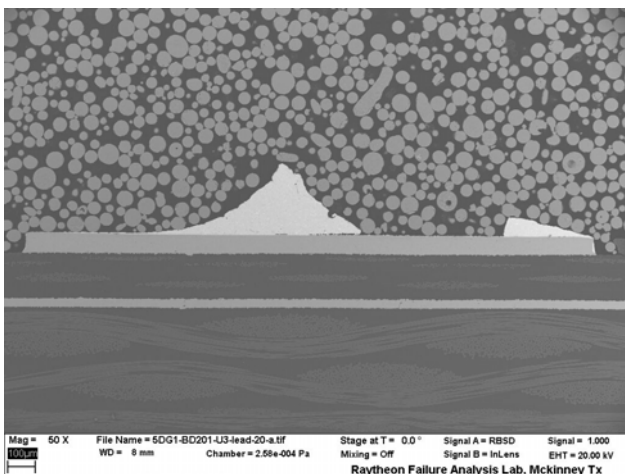


**Figure 105** SEM Micrograph of Reworked AuPdNi TQFP-208 Soldered with Tin-Silver-Copper-Bismuth Solder Alloy on Rework Test Vehicles (SN 201, U57, Lead 20) Component missing due to fractured solder.

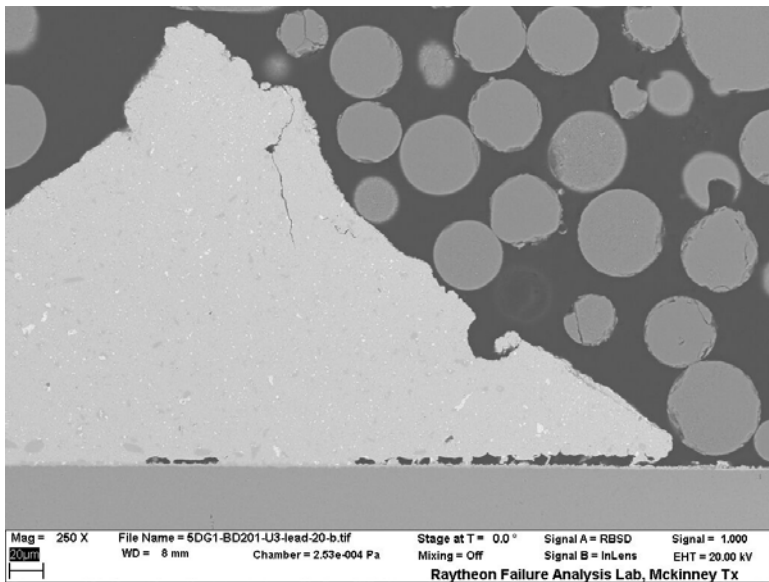


**Figure 106** SEM Micrograph of Reworked AuPdNi TQFP-208 Soldered with Tin-Silver-Copper-Bismuth Solder Alloy on Rework Test Vehicles (SN 201, U57, Lead 20) Microcracks present in the solder. Voiding at the solder to IMC interface. It appears the solder did not wet well to the board pad at the time of rework.

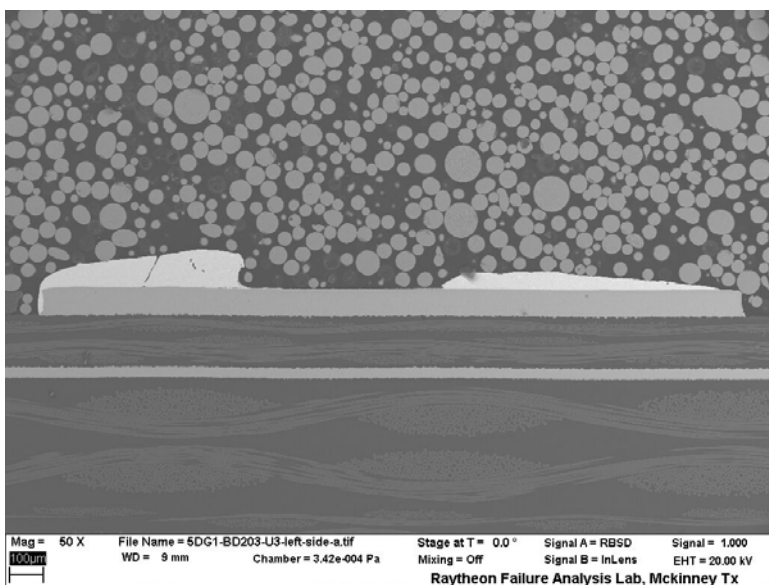


**Figure 107** SEM Micrograph of Reworked AuPdNi TQFP-208 Soldered with Tin-Silver-Copper-Bismuth Solder Alloy on Rework Test Vehicles (SN 203, U3, Lead Left) Component missing, the separation appears to have occurred at the component lead to solder interface likely due to poor wetting of the solder to the lead.

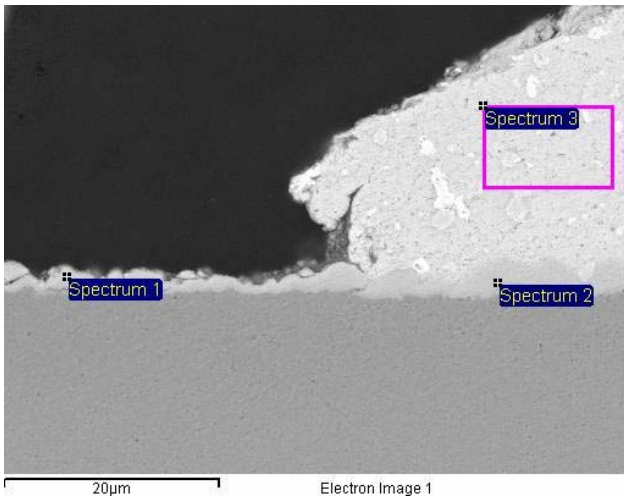


**Figure 108** SEM Micrograph of Reworked AuPdNi TQFP-208 Soldered with Tin-Silver-Copper-Bismuth Solder Alloy on Rework Test Vehicles (SN 203, U3, board interface)

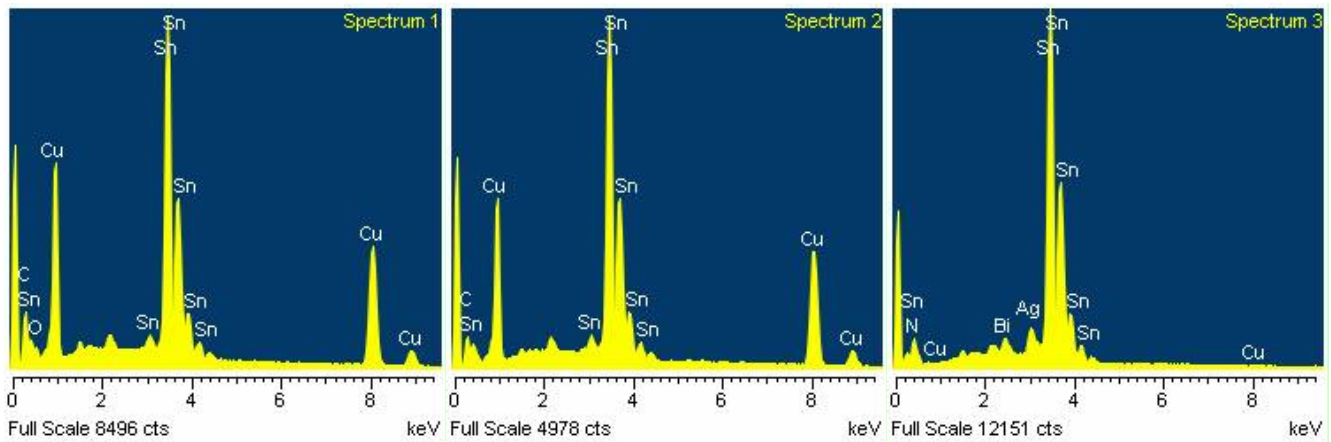


**Figure 109** EDS Spectra of Reworked AuPdNi TQFP-208 Soldered with Tin-Silver-Copper-Bismuth Solder Alloy on Rework Test Vehicles (SN 203, U3, board interface) IMC is CuSn.

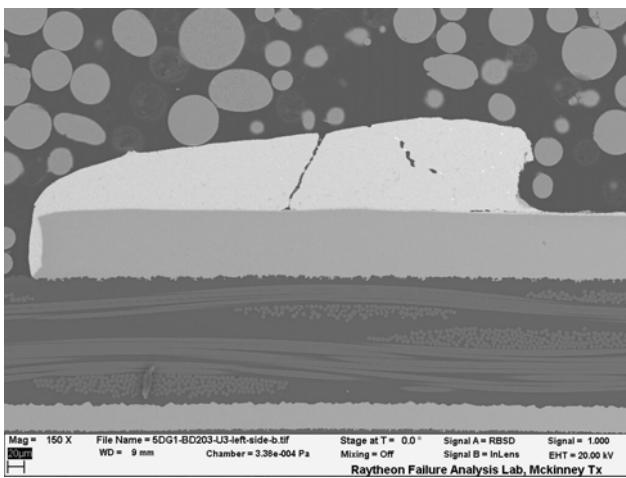


**Figure 110** SEM Micrograph of Reworked AuPdNi TQFP-208 Soldered with Tin-Silver-Copper-Bismuth Solder Alloy on Rework Test Vehicles (SN 203, U3, Lead Left) Microcracks present in the solder.

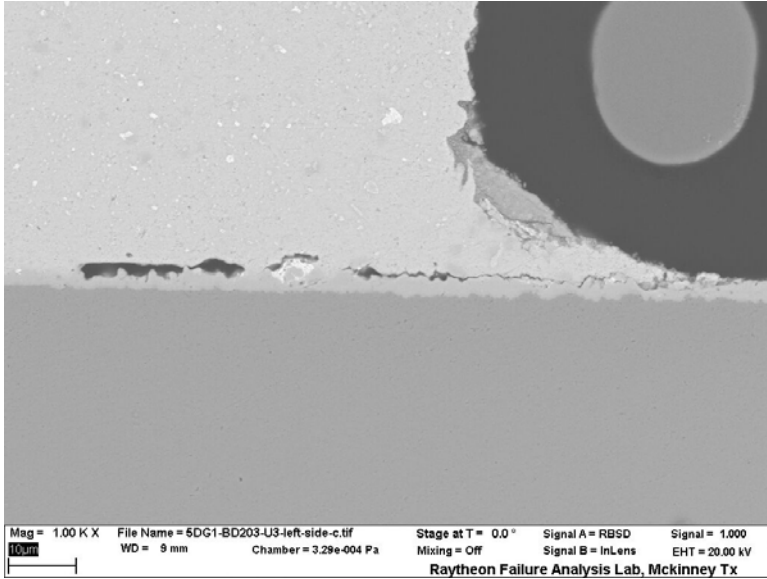


**Figure 111** SEM Micrograph of Reworked AuPdNi TQFP-208 Soldered with Tin-Silver-Copper-Bismuth Solder Alloy on Rework Test Vehicles (SN 203, U3, Lead Left) Separation at solder to IMC interface result of poor wetting of the solder.

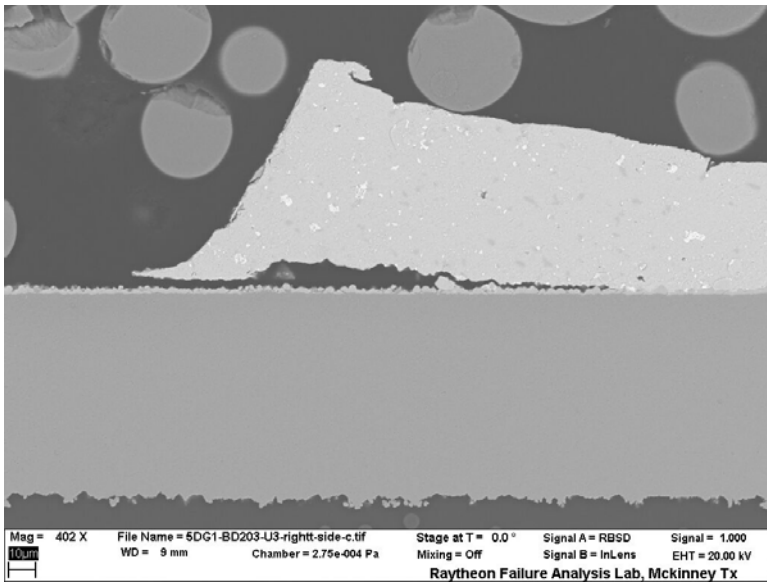


**Figure 112** SEM Micrograph of Reworked AuPdNi TQFP-208 Soldered with Tin-Silver-Copper-Bismuth Solder Alloy on Rework Test Vehicles (SN 203, U3, Lead Right) Component missing. Separation is the result of poor wetting of the solder.

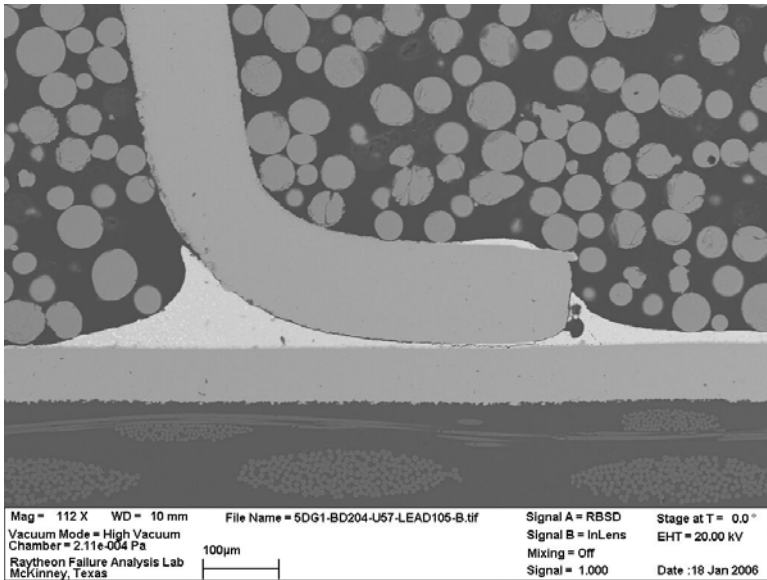


**Figure 113** SEM Micrograph of Reworked AuPdNi TQFP-208 Soldered with Tin-Silver-Copper-Bismuth Solder Alloy on Rework Test Vehicles (SN 204, U57, Lead 105) Crack extends completely through joint at lead to solder interface. Some voiding present near toe of lead.

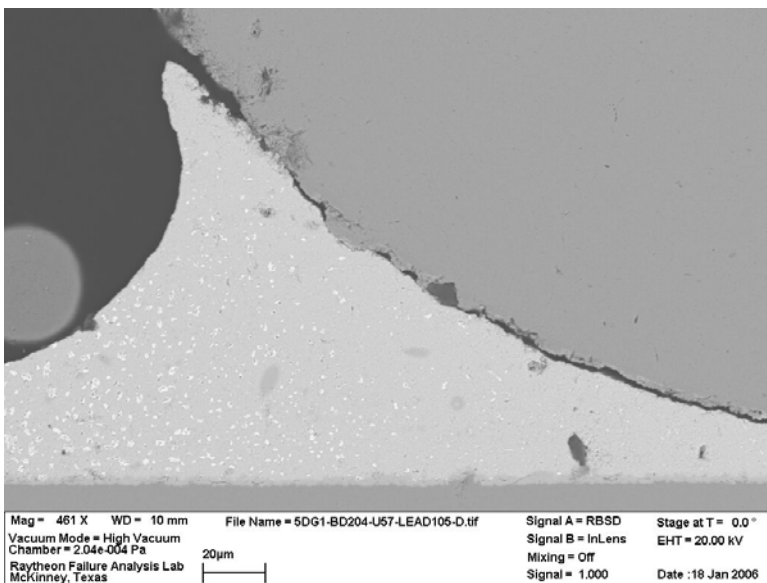


**Figure 114** SEM Micrograph of Reworked AuPdNi TQFP-208 Soldered with Tin-Silver-Copper-Bismuth Solder Alloy on Rework Test Vehicles (SN 204, U57, Lead 105) There is not an even dispersion of lead-bismuth (PbBi) phases. These phases have a heavier concentration in the solder fillet as opposed to below the lead.

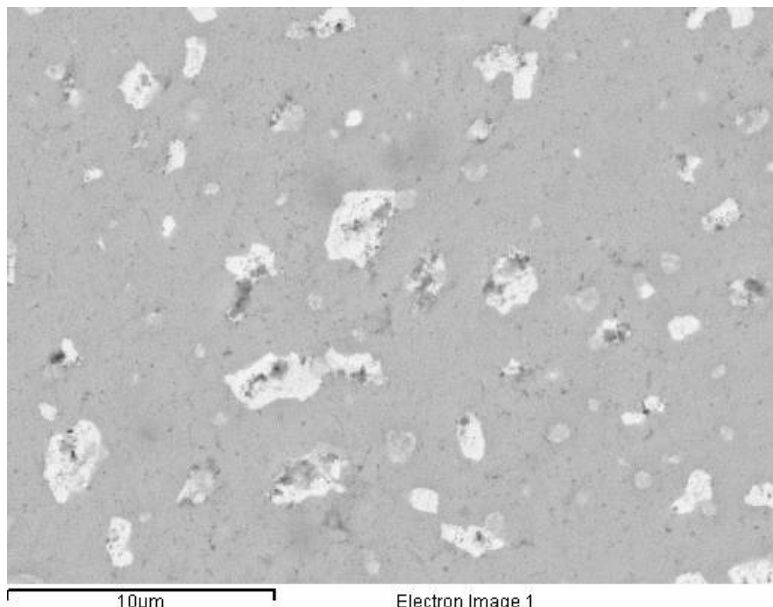


**Figure 115** SEM Micrograph of Reworked AuPdNi TQFP-208 Soldered with Tin-Silver-Copper-Bismuth Solder Alloy on Rework Test Vehicles (SN 204, U57, Lead 105) The bright phases are a PbBi alloy.

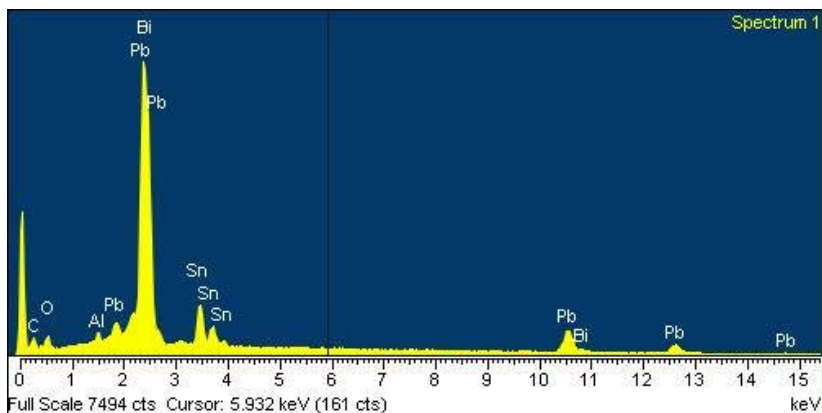


**Figure 116** EDS Spectra of Reworked AuPdNi TQFP-208 Soldered with Tin-Silver-Copper-Bismuth Solder Alloy on Rework Test Vehicles (SN 204, U57, Lead 105) Spot mode analysis was done on one of the bright phases. Pb and Bi overlap in the spectrum and are difficult to distinguish. In this particular phase the Bi is at a high enough concentration that the Bi peak can be seen at an energy of about 10.8keV. There is also evidence of Bi at about 2.4keV. There are instances where the Bi would be at too low of a concentration to be detected by EDS.

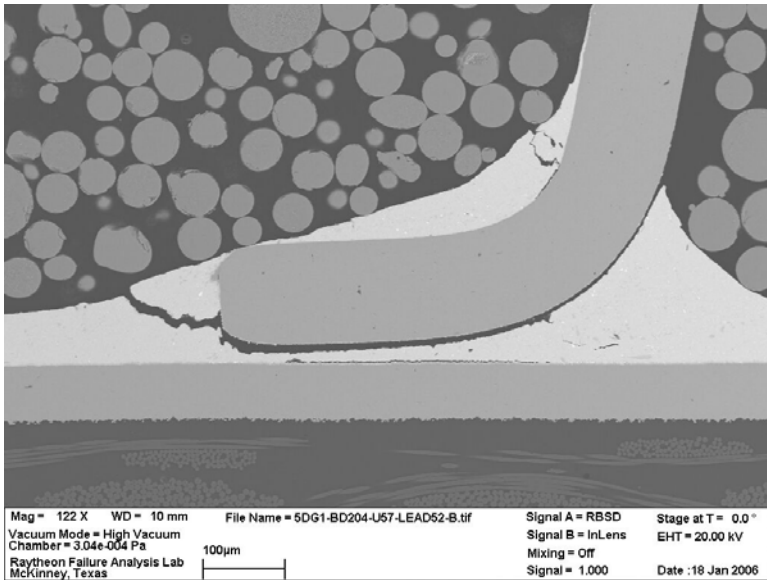


**Figure 117** SEM Micrograph of Reworked AuPdNi TQFP-208 Soldered with Tin-Silver-Copper-Bismuth Solder Alloy on Rework Test Vehicles (SN 204, U57, Lead 105) Crack extends completely through joint at lead to solder interface.

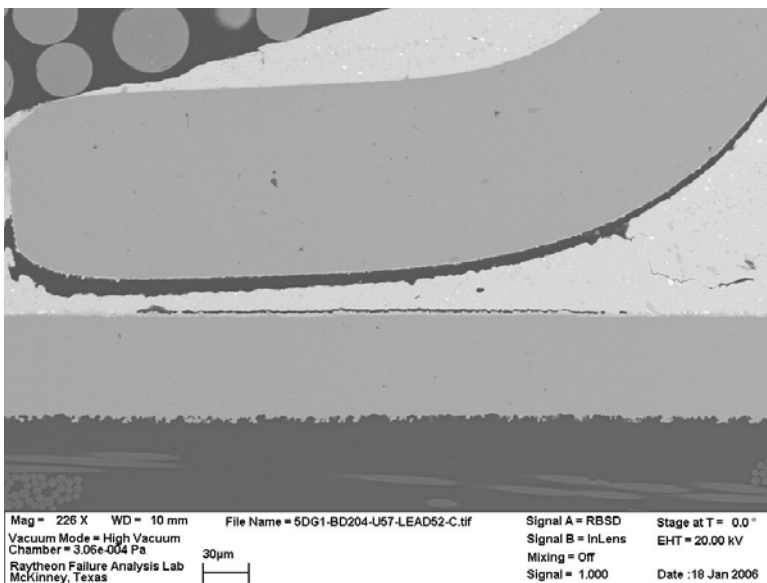


**Figure 118** SEM Micrograph of Reworked AuPdNi TQFP-208 Soldered with Tin-Silver-Copper-Bismuth Solder Alloy on Rework Test Vehicles (SN 204, U57, Lead 105) Separation at solder to board interface. This could be the result of poor wetting of the solder.

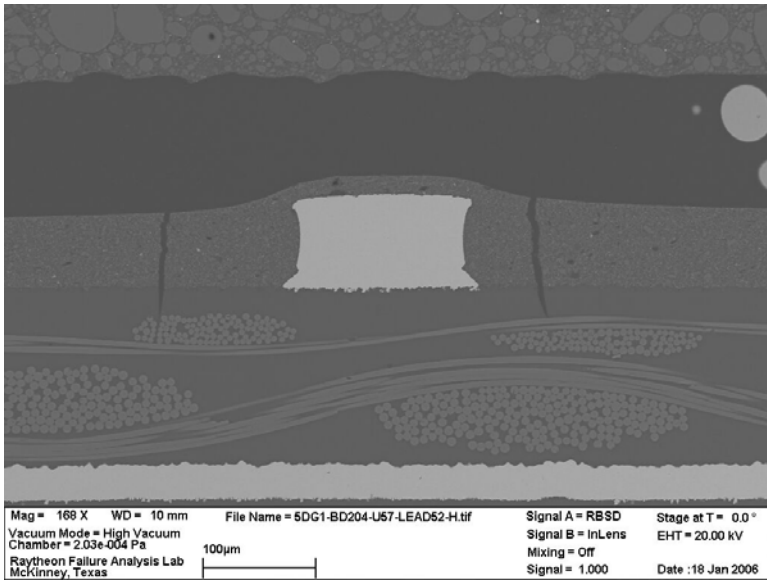


**Figure 119** SEM Micrograph of Reworked AuPdNi TQFP-208 Soldered with Tin-Silver-Copper-Bismuth Solder Alloy on Rework Test Vehicles (SN 204, U57, Lead 105) Cracks in solder mask and board below component.

### **Hybrid Test Vehicle Results and Discussion**

The hybrid test vehicles were exposed to combined environments testing for 500 cycles. One tin-silver-copper-bismuth soldered tin-silver-copper CSP-100 component failed during the second cycle and the datum was excluded from the Weibull analysis. The test vehicles were inspected for lead damage or broken wires. No apparent broken leads or wires were observed during post-test inspection at 30x magnification using a binocular microscope.

Raytheon Materials & Process Engineering selected the components to be microsectioned and is tabulated in Table 31 on page 102. The components included the early life failures, unfailed components, missing components (fell off during the test), and components with different component finish and solder alloy combinations. The SEM/EDS results are segregated by the solder alloy and component type in the following sections.

***Tin-Lead Solder***

*CSP-100*

**Table 23** Summary of Intermetallic Compound Thickness on Tin-Lead Solder Joints of CSP-100 Components on Hybrid Test Vehicles

SN	REFDES	Lead Finish	Lead	IMC Thickness, IC (um)	IMC Thickness, PWB (um)	IMC at IC	IMC at PWB	Observations
301	U36	SnPb	A	394 nm 2.83	3.36	*NiSnCu	CuAuSn	Minor cracks in solder near component interface and board interface. Other bumps similar in appearance.
301	U36	SnPb	J	541 nm 4.23	3.93	*NiSnCu	CuAuSn	Crack in solder on board side of joint extends about ¼ way into joint.
301	U37	SnPb	A	---	1.88 3.59	*NiSnCu	CuAuSn	Minor cracking in solder near component interface. Some cracking in PWB. Other bumps are similar in appearance.
301	U37	SnPb	E	1.38 7.08	2.46 4.68	*NiSnCu	CuAuSn	Some cracking in PWB. Some microcracking in intermetallics on board side.
301	U37	SnPb	J	1.14 2.63	2.86 6.10	*NiSnCu	CuAuSn	Minor cracking in solder near component interface.
302	U60	SnPb	A	458 nm 3.80	2.46	*NiSnCu	CuAuSn	Minor cracking in solder where solder comes in contact with solder mask. Other bumps similar in appearance. Some bumps have minor cracking in solder on component side.
302	U60	SnPb	J	746 nm 6.69	3.52	*NiSnCu	CuAuSn	Crack through solder on board side. Minor cracking in solder on component side.

\* The solder at the component side interface bonds to a Ni plating layer. The intermetallic (IMC) layer at this interface is comprised of NiSn and CuSn. The Cu present in the IMC layer is either migrating from the board side interface or is from the solder. The most likely scenario is the Cu is migrating from the board side since Cu is also present at the component side interface on the SnPb solder samples. At some bonds, it appears there are separate phases of NiSn and CuSn IMCs, at other locations there appears to be a ternary phase of NiSnCu.

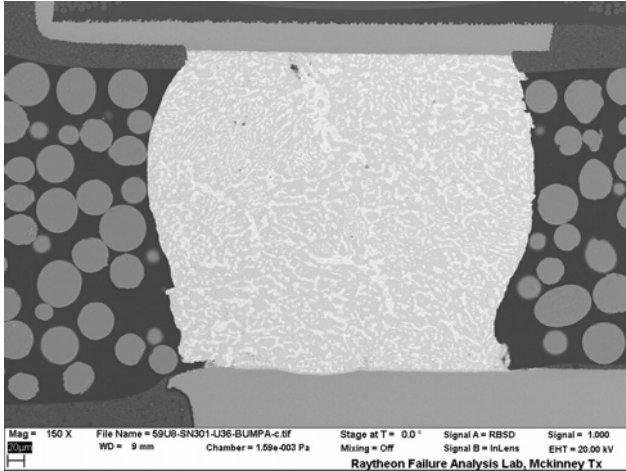


**Figure 120** SEM Micrograph of SnPb Soldered SnPb CSP-100 Components on Hybrid Test Vehicles (SN 301, U36, Bump A) The notch at the lower left corner of the bump is the result of the solder mask. Minor cracks in solder near component interface and board interface. Other bumps similar in appearance.

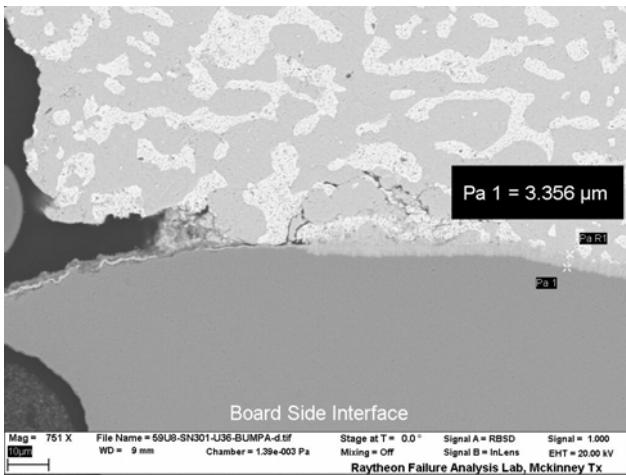


**Figure 121** SEM Micrograph of SnPb Soldered SnPb CSP-100 Components on Hybrid Test Vehicles (SN 301, U36, Bump A) Image showing minor cracking at the corner of the bump at the board interface.

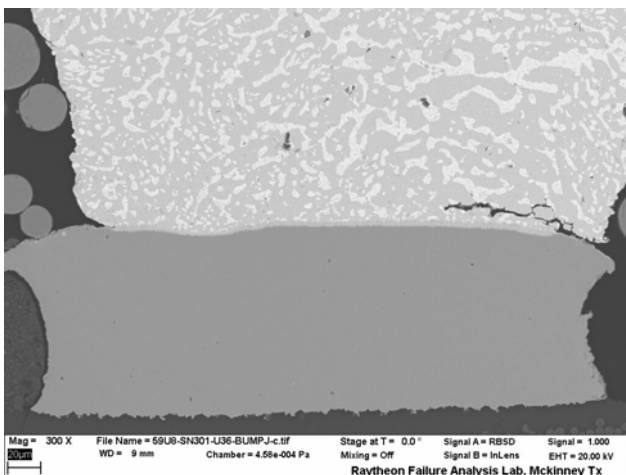


**Figure 122** SEM Micrograph of SnPb Soldered SnPb CSP-100 Components on Hybrid Test Vehicles (SN 301, U36, Bump J) Crack in solder at board interface extend about 1/4 way into joint.

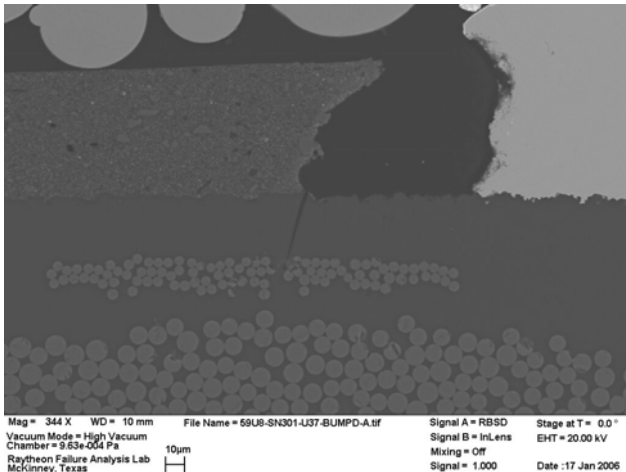


**Figure 123** SEM Micrograph of SnPb Soldered SnPb CSP-100 Components on Hybrid Test Vehicles (SN 301, U37, Bump D) Image showing crack in PWB at edge of solder mask.

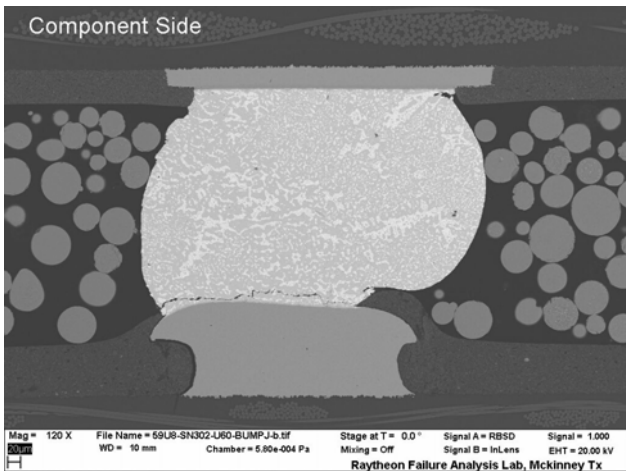


**Figure 124** SEM Micrograph of SnPb Soldered SnPb CSP-100 Components on Hybrid Test Vehicles (SN 302, U60, Bump J) Fracture extends completely through solder joint on board side. Minor cracks at corner of bump on component side.

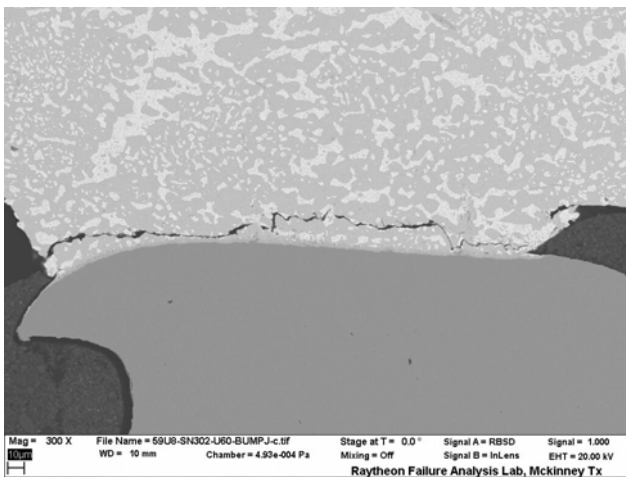


**Figure 125** SEM Micrograph of SnPb Soldered SnPb CSP-100 Components on Hybrid Test Vehicles (SN 302, U60, Bump J) High magnification view of crack seen in Figure 124.

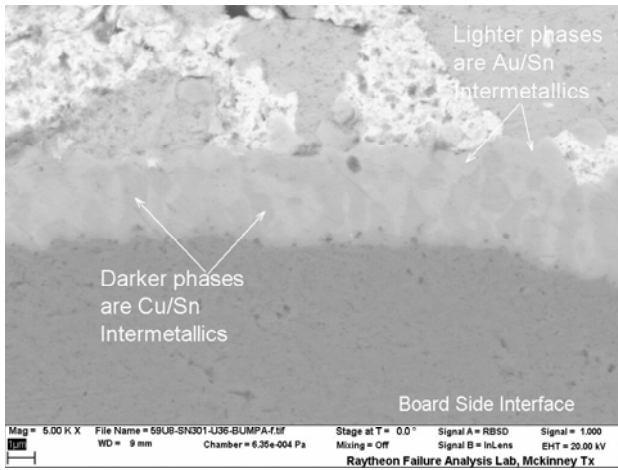


**Figure 126** SEM Micrograph of SnPb Soldered SnPb CSP-100 Components on Hybrid Test Vehicles (SN 301, U36, Bump A) Board side solder to pad interface showing the IMC layer.

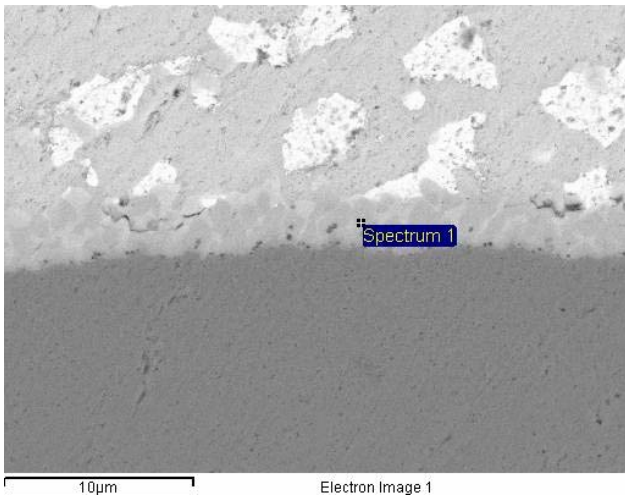


**Figure 127** SEM Micrograph of SnPb Soldered SnPb CSP-100 Components on Hybrid Test Vehicles (SN 301, U37, Bump E) The IMC layer at the board interface is CuAuSn.

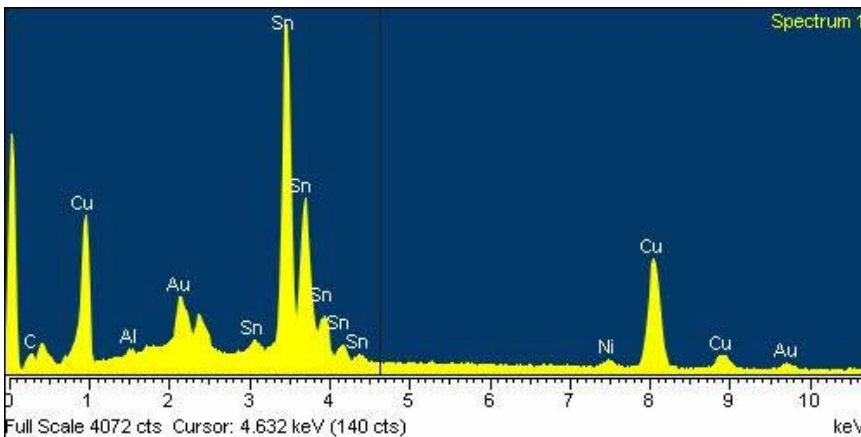


**Figure 128** EDS Spectra of SnPb Soldered SnPb CSP-100 Components on Hybrid Test Vehicles (SN 301, U37, Bump E) The IMC layer at the board interface is CuAuSn.

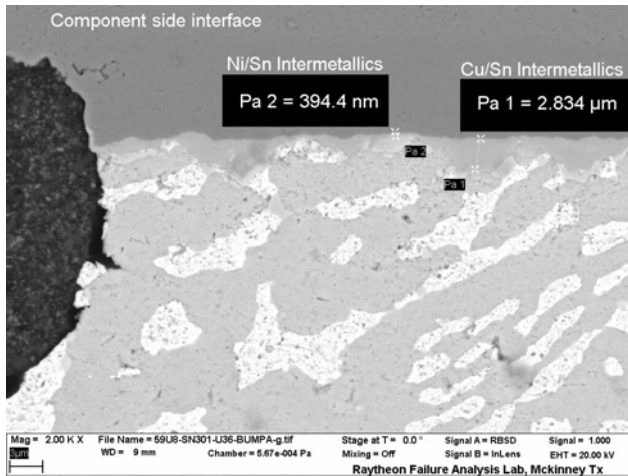


**Figure 129** SEM Micrograph of SnPb Soldered SnPb CSP-100 Components on Hybrid Test Vehicles (SN 301, U36, BUMP A) At this location there appears to be separate phases of NiSn and CuSn IMCs.

*Hybrid-30*

**Table 24** Summary of Intermetallic Compound Thickness on Tin-Lead Solder Joints of Hybrid-30 Components on Hybrid Test Vehicles

SN	REFDES	Lead Finish	Lead	IMC Thickness, IC (um)	IMC Thickness, PWB (um)	IMC at IC	IMC at PWB	Observations
301	U50	SnPb	A	286 nm 1.41	1.26 3.11	NiSn Low levels of Cu	CuSn	Cracks in board at edge of pad. Other leads have a similar appearance.
305	U33	SnPb	A	228 nm 805 nm	627 nm 1.91	NiSn Low levels of Cu	CuSn	Microcracks in solder at both component and board interfaces. Cracks in PWB. Other leads similar in appearance.
305	U33	SnPb	B	216 nm 916 nm	796 nm 3.51	NiSn Low levels of Cu	CuSn	Microcracks in solder at both component and board interfaces.
306	U50	SnPb	A	1.16 2.77	1.00 3.13	NiSn Low levels of Cu	CuSn	No anomalies identified.

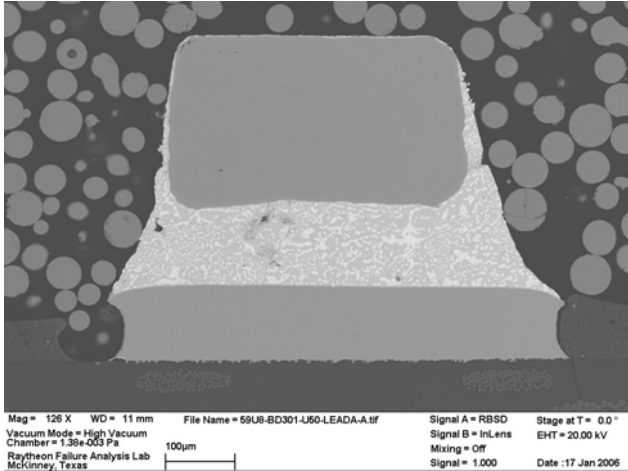


**Figure 130** SEM Micrograph of SnPb Soldered SnPb Hybrid-30 Components on Hybrid Test Vehicles (SN 301, U50, Lead A) Crack in PWB.

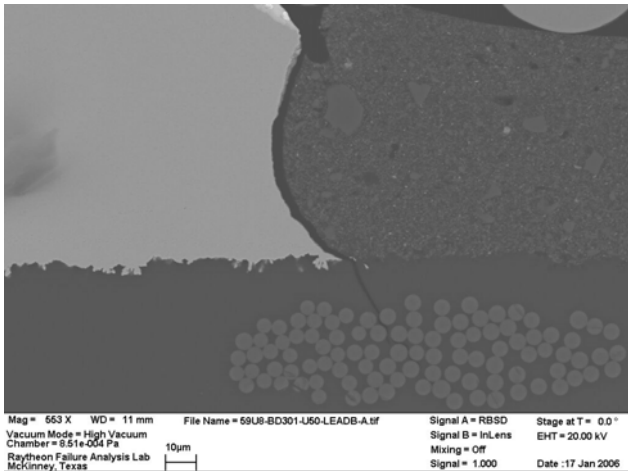


**Figure 131** SEM Micrograph of SnPb Soldered SnPb Hybrid-30 Components on Hybrid Test Vehicles (SN 301, U50, Lead A) High magnification view of crack in PWB.

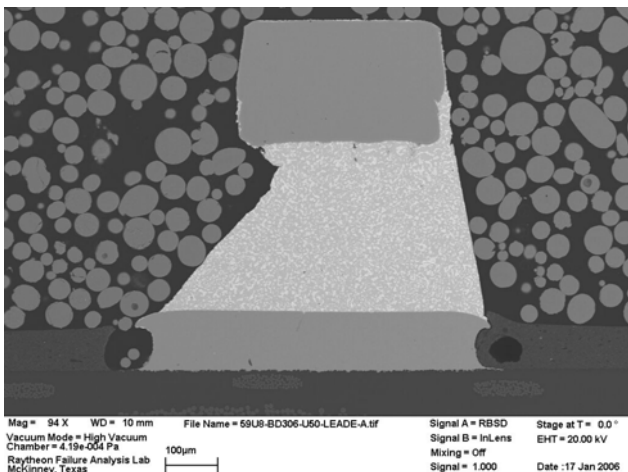


**Figure 132** SEM Micrograph of SnPb Soldered SnPb Hybrid-30 Components on Hybrid Test Vehicles (SN 306, U50, Lead E) Solder joint taller than some of the surrounding joints.

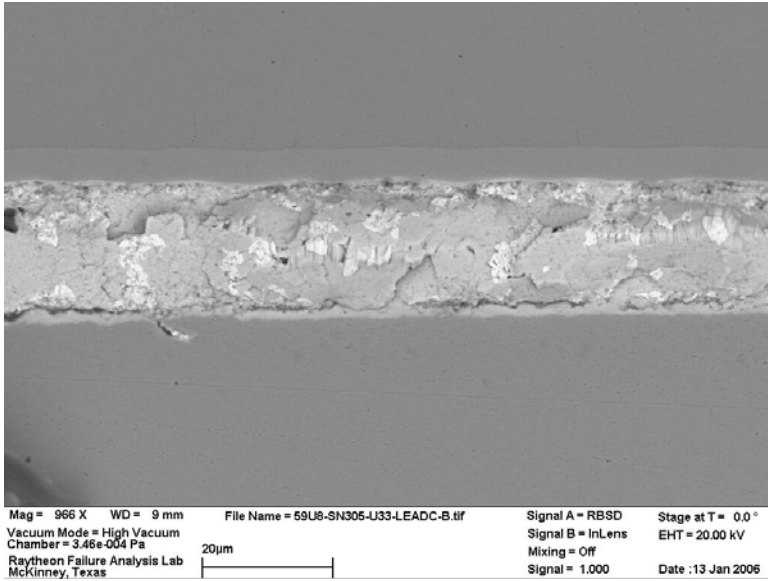


**Figure 133** SEM Micrograph of SnPb Soldered SnPb Hybrid-30 Components on Hybrid Test Vehicles (SN 305, U33, Lead C) Microcracking present in solder joint at the solder to IMC interface.

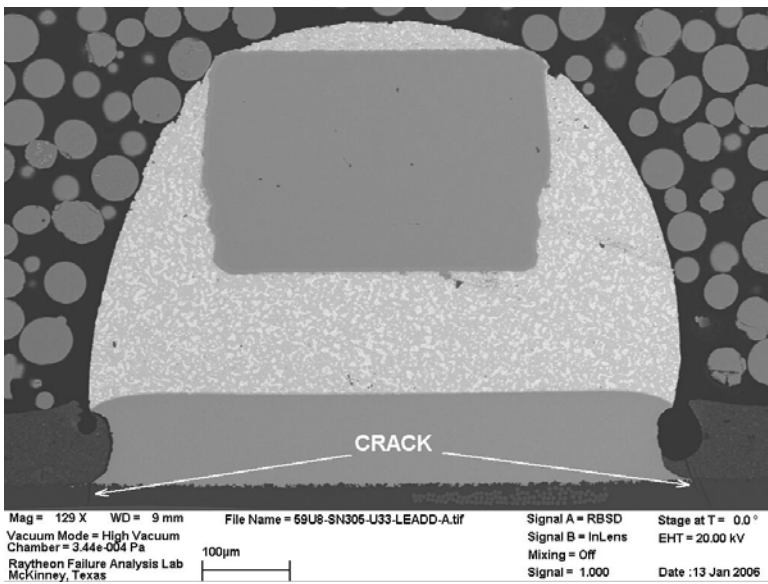


**Figure 134** SEM Micrograph of SnPb Soldered SnPb Hybrid-30 Components on Hybrid Test Vehicles (SN 305, U33, Lead D) Cracks in PWB on both sides of pad.

**Tin-Silver-Copper Solder**

*CSP-100*

**Table 25** Summary of Intermetallic Compound Thickness on Tin-Silver-Copper Solder Joints of CSP-100 Components on Hybrid Test Vehicles

SN	REFDES	Lead Finish	Lead	IMC Thickness, IC (um)	IMC Thickness, PWB (um)	IMC at IC	IMC at PWB	Observations
323	U60	SnAgCu	A	960 nm 1.97	3.76 6.74	*NiSnCu	CuAuSn	Crack through joint at PWB to solder interface. Some voiding in solder.
323	U60	SnAgCu	E	1.41 2.19	4.53 5.88	*NiSnCu	CuAuSn	Very minor voiding. Other bumps similar in appearance.
323	U60	SnAgCu	J	1.28 3.77	3.41 6.00	*NiSnCu	CuAuSn	Voiding present in solder.
325	U19	SnAgCu	A	995 nm 1.86	3.04 4.23	*NiSnCu	CuAuSn	Cracking in solder at component and PWB interface. Crack extends about ¼ to ½ way into joint. Crack in PWB at edge of pad. Other bumps with similar appearance. Some bumps have voids in solder.
325	U19	SnAgCu	G	807 nm 1.96	1.68 3.43	*NiSnCu	CuAuSn	Crack extends all the way through solder on board side. Crack in PWB. Other bumps similar in appearance.
326	U60	SnAgCu	A	1.46 4.02	6.48 6.56	*NiSnCu	CuAuSn	Crack extends completely through joint on board side.
326	U60	SnAgCu	B	---	4.59	*NiSnCu	CuAuSn	Crack extends about ½ way through joint on board side. Minor cracking on component side. Other bumps have cracks to varying degrees of severity.
326	U60	SnAgCu	J	780 nm 2.01	4.83 5.77	*NiSnCu	CuAuSn	Crack extends completely through joint on board side.

\* The solder at the component side interface bonds to a Ni plating layer. The intermetallic (IMC) layer at this interface is comprised of NiSn and CuSn. The Cu present in the IMC layer is either migrating from the board side interface or is from the solder. The most likely scenario is the Cu is migrating from the board side since Cu is also present at the component side interface on the SnPb solder samples. At some bonds, it appears there are separate phases of NiSn and CuSn IMCs, at other locations there appears to be a ternary phase of NiSnCu.

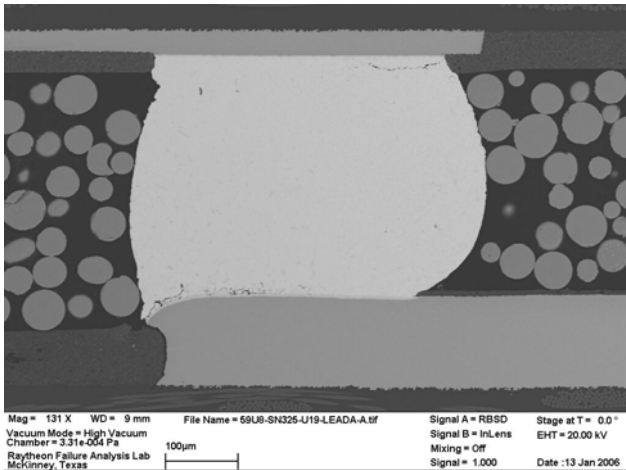


**Figure 135** SEM Micrograph of SnAgCu Soldered SnAgCu CSP-100 Components on Hybrid Test Vehicles (SN 325, U19, Bump A) Cracking in solder at component and PWB interface. Crack extends about ¼ to ½ way into joint. Crack in PWB at edge of pad. Other bumps with similar appearance.

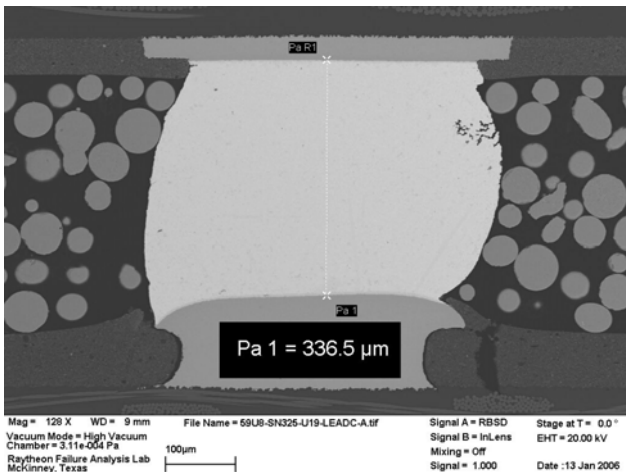


**Figure 136** SEM Micrograph of SnAgCu Soldered SnAgCu CSP-100 Components on Hybrid Test Vehicles (SN 325, U19, Bump C) Voiding in solder.

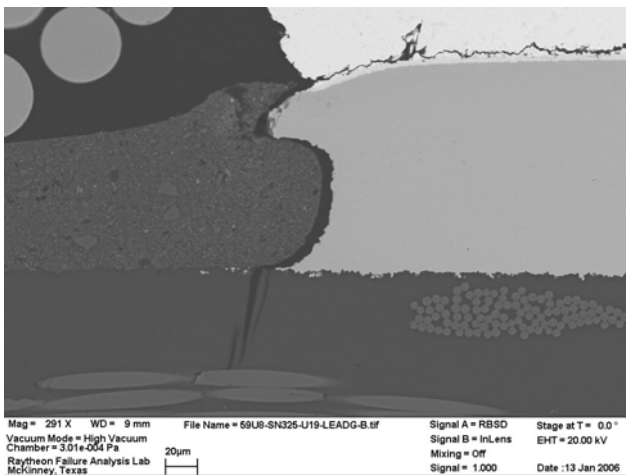


**Figure 137** SEM Micrograph of SnAgCu Soldered SnAgCu CSP-100 Components on Hybrid Test Vehicles (SN 325, U19, Bump G) Crack in PWB.

Hybrid-30

**Table 26** Summary of Intermetallic Compound Thickness on Tin-Silver-Copper Solder Joints of Hybrid-30 Components on Hybrid Test Vehicles

SN	REFDES	Lead Finish	Lead	IMC Thickness, IC (um)	IMC Thickness, PWB (um)	IMC at IC	IMC at PWB	Observations
323	U32	SnAgCu	A	585 nm 1.25	986 nm 1.79	NiSn Low levels of Cu	CuSn	Minor cracking in solder at board to solder interface. Cracking in board near edges of pad. Other leads have cracks in PWB as well.
326	U32	SnAgCu	A	1.20 3.20	1.03 2.63	NiSn Low levels of Cu	CuSn	Crack in PWB by edge of solder mask. Observed on other leads as well. Cracks present in other joints. Degree of severity varies from minor to severe.
326	U33	SnAgCu	A	608 nm 1.93	1.76 3.23	NiSn Low levels of Cu	CuSn	Cracks present in PWB near edge of solder mask. Other leads have a similar appearance.

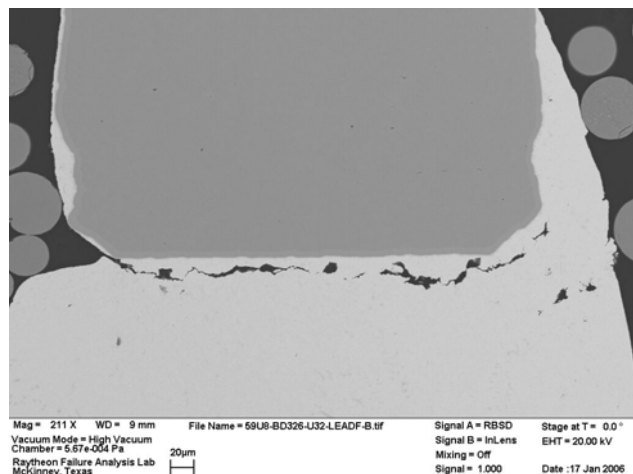


**Figure 138** SEM Micrograph of SnAgCu Soldered SnAgCu Hybrid-30 Components on Hybrid Test Vehicles (SN 326, U32, Lead F) Crack almost completely through joint near lead interface.

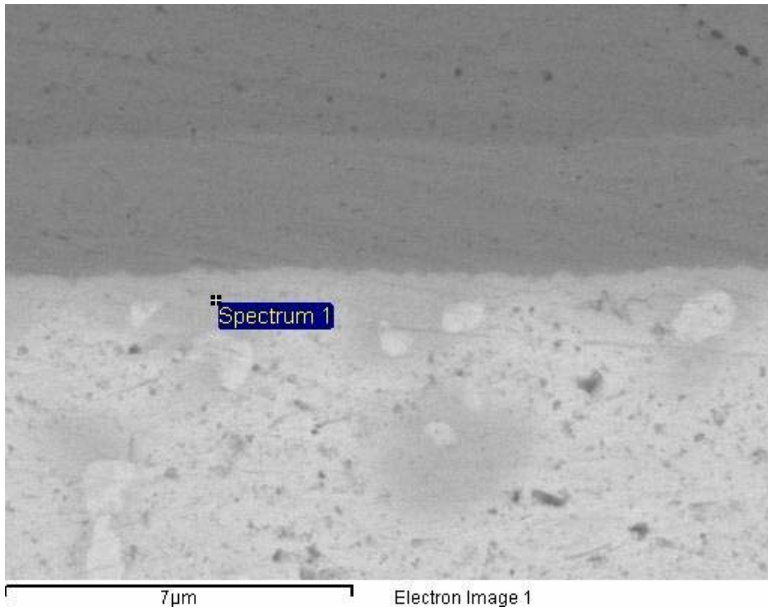


**Figure 139** SEM Micrograph of SnAgCu Soldered SnAgCu Hybrid-30 Components on Hybrid Test Vehicles (SN 326, U33, LEAD A) Component side interface, the IMC layer is NiSn however low levels of Cu are also present.

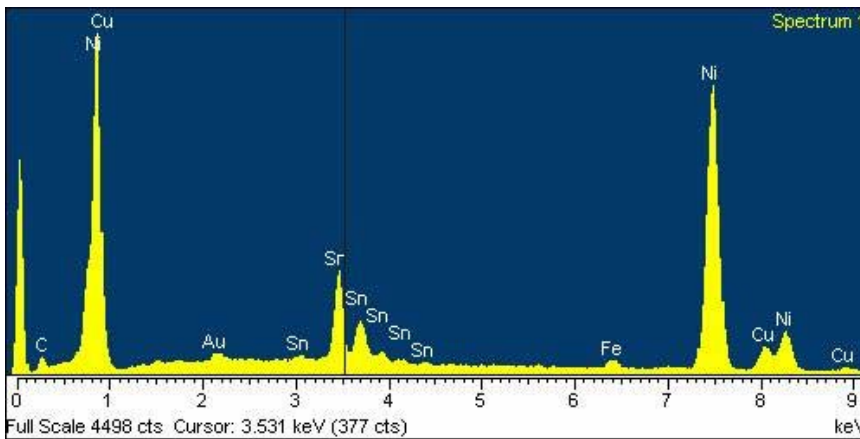


**Figure 140** EDS Spectra of SnAgCu Soldered SnAgCu Hybrid-30 Components on Hybrid Test Vehicles (SN 326, U33, LEAD A) The IMC layer is NiSn however low levels of Cu are also present.

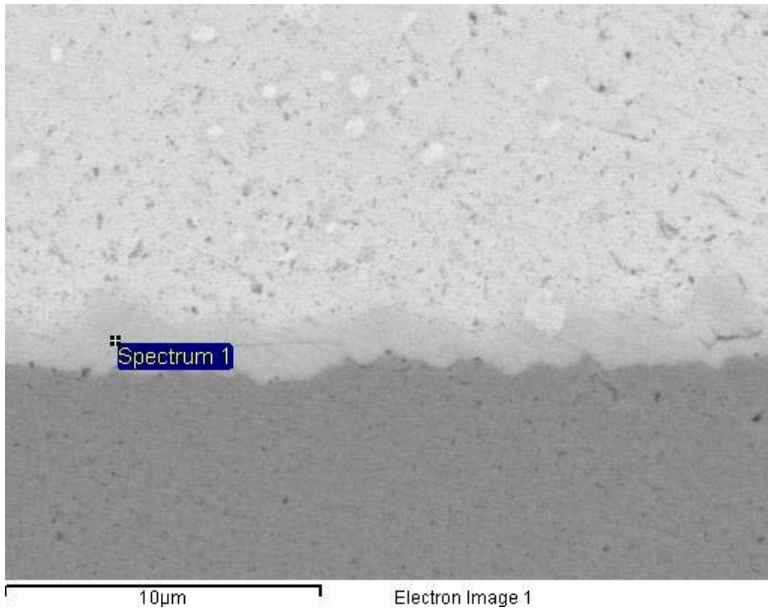


**Figure 141** SEM Micrograph of SnAgCu Soldered SnAgCu Hybrid-30 Components on Hybrid Test Vehicles (SN 326, U32, LEAD A) Board side interface, IMC layer is CuSn.

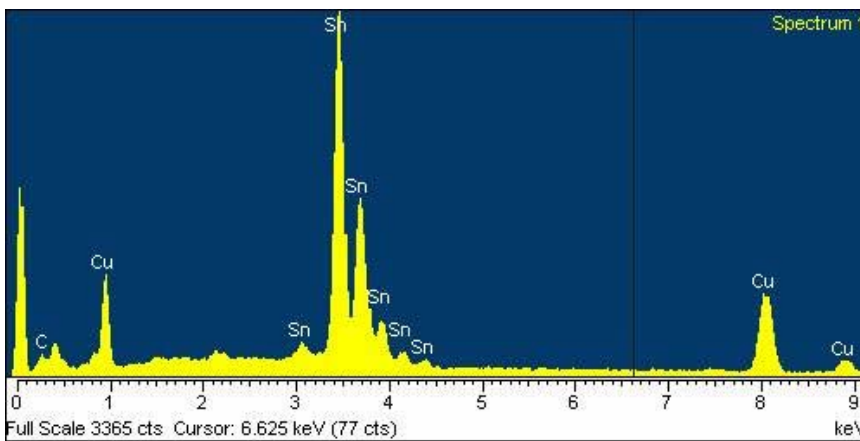


**Figure 142** EDS Spectra of SnAgCu Soldered SnAgCu Hybrid-30 Components on Hybrid Test Vehicles (SN 326, U32, LEAD A) IMC layer is CuSn.

**Tin-Silver-Copper-Bismuth Solder**

*CSP-100*

**Table 27** Summary of Intermetallic Compound Thickness on Tin-Silver-Copper-Bismuth Solder Joints of CSP-100 Components on Hybrid Test Vehicles

SN	REFDES	Lead Finish	Lead	IMC Thickness, IC (um)	IMC Thickness, PWB (um)	IMC at IC	IMC at PWB	Observations
332	U37	SnAgCu	A	1.96 2.23	2.78 7.19	*NiSnCu	CuAuSn	Crack extends completely through joint on board side. Crack in board at pad edges.
332	U37	SnAgCu	E	2.22 3.98	4.79 4.90	*NiSnCu	CuAuSn	Crack in board at pad edge. Other bumps similar in appearance.
332	U37	SnAgCu	J	1.34 2.54	3.95 5.62	*NiSnCu	CuAuSn	Crack extends completely through joint on board side.
333	U37	SnAgCu	A	1.11 2.16	2.32 4.59	*NiSnCu	CuAuSn	Crack in solder extends about ½ way through joint on component side. Other bumps have cracks to varying degrees of severity on both sides of joint. Very minor cracking on board side. Void present. Crack in PWB.
333	U37	SnAgCu	E	1.67 1.93	1.99 5.37	*NiSnCu	CuAuSn	Crack in PWB. Other bumps similar in appearance.
333	U37	SnAgCu	J	1.51 2.66	4.21 7.02	*NiSnCu	CuAuSn	Crack extends completely through joint on board side.
337	U36	SnAgCu	A	2.11	5.35	*NiSnCu	CuAuSn	Crack extends almost completely through joint on board side. Crack in PWB. Other bumps similar in appearance.
337	U36	SnAgCu	E	1.10 1.87	1.92 4.99	*NiSnCu	CuAuSn	Voiding in solder. Other bumps similar in appearance.
337	U36	SnAgCu	J	1.78 2.81	4.09 5.24	*NiSnCu	CuAuSn	Crack extends completely through joint on board side. Crack in PWB.

\* The solder at the component side interface bonds to a Ni plating layer. The intermetallic (IMC) layer at this interface is comprised of NiSn and CuSn. The Cu present in the IMC layer is either migrating from the board side interface or is from the solder. The most likely scenario is the Cu is migrating from the board side since Cu is also present at the component side interface on the SnPb solder samples. At some bonds, it appears there are separate phases of NiSn and CuSn IMCs, at other locations there appears to be a ternary phase of NiSnCu.

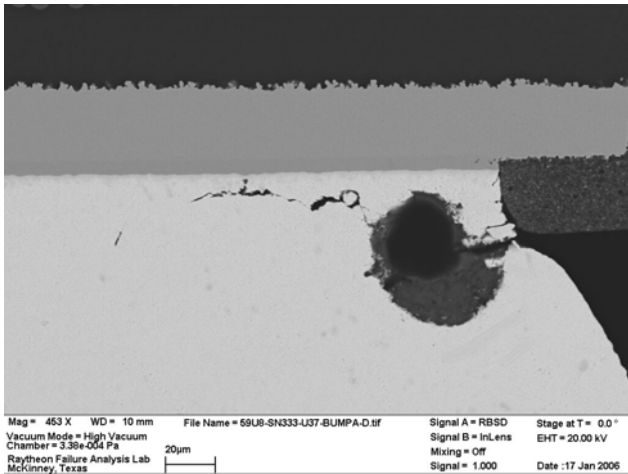


**Figure 143** SEM Micrograph of SnAgCuBi Soldered SnAgCu CSP-100 Components on Hybrid Test Vehicles (SN 333, U37, Bump A) Crack and void in solder near component interface.

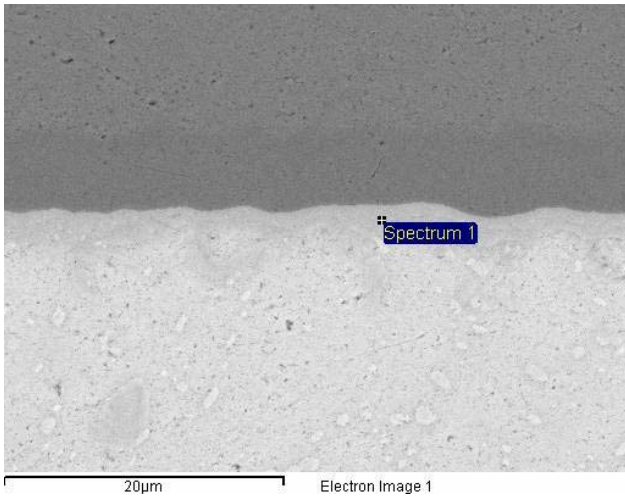


**Figure 144** SEM Micrograph of SnAgCuBi Soldered SnAgCu CSP-100 Components on Hybrid Test Vehicles (SN 333, U37, BUMP A) Component side interface

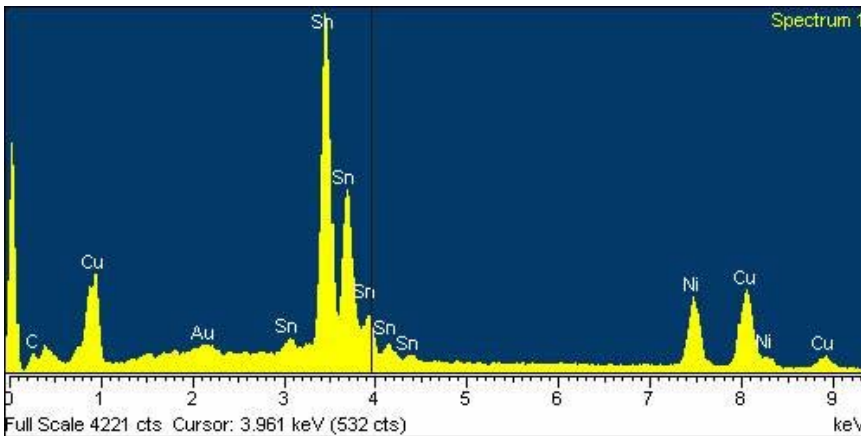


**Figure 145** EDS Spectra of SnAgCuBi Soldered SnAgCu CSP-100 Components on Hybrid Test Vehicles (SN 333, U37, BUMP A) IMC layer appears to be a ternary layer of NiSnCu.

*Hybrid-30*

**Table 28** Summary of Intermetallic Compound Thickness on Tin-Silver-Copper-Bismuth Solder Joints of Hybrid-30 Components on Hybrid Test Vehicles

SN	REFDES	Lead Finish	Lead	IMC Thickness, IC (um)	IMC Thickness, PWB (um)	IMC at IC	IMC at PWB	Observations
332	U33	SnAgCuBi	A	708 nm 1.86	1.29 2.92	NiSn Low levels of Cu	CuSn	Very minor cracking in solder on lead side of joint. Other leads have minor cracking on component side of joint.
332	U33	SnAgCuBi	G			NiSn Low levels of Cu	CuSn	Cracking in PWB at edge of solder mask. Other leads similar in appearance.
336	U50	SnAgCuBi	A	1.17 4.67	1.36 5.06	NiSn Low levels of Cu	CuSn	No anomalies.
336	U50	SnAgCuBi	B	---	---	NiSn Low levels of Cu	CuSn	Crack in PWB. Other leads have a similar appearance.
336	U50	SnAgCuBi	I	801 nm 3.13	1.58 3.99	NiSn Low levels of Cu	CuSn	Void in solder.
337	U33	SnAgCuBi	A	443 nm 1.14	1.51 4.01	NiSn Low levels of Cu	CuSn	Minor crack in solder near lead interface. Crack in PWB. Other leads have cracks in PWB.

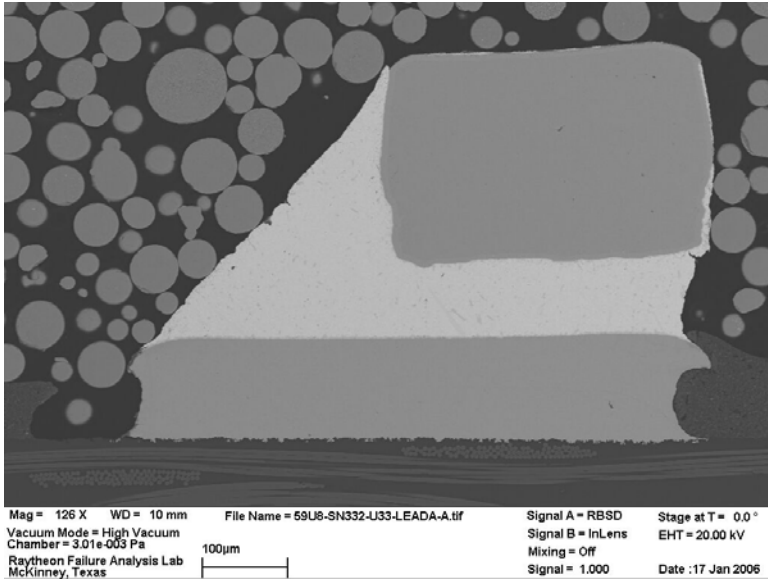


**Figure 146** SEM Micrograph of SnAgCuBi Soldered SnAgCuBi Hybrid-30 Components on Hybrid Test Vehicles (SN 332, U33, Lead A) Only very minor cracking in solder near the lead side interface. Lead not centered over the pad.

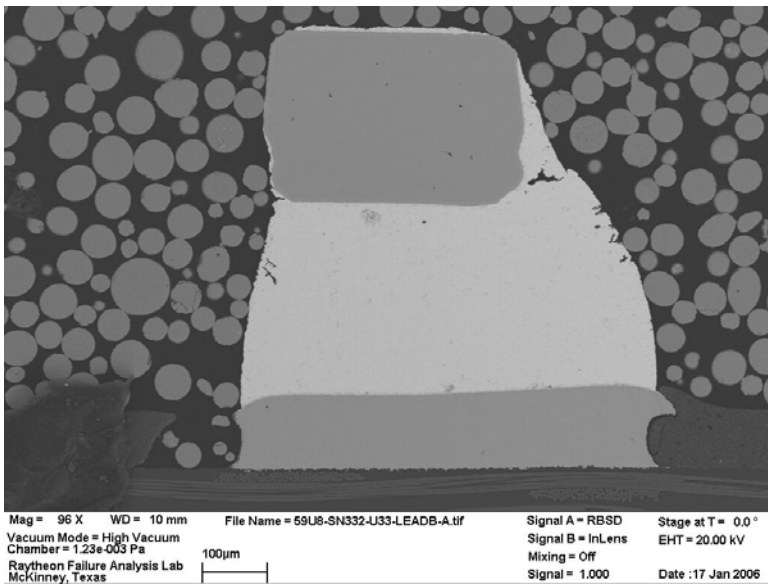


**Figure 147** SEM Micrograph of SnAgCuBi Soldered SnAgCuBi Hybrid-30 Components on Hybrid Test Vehicles (SN 332, U33, Lead B) Solder joint taller than some of the surrounding joints, minor cracking present in the solder.

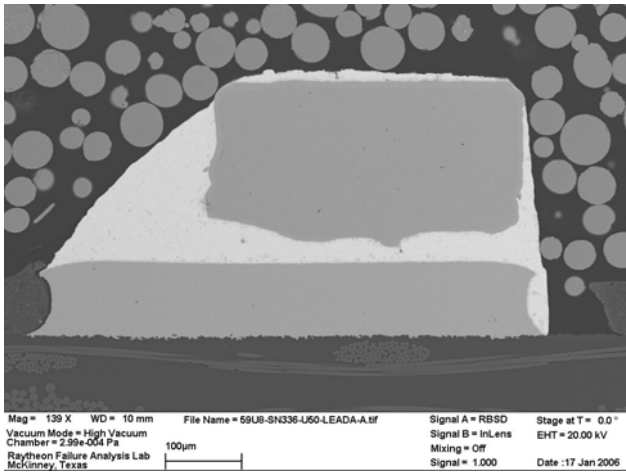


**Figure 148** SEM Micrograph of SnAgCuBi Soldered SnAgCuBi Hybrid-30 Components on Hybrid Test Vehicles (SN 336, U50, Lead A) No anomalies.

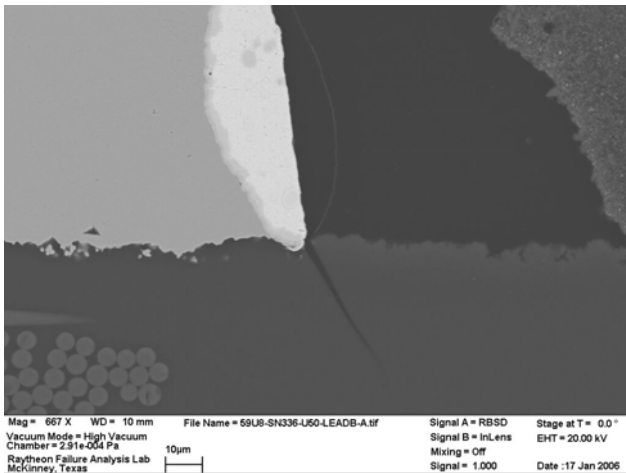


**Figure 149** SEM Micrograph of SnAgCuBi Soldered SnAgCuBi Hybrid-30 Components on Hybrid Test Vehicles (SN 336, U50, Lead B) Crack in the PWB at the corner of the pad

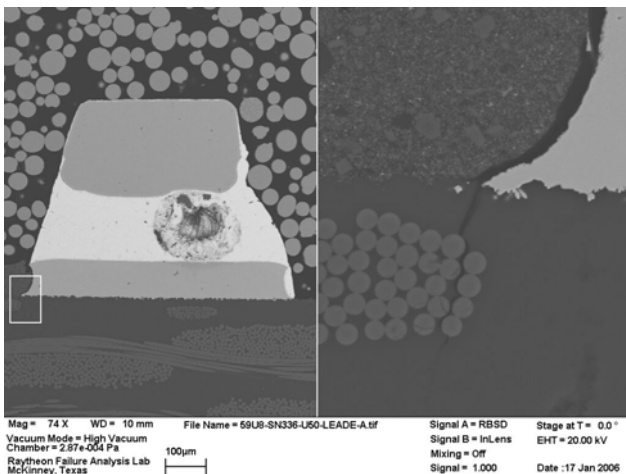


**Figure 150** SEM Micrograph of SnAgCuBi Soldered SnAgCuBi Hybrid-30 Components on Hybrid Test Vehicles (SN 336, U50, Lead E) Void in the solder and a crack in the PWB at the corner of the pad.

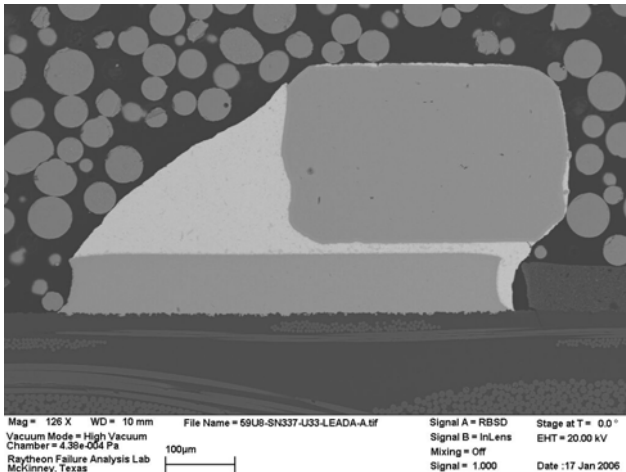


**Figure 151** SEM Micrograph of SnAgCuBi Soldered SnAgCuBi Hybrid-30 Components on Hybrid Test Vehicles (SN 337, U33, Lead A) Minor cracking in the corner of the solder near component.

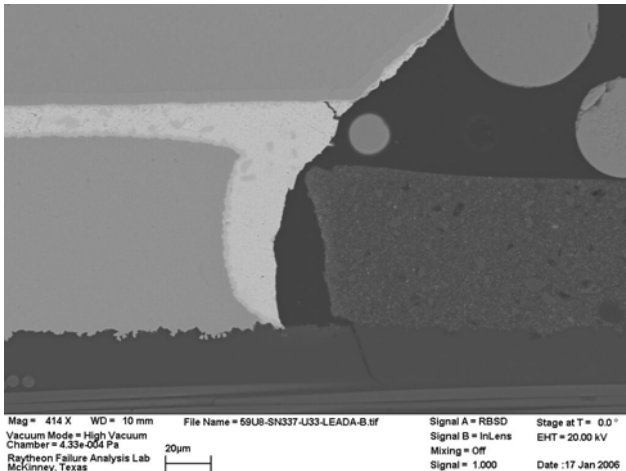


**Figure 152** SEM Micrograph of SnAgCuBi Soldered SnAgCuBi Hybrid-30 Components on Hybrid Test Vehicles (SN 337, U 33, Lead A) Minor cracking on solder and PWB.

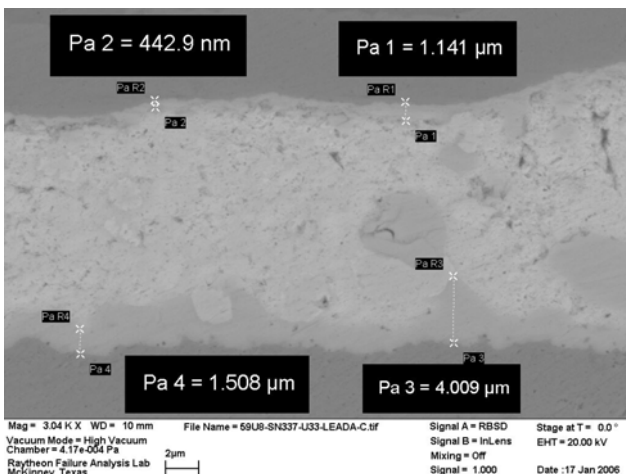


**Figure 153** SEM Micrograph of SnAgCuBi Soldered SnAgCuBi Hybrid-30 Components on Hybrid Test Vehicles (SN 337, U50, Lead A) IMC measurements at the lead and board interfaces.

## **Conclusions**

### **Manufactured Test Vehicles**

#### ***BGA-225***

BGA component U55 from board 30 with SnPb solder alloy and finish, failed after 541 cycles and had only minor cracking of the solder near the component interface. No complete fractures through the solder bump for the row examined were found to account for the device failure. It should be noted that only one plane was examined and a complete fracture through a joint may be present in another row of bumps. However, for board 32, component U43, which failed after only 175 cycles, complete fractures were found through some of the solder bumps to account for device failure. The complete fractures were through the solder near the component interface, however some cracking was also present near the board pad interface. The common failure location of BGA components when under mechanical stress is usually near the component side interface. One possible explanation for why U43 failed after only 175 cycles and U55 made it to 541 cycles may be related to the components' location on the board.

Component U55 on board 101 with SnAgCu solder with SnAgCu finish failed after 514 cycles. Some cracks near the component side interface extended all the way through the solder. Minor to severe cracking was also present near the board side. Contrast this to component U6 on board 102 with the same solder and finish failed after 100 cycles. Some bumps had cracks completely through the solder near the component interface while other bumps were cracked completely through near the board interface. The data suggest an extreme amount of movement of the component and board during the thermal cycle and vibration environment.

Component U5 on board 100 with SnAgCu solder with SnPb finish failed after only 30 cycles. Cracks were completely through the solder near the component interface. Cracks were also present of less severity near the board interface. The solder was grain coarsened near the component interface. The data do not support a reason why the solder bonds would fail after only 30 cycles. Component U44 with the same solder and finish failed after 540 cycles. Examination of the solder bumps for this device revealed minor cracking to a crack all the way through the solder near the component side interface. The failures for these two components are similar except for the cracking on the board side of U5. This indicates a higher induced stress and more movement at U5 compared to U44.

Component U4 on board 113 with SnAgCuBi solder and SnAgCu finish failed after 550 cycles. Cracks were evident all the way through the solder near both the component and board side interfaces. Component U55 on board 142 with the same solder and finish failed after 1 cycle. Cracks were present completely through the solder at both interfaces. Solder appeared severely fatigued, indicating the solder joint did not fail after 1 cycle. The early life failure may be the result of component failure and not the solder or it is possible a solder bond was defective in one of the rows not examined. Components U2 and U56 with SnAgCuBi solder and SnPb finish exhibited solder joint failures similar to U4 and U55 with cracks through the solder near component and board side interfaces.

In general, solder joint cracks on BGA components were more prevalent near the component side interface. The difference in cycles to fail could be related to the component location on the board. The induced stress a component receives during CET will vary depending on its location on the board.

#### ***CLCC-20***

All the CLCC solder joint failures occurred as the result of cracks propagating through the bulk solder. On some devices, the solder was cracked completely through on both sides and on others only on one side. Two components were missing that had SnAgCu solder and finish. Both parts appeared to have failed due to cracks extending through the bulk solder. Component U17 on board 142 with SnAgCuBi solder and finish failed after one cycle. However, the failure to the solder joint occurred due to fatigue cracks extending through the bulk solder. The failure does not match the electrical test data since the component failed on the first cycle. The cause of the electrical failure after one cycle must have been due to something besides the solder joints examined since the solder joint appears fatigued similar to late life failures. Varying levels of voiding were present below the components in the thin solder regions, however, the voiding had little contribution to the fracture failures.

***PDIP-20***

The PDIP devices with the SnPb solder and AuPdNi finish had cracks on both sides of the board. The cracks extended through the solder very close to the solder to intermetallic interface on the board side of the joint. Some voiding was present in the joints. The crack typically extended further into the joint on one side of the lead versus the other but the longer crack was not always on the same side of the lead. The SnPb solder with the Sn finish were similar in appearance to the SnPb solder with the AuPdNi finish. In addition, the device with the SnPb solder and AuPdNi finish had more voids in the joints and a crack in the PWB was observed.

In contrast, the SnAgCu solder with the Sn finish had cracks that are both near the solder to lead interface as well as solder to board interface. The majority of the cracks were near the solder to lead interface. Again, these cracks were through the solder near the intermetallic layer. Little voiding was present. A crack was identified in the board. The PDIP components with SnAgCu solder and AuPdNi finish had cracks mainly on one side of the board near the solder to board interface. Some voiding was identified.

Similar to the SnPb and SnAgCu solder, the devices with the SnCu solder and Sn finish had cracks present at the solder to lead interface near the intermetallic layer. Although some cracks were identified near the board interface, the majority of the cracks were near the lead interface. Voiding was present in the joints. Incomplete solder fill was noted in that the solder did not completely cover the lead as seen in previous joints. The solder did not extend up the curved part of the lead. Some cracks were present on the opposite side of the board but the majority of the cracks were on the one side of the board. The SnCu solder with Sn finish did not have cracks in the solder joints. The cracks identified are in the PWB.

The devices that exhibited early life failure failed through the solder whereas the devices with late failure had cracks through the board material. Solder joint cracks in devices that failed early did not extend completely through the joint in the plane examined.

***PLCC-20***

Two devices with SnPb solder and Sn finish had cracks in the solder. One device had cracks that extend about  $\frac{3}{4}$  through the joint but was near the center of the joint and did not extend out to the fillet on either side. This crack was near the lead to solder interface. Some minor cracking was also identified at the solder to board interface. The other device had minor cracking in the solder, which initiated in the fillet below the component. This crack was near the center of the solder and not at either the board or lead interface.

The device with SnAgCu solder and Sn finish had minor cracking and separation near the center of the joint, but not near the fillet edge.

Likewise, on the device with the SnAgCuBi solder and Sn finish, a small area of separation was identified between the intermetallics on the lead side and the solder. Virtually, no cracks were present.

Of the three solder types examined, the SnAgCuBi solder appeared to be in the best condition. The most severe cracking was present in the SnPb solder with Sn finish joints.

None of these devices had been identified as failures.

***TQFP-144***

Two devices were examined that have the SnPb solder and Sn finish. One device had a crack in the joint about  $\frac{1}{4}$  of the way through the solder initiating at the heel on the lead side of the joint. Microcracks were also identified in the solder on both sides of the joint at the board interface and the lead interface. The other device had a crack that extends about  $\frac{1}{2}$  way through the joint, also initiating at the heel at the solder to lead interface. Minor cracks were also identified at the toe. The other lead on this device was cracked all the way through the solder, mainly at the solder to lead interface.

Two devices were examined with the metallurgy consisting of SnAgCu solder and a Sn finish. In both devices, the cracks appeared to have initiated at the heel of the joint. The first device had a crack about  $\frac{1}{4}$  way through the

joint at the heel on one lead. On the other lead, it had cracked all the way through. On the second device, a crack was present about 1/3 way through the joint on the lead side of the joint on both leads.

Solder joints with the SnAgCuBi solder and Sn finish were determined to have cracks. The first device had a crack completely through the solder on one lead and about 3/4 way through the solder on the other lead. The crack was mainly at the intermetallic to solder interface. Some voiding was also present. The other device had cracks in the solder joints that extended 1/3 and 1/2 way through the solders at the heel on the lead side of the joint at the solder to intermetallic interface.

### ***TQFP-208***

All of the TQFP-208 microsectioned leads evaluated were found to have partial cracks in the solder that extended varying distances into the solder bond. None of the solder bonds examined were found to be fractured completely through. The cracks all initiated in the heel regions of the solder fillet. There was a slight difference in the TQFP-208 components that were soldered with SnAgCuBi solder. Once the crack made it through the bulk solder fillet of the heel, the crack continued its path along the solder to lead intermetallic interface. The components with the other solder alloys showed cracks that were close to the lead interface, but still in the bulk solder.

The data did not present a cause for the failure of component U57 on board 30 with SnPb solder alloy and finish after 51 cycles. The cracks in the solder for this component were very similar in comparison to the cracks found in all the other TQFP-208 components.

### ***TSOP-50***

The TSOP components all appear to have failed as a result of crack propagation through the solder joint. The data suggest the majority of the cracks initiated in the heel region of the solder fillet, although some of the joints may have experienced crack initiations and propagation from both the toe and heel regions. The only significant difference noted between the different groups of TSOP components was the way the TSOPs utilizing the SnAgCuBi solder alloy and SnPb finish failed. Although the cracks for this group did fracture through the bulk solder in the heel region, the data suggest the remaining crack propagation occurred along the lead intermetallic to solder interface. For all other TSOP solder alloys and finish combinations, the crack propagation was through the bulk solder from start to finish. It should be noted that the components were all missing from this particular group after test, therefore these conclusions are based on analysis of the remaining solder at the board pad interface only. It was noted from the test data that the group of TSOPs with the SnAgCuBi solder alloy with SnPb finish did fail with less cycles than all other solder alloy groups and finishes. The data suggest the bonds may have been weaker at the solder to lead interface for this particular group.

## **Reworked Tin-Silver-Copper-Bismuth Soldered TQFP-208 Components on Rework Test Vehicles**

The U57 devices had separation between the lead intermetallics and solder. The separation was not through the solder as seen on many of the other failures examined during this study. Some voiding was present between the solder and intermetallics. Cracks were present in the solder mask and PWB below the component.

The U3 devices were missing due to the fracture of the joints. Microcracks were identified in the solder. Some voiding was present at the solder to intermetallic interface. It appeared the solder did not wet well at the time of rework as evidenced by the microvoiding near the interface. The U3 devices failed very early on in comparison to the U57 devices. Most likely this is the result of poor wetting of the solder at the time of rework.

## **Hybrid Test Vehicles**

### ***CSP-100***

All of the CSP-100 devices examined had minor cracking in the PWB near the edges of the pad.

Solder joints made of SnPb solder and SnPb finish had minor cracks in the solder on the PWB side of the joint. One of the devices also had minor cracks in the solder on the component side of the joint. Two of the devices, one an early failure and one a late failure, did not have any cracks severe enough to cause a failure in the plane examined. One device had cracks all the way through which could account for the failure.

The devices with the SnAgCu solder and SnAgCu finish had solder joints with cracks that extended completely through the solder on the PWB side of the joint. The cracks identified on the component side of the joint were not as severe.

Solder joints with the SnAgCuBi solder and SnAgCu finish had cracks that varied in severity, some of which extended completely through the solder on the board side of the joints.

No differences were identified that could explain the difference between the early and late failures. In instances where the device was identified as an electrical failure but the joints did not crack all the way through may be explained by the plane analyzed. Only a single plane in the joint is examined in a cross section, the failure may have occurred in a different plane on a different bump. Board location may also result in varying degrees of crack severity. Different parts of the board will see different levels of stress dependent on test conditions.

### ***Hybrid-30***

Of the Hybrid devices examined, all but one had cracks in the PWB. These cracks were minor and were located either at the edge of the pad on the PWB or at the edge of the solder mask. There was no trend with solder or finish to determine location of these minor cracks. The solder joint thickness also varied from lead to lead. It appeared to depend on whether the lead was bent slightly upward.

Solder joints from two of the devices made with SnPb solder and SnPb finish did not contain cracks. There was no evidence to indicate failure cause. However, only one side of the component was microsectioned, therefore the failure could have been on the other side. These devices failed after 315 and 449 cycles. The other device with the same solder and finish had microcracks in the solder at both the component and board interfaces. This device failed after 36 cycles. None of the joints examined fractured completely through.

The next group of devices compared had a SnAgCu solder with SnAgCu lead finish. Of these three devices, one had no cracks in the solder joints (failed after 105 cycles), one had minor cracks in the solder on the board side of the joint (failed after 356 cycles) and one had cracks completely through the solder on the board side and minor cracks through the solder on the lead side (failed after 229 cycles).

Solder joints made with SnAgCuBi solder and SnAgCuBi finish were also compared. Two of these devices had minor cracks in the solder on the lead side of the joints. The other device did not contain solder cracks. The device that did not contain solder cracks did have some voiding present in the joints. No anomalies were identified to explain failure. Similar to above, the cracks may have been on the opposite side of the device. It should be noted that the sides chosen for microsectioning appeared to be the side that most likely contained cracks based on an optical surface examination.

**References**

Bradford, Jeff, Joe Felty, and Bill Russell. "JCAA/JG-PP Lead-Free Solder Project: Combined Environments Test". EER-2005-34171-002. Raytheon, August 15, 2005.

IPC-9701. Performance Test Methods and Qualification Requirements for Surface Mount Solder Attachments. January 2002.

IPC/EIA J-STD-001. Requirements for Soldered Electrical and Electronic Assemblies. March 2000.

IPC-SM-785. Guidelines for Accelerated Reliability Testing of Surface Mount Solder Attachments. November 1992.

Joint Group on Pollution Prevention. Joint Test Protocol J-01-EM-026-P1 for Validation of Alternatives to Eutectic Tin-Lead Solders used in Manufacturing and Rework of Printed Wiring Assemblies. April 2004.

MIL-STD-810F, Method 520.2. Temperature, Humidity, Vibration, and Altitude.

**Appendixes**

**Appendix A: List of Microsectioned Components From Manufactured Test Vehicles**

**Appendix B: List of Microsectioned Components From Rework Test Vehicles**

**Appendix C: List of Microsectioned Components From Hybrid Test Vehicles**

**Appendix A: List of Microsectioned Components on Manufactured Test Vehicles**

**Table 29 List of Microsectioned Components on Manufactured Test Vehicles**

SN	RefDes	Component	Finish	Solder	Actual Cycles at Failure	Missing
30	U1	TQFP-144	Sn	SnPb	549	
30	U55	BGA-225	SnPb	SnPb	541	
30	U57	TQFP-208	AuPdNi	SnPb	51	
31	U22	CLCC-20	SnPb	SnPb	319	
31	U24	TSOP-50	SnPb	SnPb	549	
31	U30	PDIP-20	Sn	SnPb	-	
31	U46	CLCC-20	SnPb	SnPb	469	
32	U26	TSOP-50	SnPb	SnPb	347	
32	U43	BGA-225	SnPb	SnPb	175	
33	U1	TQFP-144	Sn	SnPb	327	
34	U27	PLCC-20	Sn	SnPb	-	
34	U3	TQFP-208	AuPdNi	SnPb	537	
34	U49	PDIP-20	AuPdNi	SnPb	51	
34	U59	PDIP-20	AuPdNi	SnPb	11	
99	U11	PDIP-20	Sn	SAC	-	
99	U16	TSOP-50	SnPb	SAC	323	
99	U23	PDIP-20	AuPdNi	SAC	-	
99	U46	CLCC-20	SnPb	SAC	353	
100	U39	TSOP-50	SnCu	SAC	506	
100	U5	BGA-225	SnPb	SAC	30	
101	U17	CLCC-20	SAC	SAC	303	X
101	U3	TQFP-208	AuPdNi	SAC	455	
101	U55	BGA-225	SAC	SAC	514	
101	U58	TQFP-144	Sn	SAC	550	
101	U62	TSOP-50	SnPb	SAC	520	
102	U12	TSOP-50	SnCu	SAC	221	
102	U14	CLCC-20	SAC	SAC	168	X
102	U31	TQFP-208	AuPdNi	SAC	526	
102	U44	BGA-225	SnPb	SAC	540	
102	U47	PLCC-20	Sn	SAC	-	
102	U6	BGA-225	SAC	SAC	100	
102	U7	TQFP-144	Sn	SAC	308	
103	U53	CLCC-20	SnPb	SAC	304	
113	U4	BGA-225	SAC	SACB	550	
113	U9	CLCC-20	SnPb	SACB	351	
139	U1	TQFP-144	Sn	SACB	353	
139	U57	TQFP-208	AuPdNi	SACB	221	
140	U51	PDIP-20	Sn	SnCu	-	
140	U54	PLCC-20	Sn	SACB	-	
140	U56	BGA-225	SnPb	SACB	522	
141	U2	BGA-225	SnPb	SACB	223	
141	U24	TSOP-50	SnPb	SACB	212	

**JCAA/JG-PP Lead-Free Solder Project: Failure Analysis of Test Vehicles Subjected to Combined Environments Test**

**Appendixes**

SN	RefDes	Component	Finish	Solder	Actual Cycles at Failure	Missing
141	U45	CLCC-20	SACB	SACB	518	
141	U46	CLCC-20	SnPb	SACB	501	
142	U17	CLCC-20	SACB	SACB	1	
142	U24	TSOP-50	SnPb	SACB	178	
142	U25	TSOP-50	SnCu	SACB	524	
142	U29	TSOP-50	SnCu	SACB	367	
142	U31	TQFP-208	AuPdNi	SACB	536	
142	U35	PDIP-20	AuPdNi	SnCu	317	
142	U55	BGA-225	SAC	SACB	1	
142	U58	TQFP-144	Sn	SACB	530	

**Appendix B: List of Microsectioned Components From Rework Test Vehicles**

**Table 30** List of Microsectioned Components From Rework Test Vehicles

SN	RefDes	Component	Component Finish Before Rework	Component Finish After Rework	Rework Wire	Cycles at Failure	Missing
45	U25	TSOP-50	SnPb	SnPb	SnPb	186	
45	U3	TQFP-208	AuPdNi	AuPdNi	SnPb	505	
45	U4	BGA-225	SnPb	SnPb		-	
45	U57	TQFP-208	AuPdNi	AuPdNi	SnPb	-	
66	U25	TSOP-50	SnPb	SnPb	SnPb	210	
66	U59	PDIP-20	AuPdNi	SnPb	SnPb	-	
68	U3	TQFP-208	AuPdNi	AuPdNi	SnPb	307	
68	U57	TQFP-208	AuPdNi	AuPdNi	SnPb	305	X
70	U23	PDIP-20	AuPdNi	AuPdNi	SnPb	528	
70	U4	BGA-225	SnPb	SnPb		252	
172	U25	TSOP-50	SnPb	SnCu	SAC	470	
172	U3	TQFP-208	AuPdNi	AuPdNi	SAC	52	
172	U59	PDIP-20	AuPdNi	AuPdNi	SAC	531	
173	U57	TQFP-208	AuPdNi	AuPdNi	SAC	256	
174	U3	TQFP-208	AuPdNi	AuPdNi	SAC	521	
174	U4	BGA-225	SnPb	SAC		169	
174	U57	TQFP-208	AuPdNi	AuPdNi	SAC	508	
174	U59	PDIP-20	AuPdNi	AuPdNi	SAC	334	
175	U12	TSOP-50	SnPb	SnCu	SAC	156	
200	U25	TSOP-50	SnPb	SnCu	SACB	22	X
200	U57	TQFP-208	AuPdNi	AuPdNi	SACB	521	
201	U25	TSOP-50	SnPb	SnCu	SACB	201	
201	U3	TQFP-208	AuPdNi	AuPdNi	SACB	2	X
201	U59	PDIP-20	AuPdNi	AuPdNi	SnCu	428	
203	U3	TQFP-208	AuPdNi	AuPdNi	SACB	42	X
204	U4	BGA-225	SnPb	SAC		-	
204	U57	TQFP-208	AuPdNi	AuPdNi	SACB	512	
204	U59	PDIP-20	AuPdNi	AuPdNi	SnCu	523	

**Appendix C: List of Microsectioned Components From Hybrid Test Vehicles**

**Table 31 List of Microsectioned Components From Hybrid Test Vehicles**

SN	RefDes	Component	Finish	Paste	Cycles at Failure
301	U36	CSP-100	SnPb	SnPb	280
301	U37	CSP-100	SnPb	SnPb	15
301	U50	Hybrid-30	SnPb	SnPb	449
302	U60	CSP-100	SnPb	SnPb	449
305	U33	Hybrid-30	SnPb	SnPb	36
306	U50	Hybrid-30	SnPb	SnPb	315
323	U32	Hybrid-30	SnAgCu	SnAgCu	356
323	U60	CSP-100	SnAgCu	SnAgCu	332
325	U19	CSP-100	SnAgCu	SnAgCu	24
326	U32	Hybrid-30	SnAgCu	SnAgCu	229
326	U33	Hybrid-30	SnAgCu	SnAgCu	105
326	U60	CSP-100	SnAgCu	SnAgCu	146
332	U33	Hybrid-30	SnAgCuBi	SnAgCuBi	232
332	U37	CSP-100	SnAgCu	SnAgCuBi	135
333	U37	CSP-100	SnAgCu	SnAgCuBi	230
336	U50	Hybrid-30	SnAgCuBi	SnAgCuBi	343
337	U33	Hybrid-30	SnAgCuBi	SnAgCuBi	475
337	U36	CSP-100	SnAgCu	SnAgCuBi	2

## **JCAA/JG-PP Lead-Free Solder Project: Failure Analysis of Test Vehicles Subjected to Combined Environments Test**

### **List of Symbols, Abbreviations and Acronyms**

#### **List of Symbols, Abbreviations and Acronyms**

Ag	Silver
Au	Gold
AuPdNi	Gold-Palladium-Nickel finish
BGA	Ball grid array
Bi	Bismuth
CCA	Circuit card assembly
CET	Combined environments test
CLCC	Ceramic leadless chip carrier
CSP	Chip scale package
Cu	Copper
DoD	Department of Defense
EDS	Energy dispersive spectroscopy
EPA	Environmental Protection Agency
ETL	Environmental Test Laboratory
FAL	Failure Analysis Laboratory
HASL	Hot air solder level
HALT	Highly accelerated life test
HASS	Highly accelerated stress screen
IMC	Intermetallic compound
I/O	Input/output
JCAA	Joint Council on Aging Aircraft
JG-PP	Joint Group on Pollution Prevention
JTP	Joint Test Protocol
JTR	Joint Test Report
NASA	National Aeronautical and Space Administration
KeV	Kilo electron volt
Ni	Nickel
OSP	Organic solderability preservative

**JCAA/JG-PP Lead-Free Solder Project: Failure Analysis of  
Test Vehicles Subjected to Combined Environments TestList of Symbols, Abbreviations and Acronyms**

Pd	Palladium
PDIP	Plastic dual-inline package
PLCC	Plastic leaded chip carrier
PTH	Plated-through hole
PWB	Printed wiring board
RoHS	Restriction of Hazardous Substances
SAC	Tin-Silver-Copper solder alloy
SACB	Tin-Silver-Copper-Bismuth solder alloy
SEM	Scanning electron microscope or scanning electron microscopy
SMT	Surface mount technology
Sn	Tin
SnAgCu	Tin-Silver-Copper solder alloy
SnAgCuBi	Tin-Silver-Copper-Bismuth solder alloy
SnCu	Tin-Copper solder alloy
SnPb	Tin-Lead solder alloy
Tg	Glass transition temperature
TQFP	Thin quad flat package
TSOP	Thin small outline package
um	Micrometer or micron
W	Tungsten
WEEE	Waste from Electrical and Electronic Equipment Directive